# Innovative adsorbent materials for reactive capping of contaminated marine sediments

Abstract
The development of anthropogenic coastal activities has led to the contamination of marine sediments with hazardous substances, posing serious risks to the health and well-being of humans and the environment. It is of paramount importance to develop sustainable technologies for the simultaneous treatment of different contaminants, providing a permanent solution to reduce the hazardousness of sediments in aquatic environments.
Recently, nanomaterials are gaining ground in the remediation sector, so the need arises to develop ever-new ones concerning sustainability. Materials that have natural substances or waste as precursors are ideal candidates.
This study aimed to develop sustainable materials for the remediation of contaminated marine sediments. The synthesis of the materials involves oxidation of the precursors (cellulose) with 2,2,6,6-tetramethylpiperidine-1-oxyl (TEMPO), acidification and branching with branched polyethyleneimine (bPEI), and freezing overnight. The better method to obtain this material was individuated between freeze-drying, Soxhlet extractor or a combination of both. A Soxhlet extractor with ethanol as solvent was the best way in terms of time and yield and it was used to obtain the chitin-based material. After being chemically and microstructurally characterized, the materials obtained was subjected to adsorption tests with three organic tracers: Methylene Blue, 4-Nitrobenzaldehyde and 4-Nitrophenol, and two heavy metals: Chromium and Cadmium.
All the experiments were implemented with LCA analysis to evaluate the environmental impact.

Photo of the two materials: First on the left is chitin-based material with its SEM image; on the bottom a photo of Mar Piccolo of Taranto and a schematic view of how capping works.

DICATECh

2024

Milvia Elena Di Clemente

Innovative adsorbent materials for reactive capping of contaminated marine sediments

12

# D.R.S.A.T.E.

Doctor in Risk And Environmental, Territorial And Building Development

POLITECNICO DI BARI

12

2024

Coordinator: Prof. Vito Iacobellis

XXXVI CYCLE
Ing/Ind 22 - Material Science and Technology

DICATECh
Department of Civil, Environmental, Building Engineering and Chemistry

Milvia Elena Di Clemente

## Innovative adsorbent materials for reactive capping of contaminated marine sediments

Prof. Michele Notarnicola
Prof. Roberto Grisorio
DICATECh, Politechnic of Bari

Prof. Carmen Teodosiu
Department Environmental Engineering and Management
"Gheorghe Asachi" Technical University Iasi

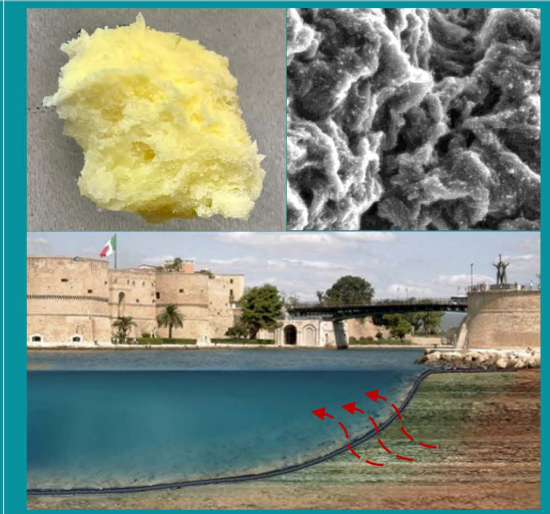

Abstract
The development of anthropogenic coastal activities has led to the contamination of marine sediments with hazardous substances, posing serious risks to the health and well-being of humans and the environment. It is of paramount importance to develop sustainable technologies for the simultaneous treatment of different contaminants, providing a permanent solution to reduce the hazardousness of sediments in aquatic environments.
Recently, nanomaterials are gaining ground in the remediation sector, so the need arises to develop ever-new ones concerning sustainability. Materials that have natural substances or waste as precursors are ideal candidates.
This study aimed to develop sustainable materials for the remediation of contaminated marine sediments. The synthesis of the materials involves oxidation of the precursors (cellulose) with 2,2,6,6-tetramethylpiperidine-1-oxyl (TEMPO), acidification and branching with branched polyethyleneimine (bPEI), and freezing overnight. The better method to obtain this material was individuated between freeze-drying, Soxhlet extractor or a combination of both. A Soxhlet extractor with ethanol as solvent was the best way in terms of time and yield and it was used to obtain the chitin-based material. After being chemically and microstructurally characterized, the materials obtained was subjected to adsorption tests with three organic tracers: Methylene Blue, 4-Nitrobenzaldehyde and 4-Nitrophenol, and two heavy metals: Chromium and Cadmium.
All the experiments were implemented with LCA analysis to verify the environmental impact.

DICATECh

2024

Milvia Elena Di Clemente

**Innovative adsorbent materials for reactive capping of contaminated marine sediments**

**12**

**D.R.S.A.T.E.**

Doctor in Risk And Environmental, Territorial And Building Development

Coordinator: Prof. Vito Iacobellis

XXXVI CYCLE
Ing/Ind 22 – Material Science and Technology

DICATECh
Department of Civil, Environmental, Building Engineering and Chemistry

**POLITECNICO DI BARI**

Milvia Elena Di Clemente

**Innovative adsorbent materials for reactive capping of contaminated marine sediments**

Prof. Michele Notarnicola
Prof. Roberto Grisorio
DICATECh, Politechnic of Bari

Prof. Carmen Teodosiu
Department Environmental Engineering and Management
"Gheorghe Asachi" Technical University Iasi

**12**

**2024**

Politecnico di Bari

LIBERATORIA PER L'ARCHIVIAZIONE DELLA TESI DI DOTTORATO

Al Magnifico Rettore
del Politecnico di Bari

La sottoscritta Milvia Elena Di Clemente nata a Terlizzi (BA) il 12/04/1990

residente a Bari (BA) in via Monte Grappa, 9 e-mail milviaelena.diclemente@poliba.it

iscritto al 3° anno di Corso di Dottorato di Ricerca in Rischio, Sviluppo, Ambientale, del Territorio ed Edilizio ciclo XXXVI

ed essendo stato ammesso a sostenere l'esame finale con la prevista discussione della tesi dal titolo:

Innovative adsorbent materials for reactive capping of contaminated marine sediments

**DICHIARA**

1) di essere consapevole che, ai sensi del D.P.R. n. 445 del 28.12.2000, le dichiarazioni mendaci, la falsità negli atti e l'uso di atti falsi sono puniti ai sensi del codice penale e delle Leggi speciali in materia, e che nel caso ricorressero dette ipotesi, decade fin dall'inizio e senza necessità di nessuna formalità dai benefici conseguenti al provvedimento emanato sulla base di tali dichiarazioni;
2) di essere iscritto al Corso di Dottorato di ricerca Rischio, Sviluppo, Ambientale, del Territorio ed Edilizio ciclo XXXVI, corso attivato ai sensi del "*Regolamento dei Corsi di Dottorato di ricerca del Politecnico di Bari"*, emanato con D.R. n.286 del 01.07.2013;
3) di essere pienamente a conoscenza delle disposizioni contenute nel predetto Regolamento in merito alla procedura di deposito, pubblicazione e autoarchiviazione della tesi di dottorato nell'Archivio Istituzionale ad accesso aperto alla letteratura scientifica;
4) di essere consapevole che attraverso l'autoarchiviazione delle tesi nell'Archivio Istituzionale ad accesso aperto alla letteratura scientifica del Politecnico di Bari (IRIS-POLIBA), l'Ateneo archivierà e renderà consultabile in rete (nel rispetto della Policy di Ateneo di cui al D.R. 642 del 13.11.2015) il testo completo della tesi di dottorato, fatta salva la possibilità di sottoscrizione di apposite licenze per le relative condizioni di utilizzo (di cui al sito http://www.creativecommons.it/Licenze), e fatte salve, altresì, le eventuali esigenze di "embargo", legate a strette considerazioni sulla tutelabilità e sfruttamento industriale/commerciale dei contenuti della tesi, da rappresentarsi mediante compilazione e sottoscrizione del modulo in calce (Richiesta di embargo);
5) che la tesi da depositare in IRIS-POLIBA, in formato digitale (PDF/A) sarà del tutto identica a quelle **consegnate**/inviate/da inviarsi ai componenti della commissione per l'esame finale e a qualsiasi altra copia depositata presso gli Uffici del Politecnico di Bari in forma cartacea o digitale, ovvero a quella da discutere in sede di esame finale, a quella da depositare, a cura dell'Ateneo, presso le Biblioteche Nazionali Centrali di Roma e Firenze e presso tutti gli Uffici competenti per legge al momento del deposito stesso, e che di conseguenza va esclusa qualsiasi responsabilità del Politecnico di Bari per quanto riguarda eventuali errori, imprecisioni o omissioni nei contenuti della tesi;
6) che il contenuto e l'organizzazione della tesi è opera originale realizzata dal sottoscritto e non compromette in alcun modo i diritti di terzi, ivi compresi quelli relativi alla sicurezza dei dati personali; che pertanto il Politecnico di Bari ed i suoi funzionari sono in ogni caso esenti da responsabilità di qualsivoglia natura: civile, amministrativa e penale e saranno dal sottoscritto tenuti indenni da qualsiasi richiesta o rivendicazione da parte di terzi;
7) che il contenuto della tesi non infrange in alcun modo il diritto d'Autore né gli obblighi connessi alla salvaguardia di diritti morali od economici di altri autori o di altri aventi diritto, sia per testi, immagini, foto, tabelle, o altre parti di cui la tesi è composta.

Luogo e data 05/07/2024 Firma Milvia Elena Di Clemente

Il/La sottoscritto, con l'autoarchiviazione della propria tesi di dottorato nell'Archivio Istituzionale ad accesso aperto del Politecnico di Bari (POLIBA-IRIS), pur mantenendo su di essa tutti i diritti d'autore, morali ed economici, ai sensi della normativa vigente (Legge 633/1941 e ss.mm.ii.),

**CONCEDE**

- al Politecnico di Bari il permesso di trasferire l'opera su qualsiasi supporto e di convertirla in qualsiasi formato al fine di una corretta conservazione nel tempo. Il Politecnico di Bari garantisce che non verrà effettuata alcuna modifica al contenuto e alla struttura dell'opera.
- al Politecnico di Bari la possibilità di riprodurre l'opera in più di una copia per fini di sicurezza, back-up e conservazione.

Luogo e data 05/07/2024 Firma Milvia Elena Di Clemente

Politecnico di Bari

RICHIESTA DI EMBARGO

Sottoscrivere solo nel caso in cui si intenda auto-archiviare la tesi di dottorato nell'Archivio Istituzionale ad accesso aperto alla letteratura scientifica POLIBA-IRIS (https://iris.poliba.it) ) non in modalità "Accesso Aperto", per motivi di segretezza e/o di proprietà dei risultati e/o informazioni sensibili o sussistano motivi di segretezza e/o di proprietà dei risultati e informazioni di Enti esterni o Aziende private che hanno partecipato alla realizzazione della ricerca.

La sottoscritta MIlvia Elena Di Clemente nata a Terlizzi (BA)

Il 12/04/1990 residente a Bari (BA) alla via Monte Grappa, 9 indirizzo e-mail milviaelena.diclemente@poliba.it

iscritto/a al corso di dottorato di ricerca Rischio, Sviluppo, Ambientale, del Territorio ed Edilizio ciclo XXXVI

Autore della tesi di dottorato dal titolo Innovative adsorbent materials for reactive capping of contaminated marine sediments

e ammesso a sostenere l'esame finale:

**NON AUTORIZZA**

Il Politecnico di Bari a pubblicare nell'Archivio Istituzionale di Ateneo ad accesso aperto il testo completo della tesi depositata per un periodo comunque non superiore a 12 (dodici) mesi decorrenti dalla data di esame finale.

Specificare la motivazione *(apporre una crocetta sulla motivazione):*

☒ Brevetto (*indicare nel campo libero la data della domanda di deposito*) 20/12/2023

☐ Segreto industriale, se è stato firmato un accordo di non divulgazione.
*(indicare nel campo libero gli estremi dell'accordo)*_____

☐ Segreto d'ufficio a tutela di progetti _____

☐ Motivi di priorità nella ricerca (previo accordo con terze parti) _____

☐ Motivi editoriali _____

☐ Altro (*specificare*) _____

Saranno comunque consultabili ad accesso aperto i dati bibliografici e l'abstract.

Il sottoscritto dottorando dichiara in virtù di quanto sopra che si rende opportuno procrastinare la pubblicazione della tesi attraverso l'Archivio Istituzionale ad accesso aperto (POLIBA -IRIS) e di impostare la data di embargo, in fase di deposito della tesi di dottorato in formato elettronico (pdf/A) per un periodo *di embargo* non superiore a 12 (dodici) mesi decorrenti dalla data di esame finale.

Il sottoscritto dottorando dichiara di essere a conoscenza che a scadenza della data di embargo su riportata, la tesi verrà pubblicata attraverso l'Archivio Istituzionale ad accesso aperto alla letteratura scientifica del Politecnico di Bari.

Luogo e data 05/07/2024

Firma Dottorando 

Firma Relatore Michele Notarnicola

| | | | |
|---|---|---|---|
| | |  | |
| | **D.R.S.A.T.E.** | **POLITECNICO DI BARI** | **12** |
| | Doctor in Risk And Environmental, Territorial And Building Development | | **2024** |
| | Coordinator: Prof. Vito Iacobellis | | |
| | XXXVI CYCLE<br>Ing/Ind 22 – Material Science and Technology | | |
| | DICATECh<br>Department of Civil, Environmental, Building Engineering and Chemistry | | |
| | | Milvia Elena Di Clemente | |
| | | **Innovative adsorbent materials for reactive capping of contaminated marine sediments** | |
| | | Prof. Michele Notarnicola<br>Prof. Roberto Grisorio<br>DICATECh, Politechnic of Bari<br><br>Prof. Carmen Teodosiu<br>Department Environmental Engineering and Management<br>"Gheorghe Asachi" Technical University Iasi | |
| | | | |
| | | | |

# **EXTENDED ABSTRACT** (Eng)

The management of contaminated marine sediment is a major global environmental problem. Therefore, it is crucial to develop sustainable technologies for the simultaneous treatment of different contaminants by providing a permanent solution to the reduction of sediment toxicity in aquatic environments.

Among the various technologies of remediation in situ there is the use of Reactive Core Mats (RCM), that is, mats containing, inside two layers of fabric/ non-woven, a material capable of blocking and/ or degrading the contaminated sediment. Currently, the materials most commonly used for the adsorption of contaminants are organic clays and activated carbon.

In this context, this thesis aims to identify new sustainable materials, both from an environmental and economic point of view, with high remediation performance.

In particular, two materials were developed through the synthesis of cellulose- and chitin. Both are natural polymers: cellulose is the most abundant, renewable and biodegradable source in the biosphere, making it a good alternative to petroleum-derived materials. Nearby chitin is the second biopolymer most abundant in nature, which is derived from shrimp shells, fungi and exoskeletons of arthropods. A big advantage of this polymer is that the industrial product is always obtained by one of the major by-products of the seafood industry.

The experimental plan carried out in this thesis concerns the development of a synthesis protocol, characterization and adsorption tests of cellulose- and chitin-based material.

First, different protocols to obtain cellulose-based material are compared to find the best way to obtain it., comparing methods such as

freeze-drying, Soxhlet extractor and the combination of both, and three different solvents for the Soxhlet extractor (Acetone, Methanol and Ethanol). The materials were chemically (FTIR spectroscopy) and morphologically (SEM microscopy) characterized and tested with three different organic dyes (4-nitrophenol, 4-Nitrobenzaldehyde and Methylene Blue). The results allowed us to determine which was the synthesis protocol that best-combined functionality and speed of implementation. The protocol identified has been applied to chitin with the appropriate improvements and subsequently the possibility of implementing a scale-up to synthesis with a view to an industrial development of these materials.

The cellulose- and chitin-based materials thus obtained were tested with the three organic dyes, in deionized water and marine water, which showed comparable results, and tested also with two heavy metals (Cd and Cr), which showed some better results for the chitin-based material.

The experimentation was completed by Life Cycle Assessment (LCA) in order to individuate the less environmentally impactful synthesis protocol. Thanks to LCA analysis was possible to observe that the environmental impact of both synthesis protocols is more affected by the electricity needed to use the laboratory equipment.

The results obtained lay the foundation for the use of these reactive materials within the Reactive core mats.

**Keywords:** environmental remediation, contaminated sediments, new materials, cellulose, chitin

# **EXTENDED ABSTRACT** (Ita)

La gestione dei sedimenti marini contaminati è un notevole problema ambientale riconosciuto a livello mondiale. Pertanto, è di fondamentale importanza sviluppare tecnologie sostenibili per il trattamento simultaneo di diversi contaminanti fornendo una soluzione permanente alla riduzione della tossicità dei sedimenti presenti negli ambienti acquatici.

Tra le varie tecnologie di bonifica in situ vi è l'impiego di Reactive Core Mats (RCM), ovvero dei materassini contenenti, all'interno di due strati di tessuto/non-tessuto, un materiale in grado di bloccare e/o degradare i contaminati presenti nei sedimenti. Attualmente i materiali maggiormente utilizzati per l'adsorbimento dei contaminanti sono le argille organiche e il carbone attivo.

In questo contesto si inquadra il presente lavoro di tesi che mira ad individuare nel panorama dei materiali innovativi ed ancora in fase di sviluppo, nuovi materiali che siano sostenibili, sia da un punto di vista ambientale che economico, pur mantenendo elevate prestazioni.

I due materiali sviluppati sono a base di cellulosa e chitina. Entrambi sono polimeri naturali: la cellulosa è la fonte più abbondante, rinnovabile e biodegradabile nella biosfera, rendendola una buona alternativa ai materiali derivati dal petrolio. La chitina vicina è il secondo biopolimero più abbondante in natura, che deriva dai gusci dei gamberetti, dai funghi e dagli esoscheletri degli artropodi. Un grande vantaggio di questo polimero è che il prodotto industriale è sempre ottenuto da uno dei principali sottoprodotti dell'industria ittica.

La parte sperimentale svolta in questa tesi riguarda lo sviluppo di un protocollo di sintesi, prove di caratterizzazione e adsorbimento di materiali a base di cellulosa e chitina.

In primo luogo, diversi protocolli per ottenere materiale a base di cellulosa vengono confrontati per trovare il modo migliore per ottenerlo. ,

confrontando metodi come liofilizzazione, estrattore Soxhlet e la combinazione di entrambi, e tre diversi solventi per l'estrattore Soxhlet (acetone, metanolo ed etanolo). I materiali sono stati chimicamente (spettroscopia FTIR) e morfologicamente (microscopia SEM) caratterizzati e testati con tre diversi coloranti organici (4-nitrofenolo, 4-nitrobenzaldeide e blu di metilene). I risultati ci hanno permesso di determinare quale era il protocollo di sintesi che meglio combinava funzionalità e velocità di implementazione. Il protocollo individuato è stato applicato alla chitina con gli opportuni miglioramenti e successivamente la possibilità di attuare una scale-up di sintesi in vista di uno sviluppo industriale di questi materiali.

I materiali a base di cellulosa e chitina così ottenuti sono stati testati con i tre coloranti organici, in acqua deionizzata e acqua marina, che hanno mostrato risultati comparabili, e testati anche con due metalli pesanti (Cd e Cr), che hanno mostrato risultati migliori per il materiale a base di chitina.

La parte sperimentale è stata accompagnata dall'analisi LCA per individuare il protocollo di sintesi meno impattante per l'ambiente. Grazie all'analisi di LCA è stato possibile osservare che l'impatto ambientale di entrambi i protocolli di sintesi è più influenzato dall'energia elettrica necessaria per utilizzare le apparecchiature di laboratorio.

I risultati ottenuti hanno gettato le basi per l'uso di questi materiali reattivi all'interno dei Reactive Core Mat.

**Keywords:** Bonifica, sedimenti contaminati, nuovi materiali, cellulosa, chitina

# *INDEX*

# INTRODUCTION

A huge problem of this century is the pollution of seawater and its sediments. The development of human activities, such as agriculture, urbanization, and industry, on the coast during the century has led to the release of many hazardous chemicals in the aquatic environment. Aquatic sediments have been identified as the ultimate receptor for these pollutants – contaminants then re-enter the overlying water due to the variation of the physical-chemical characteristics of the water. Contaminants are thus available for benthic organisms and subsequently enter aquatic food chains.

The remediation of contaminated sediments is nowadays one of the most challenging problems in the environmental protection area.

Among all the in-situ strategies, capping is one of the most sustainable options, i.e. in terms of efficacy, durability, and economy. This technology consists of placing a layer of clean materials over contaminated sediments to isolate the contaminant from the overlying water column and biota, to reduce contaminant flux into the biologically active portion of the sediment, and to create new habitats for aquatic organisms.

This technology can be divided into two macro-types: the first consists of using an inert material (e.g. sand) to block contaminants in the area underneath; the second, on other hand, consists of using a material called reactive capping that allows contaminants to be blocked and/or degraded.

Appropriate materials have been developed and put in place to block or degrade contaminants in the marine sediment and to prevent them from returning to overlying water (Wang et al., 1991). In the last two decades, the most used materials are Activated carbon, Apatite, Biochar, Coke, Organoclay, Zeolites, and Zero Valent Iron (Zhang et al., 2016a). Many studies were carried out on the actual effectiveness of these materials, but nowadays the focus is more and more on materials with nanometric sizes.

Nanomaterials are materials with sizes at the nano-scale (1–100 nm) in at least one of their three dimensions and include nano-objects and nanoparticles (Hristozov & Malsch, 2009; Stone et al., 2010).

They are very appreciated because they are considered excellent remarkable absorbents and catalysts thanks to their much larger specific surface areas, more associated sorption sites, lower temperature modification, shorter interparticle diffusion distance, more tunable pore size, and different surface chemistry than other materials (Tang et al., 2014a).

Although nanomaterials are a promising resource for the remediation of heavy metal(loid) polluted sediments, few studies have been published on immobilizing/adsorbing heavy metal(loid)s by utilizing nanomaterials for sediment remediation.

This thesis work aimed to identify a new reactive material both exhibiting a good response with as many contaminant classes as possible and meeting the fundamentals of sustainability. To pursue this objective, the research was focused on *i*) the appropriate development of a synthesis protocol for two biobased materials (cellulose and chitin), *ii*) the increasing of the quantities produced by a suitable scale-up protocol, *iii*) the adsorption tests with organic dyes and heavy metals, and *iv*) Life Cycle Assessment (LCA) analysis to evaluate the environmental impact of the previous activities.

The experimental data give important results to set the first step of the development and use of new materials for environmental remediation. In particular, the most significant results are the development of a new adsorbent material (hereafter, Chn-based material) which has a structure similar to the cellulose-based material, the possibility to scale up simply the production of this material and a lower environmental impact than the cellulose-based material because secondary products of the seafood sector always obtain the chitin used as a precursor.

The results obtained from this work lay the foundation for the development of materials and technology that are sustainable and effective for the environmental remediation of contaminated marine sediments.

# 1. CONTAMINATED MARINE SEDIMENTS

## *1.1 Introduction*

Contaminated marine sediments are a common problem throughout the industrialized world and trying to clean them up is a real challenge. The biggest problem caused by contaminants in sediments is their migration into the overlying water column, which leads to the diffusion of these contaminants into the marine flora, thus spreading to animal organisms via the food chain.

The contaminants usually present in sediments are PCBs, PAHs, pesticides, nutrients, and metals. The metals that are typically detected and considered toxic are arsenic, cadmium, chromium, copper, lead, mercury, and nickel. (Peng et al., 2009)

## *1.2 Regulatory issues*

As the field of remediation is a real challenge, it is necessary to regulate what is meant by contaminated sediments and when the presence of a contaminant in a certain quantity may not be defined as risky.

The laws regulating these aspects are not globally uniform to date. In fact, in the United States, the most complete set of Preliminary Remediation Goals (PRGs) comes from the Environmental Protection Agency (EPA). In Europe a set of standards often used is represented by the so-called "Dutch Standards", environmental pollutant reference values (i.e., concentrations in environmental medium) for environmental remediation, investigation, and clean-up.

In Italy, the national environmental reference law in the Legislative Decree 152 of 3 April 2006, known as the Environmental Code or Consolidated Environmental Act, defines and regulates everything concerning waste management and the remediation of contaminated sediments.

In particular, Title V of Part IV regulates the remediation and environmental restoration of contaminated sites and defines procedures, criteria, and

methods for carrying out the necessary activities in harmony with community principles.

The fundamental principles on which it is based are:

- The main party obliged to carry out remediation is the polluter, even before the owner of the contaminated site;
- The obligation of remediation exists regardless of the date on which the pollution occurred;
- The remediation can only be implemented after formal approval of a project by the competent authority;
- Emergency safety measures must be implemented immediately by the polluter or site owner, without the need for approval by the competent authority.

And also it defines threshold levels:

- Threshold contamination concentration, defined as the level of contamination of environmental matrices above which site characterisation and site-specific site characterisation and site-specific risk analysis become mandatory;
- Threshold Risk Concentration, defined as the level of contamination level of the environmental matrices beyond which the safety and safety and remediation procedure becomes mandatory. The Threshold Risk Concentration represents the remediation objectives and, unlike the Threshold contamination concentration, is not tabulated, i.e. known in advance, so they must be determined on a case-by-case basis through the application of a site-specific risk analysis;
- Site-specific risk analysis, defined as the analysis of the effects on human health resulting from long-term exposure to pollutants in environmental matrices.

From these definitions derive the definitions of potentially contaminated site and contaminated site:

- A site is potentially contaminated when the concentration values of the pollutants detected in the environmental matrices are higher

than the Threshold contamination concentration, pending the characterization and site-specific risk analysis operations which make it possible to confirm the state of contamination or not on the basis of the Threshold Risk Concentration;

- A site is contaminated when the Threshold Risk Concentration values determined by the application of the site-specific risk analysis, whose input data are the results of the characterization activity, are exceeded.

Italian law is also supplemented with European laws for what concerns water protection and management, the following regulations should also be considered: (a) Directive 91/156/EEC about waste, (b) Directive 91/689/EEC about hazardous waste, (c) Directive 2004/95/EC about the environmental responsibilities on prevention and remediation of the environmental damage, (d) Ministerial Decree 56/09 about marine coastal water transposing part of the European Directive 2008/105/EC and the Ministerial Decree 260/10 for monitoring and classification of superficial water bodies.

At the European level, there are two fundamental directives: (i) Directive 2004/35/CE of the European Parliament and of the Council of 21 April 2004 lay the foundations for environmental liability concerning the prevention and remediation of environmental damage, and (ii) Directive 2000/60/EC of the European Parliament and the Council established a framework for Community action in the field of water policy, specifically for the protection of inland surface waters, transitional waters, coastal waters, and groundwaters. In particular, the latter directive recommends certain actions to be followed: (a) avoiding further deterioration and protecting the status of aquatic ecosystems, (b) promoting sustainable water use based on long-term protection, (c) aiming at enhanced protection and improving the aquatic environment, (d) safeguarding groundwater quality from further pollution and reducing the one already present, and (e) mitigating the effects of floods and droughts.

The Environmental Quality Standards Directive (EQSD) (Directive 2008/105/EC of the European Parliament and of the Council of 16 December 2008), included in Directive of the Water Framework Directive 2000/60/EC and it sets out environmental quality standards (EQSs) regarding the presence in surface water of priority pollutants because of the significant risk to the aquatic environment.

Instead, the main European regulations about waste management are: (a) the Council Directive 91/156/EEC of 18 March 1991 amending Directive 75/442/EEC on waste, (b) the Landfill Directive, more formally Council Directive 1999/31/EC of 26 April 1999 and (c) the Waste Framework Directive, or Directive 2008/98/EC of the European Parliament and of the Council of 19 November 2008. They are based on the principle of re-use of waste as a new resource, including dredged sediments.

### *1.3 Contaminants*

Contaminants are substances that can accumulate within sediments and their release can cause dramatic changes to the biological characteristics of the overlying water. The contaminants that accumulate within the sediments are hydrophobic and related to the chemical components of the sediments. These substances include polycyclic aromatic hydrocarbons (PAHs), chlorinated aromatics (such as multiple chlorinated benzenes), polychlorinated biphenyls (PCBs), and heavy metals.(Vandermeersch et al., 2015)

The phenomenon that most happens to contaminants in sediments is adsorption, which is characterised by a sediment-water partition coefficient, $k_d$. The sediment-water partition coefficient is defined by:

$$k_d = \frac{W_s}{C} \qquad (1.1)$$

where $W_s$ (mg/kg) is the solid phase concentration and C (mg/kg) is the adjacent water phase concentration.

Another phenomenon is sorption and it is predominant for hydrophobic organic contaminants which are sorbed into the organic carbon fraction of

the sediments and thus the sediment-water partition coefficient is often defined as:

$$k_d = k_{oc} f_{oc} \qquad (1.2)$$

where $k_{oc}$ is the organic carbon-based partition coefficient, a measure of the hydrophobicity of the compound, and $f_{oc}$ is the fraction of organic carbon, a single indicator of the sorption capacity of the sediment for hydrophobic organic compounds. This relationship is a good approximation for the sorption of organic contaminants in natural organic matter that is made of amorphous carbon also called soft organic matter. In this case, the organic carbon-based partition coefficient is related to a measure of the hydrophobicity of the compound. The organic carbon-based partition coefficient is commonly correlated with the octanol-water partition coefficient of the compounds. For example (Baker, 1997),

$$Logk_{oc} = 0.903 Logk_{ow} + 0.094 \qquad (1.3)$$

Common PAHs exhibit octanol-water partition coefficients ($Logk_{ow}$) between 3.37 (naphthalene) and 6 or more (e.g., benzo α pyrene). Pyrene has a $Logk_{ow}$ of 5.18 and therefore Equation 1.3 suggests a $Logk_{oc}$ of 4.77.

Metals interact with sediments in different complicated manners. Metals do not absorb into the organic fraction of the sediments, but they can absorb onto sediment mineral surfaces and precipitate onto solids. Another possibility is that electrostatically attracted to charged sediment surface and then can be released by a cation exchange reaction introducing other cations or acidification of the sediments. In brief, it is possible to divide the behaviour of the metals in sediments into two different categories: the formation of metal precipitates, which is an irreversible phenomenon, and a reversible phenomenon. The most important of the metal precipitates are metal sulfides which are effectively insoluble and form under strongly reducing conditions. This happens a few centimetres below the sediment's surface, in fact, at the surface oxic conditions can lead to sulphide oxidation

and release of the metal ions (Hong et al., 2011a). _Under static conditions, only the exchangeable and adsorbed portion can be partitioned between the sediments and adjacent porewater. This is generally modelled with an effective partition coefficient, $K_{sw}$, but this is not easily modelled and changes in pH and oxygen conditions can affect the partition coefficient (Hong et al., 2011b).

The values were compared with the limits defined by both site-specific law (ICRAM, 2007) and national law (D.Lgs. 152/2006). The values are reported in Tab. 1.1 for each heavy metal considered.

Table 1.1 - Limits of heavy metal concentration

| Metals | Unit | Site-specific law ICRAM 2024 | National law D.Lgs. 152/2006 |
|---|---|---|---|
| As | mg/kg ss | 20 | 50 |
| Be | mg/kg ss | X | 10 |
| Cd | mg/kg ss | 1 | 15 |
| Co | mg/kg ss | X | 250 |
| Cr | mg/kg ss | 160 | 800 |
| Cu | mg/kg ss | 45 | 600 |
| Hg | mg/kg ss | 0.8 | 5 |
| Ni | mg/kg ss | 100 | 500 |
| Pb | mg/kg ss | 50 | 1000 |
| V | mg/kg ss | X | 250 |
| Zn | mg/kg ss | 110 | 1500 |

The concentrations of the persistent organic compounds (Polycyclic Aromatic Hydrocarbons, PAHs, and Polychlorinated Biphenyls, PCBs) are described and compared with the thresholds reported in Tab. 1.2.

Table 1.2 - Limits of PAHs and PCBs concentration.

| Compounds | Unit | Site-specific law ICRAM 2004 | National law D.Lgs. 152/2006 |
|---|---|---|---|
| PAHs | mg/Kg ss | 4 | 100 |
| PCBs | mg/Kg ss | 0.19 | 5 |

# 2. IN SITU CAPPING

Unlike ex-situ treatments, in-situ treatments have the great advantage of being able to treat soils and sediments without removing and transporting them, thus significantly lowering costs. On the other hand, in-situ treatment requires a longer period, and there is less certainty about the uniformity of the treatment because of the variability in soil and aquifer characteristics and because the efficiency of the process is more difficult to verify. In-situ treatments involve the use of different processes (biological, physical/chemical or thermal treatment) that can be employed independently or simultaneously to remove or immobilize contaminants without removing the bulk soil/sediment. Unfortunately, not all the treatments could be used for sediment.

Treatment methods can be divided into three categories according to the mechanism of operation:

- physical/ chemical treatment (i.e. in situ stabilisation/solidification, chemical oxidation, electrokinetic separation, soil flushing and sediment capping). This type of treatment uses the physical properties of the contaminants or the contaminated medium to destroy (i.e., chemically convert), separate, or contain the contamination. Its advantages are cost-effectivity, it can be completed in short periods, and its equipment is readily available and not engineering or energy-intensive (Peng et al., 2018a).
- biological treatment (i.e. phytoremediation, monitored natural attenuation, enhanced natural attenuation). This type of treatment uses microorganisms or vegetation (phytoremediation). Usually, bacteria and fungi are employed because they can transform hazardous chemicals into substances that may be less hazardous than the original compounds or they can immobilize contaminants. It is possible because several plant species can bioaccumulate heavy metals from soil, and some tree species can sequester contaminants and destroy them (Cecchi et al., 2021).

- Thermal treatment (i.e. electrical resistance heating, steam injection and extraction, conductive heating, radio-frequency heating, vitrification). This technique is useful in the presence of volatile and semi-volatile contaminants that evaporate as a result of heat addition to the soil. In case focusing on areas below the groundwater table, the heating cost for all thermal heating technologies rapidly increases and may result in low competitiveness (Crocetti et al., 2022).

In the broad landscape of in situ remediation technology, one of the most promising is reactive capping. Two main approaches could be used to remediate contaminated sediment with in-situ technology:

- Active mixing: It consists of mixing contaminated sediments with natural substrates or inert material. the bioactive surface layer of sediment can transfer contaminants from sediment to strongly binding sorbent particles, reducing their bioavailability to benthic organisms and contaminant flux into the water column and thus the potential general accumulation in the aquatic food web (Ghosh et al., 2011).
- Thin capping: It consists of one or more layers of amendment actively reducing the overall cap thickness required to stop the contaminant. (Perelo, 2010).

Over the past 25 years, researchers' attention has shifted to the possibility of introducing sorbent materials such as activated carbon (AC), organoclay, apatite, biochar, coke, zeolites, and zerovalent iron (ZVI) into contaminated sediments (USEPA, 2013). Additives tend to modify sediment geochemistry by increasing the binding and stability of contaminants to reduce the risk to human health and the environment.

Reactive materials can degrade and/or adsorb contaminants while allowing upward groundwater flow. The use of reactive materials can significantly reduce the thickness required for cap compared to conventional sand caps (Perelo, 2010).

The most common sorptive materials applied in pilot experiments include:

- Apatites (Knox et al., 2012a): it generally consist of a matrix of calcium phosphate and various other common anions, including fluoride, chloride, hydroxide, and occasionally carbonate, capable of sequestering metals in soils and sediments (X. Chen et al., 2000; Peld et al., 2002).
- Zeolites (Velarde et al., 2023) which adsorb and complex different metals;
- Organophilic clay (Erten et al., 2012; Olsta, 2010);
- Biochar or activated carbon (Silvani et al., 2017) which effectively adsorb organic compounds;
- Zero-valent iron (ZVI) for treating nitroaromatics, chromium, lead, DDT, and related compounds (Chapman et al., 2020; Gil-Díaz et al., 2017).

Capping systems utilizing organoclay, achieved through the incorporation of organic molecules into clay structures, have demonstrated efficacy in mitigating various contaminants in soil and water, owing to their impressive sorption capabilities. Organoclay is derived from the fusion of clay minerals with surfactants, including quaternary alkyl ammonium salts among others. Numerous studies in the literature have showcased its effectiveness in adsorbing non-aqueous phase liquids and other organic contaminants (Guégan, 2019; Knox et al., 2012b).

Due to its notable organic adsorption capacity, organoclay can offer a cost-effective alternative to activated carbon.(Olsta & Asce, 2007)

Out of all options, activated carbon (AC), organic clay, and apatite have emerged as notably promising adsorbent amendments for in situ sediment remediation. However, comprehensive data on their potential side effects remain limited. Except for activated carbon (AC) and zero-valent iron (ZVI), information regarding (eco)toxicity is either scarce or not yet accessible.

The materials used today and the new materials that can be used in in-situ treatments will be discussed in more detail in Chapter 3.

### *2.1 REACTIVE CORE MAT*

All the amendments seen so far can be used as active materials in in-situ capping. This technology is perfect for increasing the low absorption capacity of classical sand caps and reducing the cap thickness. Reactive materials can be encapsulated in two permeable geotextile layers and then laid down on the contaminated sediments.

Reactive Core Mat (RCM) is a patented permeable composite mat invented by CETCO (Meric et al., 2011). This technology can therefore be for all intents and purposes identified as a new class of sediment remediation technique, consisting of a reactive layer containing one or more neutralizing or otherwise reactive materials (e.g., organoclay) that are confined between two permeable geotextile layers (Meric et al., 2013). Geotextiles are fabric materials made from synthetic fibers that resist biodegradation, creating flexible and permeable fabrics. Geotextiles primarily serve four key functions: drainage, separation, reinforcement, and filtration. Thanks to these functions, the use of geotextiles can efficiently prevent the buoyancy of low-density materials enclosed within two layers of geotextile. Reactive mats have been fabricated by CETCO using two methods: (i) needle-punching which has been used since the late 1980s to manufacture geosynthetic clay liners; in this manner is possible to obtain a thickness of 6 mm. (ii) laminating method that has two main benefits: a higher mass per unit area than needle-punching and the possibility to use abrasive reactive materials that cannot be needle-punched. On the other hand, the laminated mat is thick 11 mm (Olsta & Darlington, 2006).

Mats have a lot of advantages. Indeed, for the same amendment and amount used, the amendment enclosed within the mat is more effective than the amendment mixed with the contaminated sediment. Since reactive materials are more expensive than inert materials in economic terms, it is very advantageous to be able to use only a thin layer of them or mix two different amendments with different characteristics that are confined between two permeable geotextile layers. The placement of these mats needs to be

accurate because of amendments with high total organic content and low density that could otherwise become suspended during placement. It is also important to remove rock and debris from the sediment surface before the mat is installed to minimize potential damage to the mat and provide a more even surface for placement (Labianca et al., 2022). The presence of synthetic geotextiles on the outside of the mat also provides a bioturbation barrier, prevents the mixing of amendments with underlying sediments, allows a more uniform application of amendments, and reduces erosion.

After the deposition of the mat on the surface of the sediment, these mats are generally covered with conventional capping materials and, if needed, armouring layers to provide physical stability and further isolation. A layer of 10-15 cm of sand or soil is placed on top of the mat and it acts as an armour layer to protect the underlying thin sorbent layer from erosion forces and provides a habitat for benthic organisms to colonize and lengthen contaminant breakthrough paths. The addition of sand or soil is also useful to prevent contaminant migration through the seams in case of damage. Finally, the amendments and components of the mat could not sink readily, so it is necessary to use geotextiles with a higher specific gravity or mix a fraction of sand with the amendment to create a mat that is easier to sink.

Amendment mats of this kind are accessible on the market through a few select companies. Nonetheless, this strategy has been implemented in various EPA Superfund site projects, featuring standard thicknesses of 6 and 11 mm.

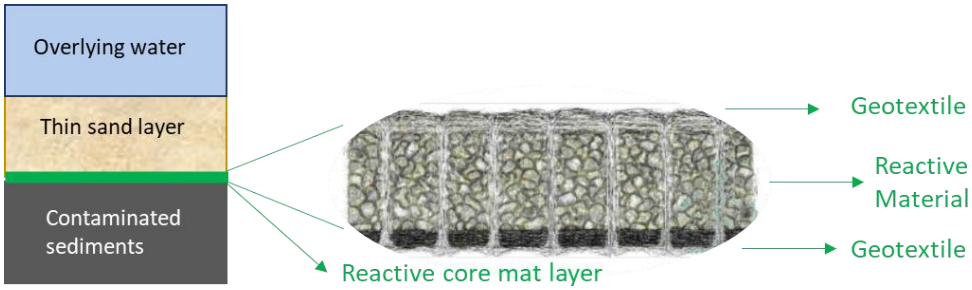


Fig. 2.1 - Scheme of a set-up of capping and an overview of the inner layer of a Reactive core mat.

# 3. REACTIVE NANOMATERIALS FOR ENVIRONMENTAL REMEDIATION

In the last years, researchers evaluated several sorbent materials as in situ amendments. The most used nowadays are Activated Carbon (AC), organoclay, apatite, biochar, coke, zeolites and zerovalent iron (ZVI) (Zhang et al., 2016b). These amendments change the sediment geochemistry increasing contaminant binding and stability to reduce its risk to human health and the environment.

The interest of researchers is now shifting towards other materials, especially nanomaterials, but above all materials that can be produced from secondary raw materials, to reduce the environmental impact of the production process.

Nanomaterials are materials with sizes at the nano-scale (1–100 nm) in at least one and include nano-objects and nanoparticles (Hristozov & Malsch, 2009; Stone et al., 2010).

They are very appreciated because they are considered excellent remarkable absorbents and catalysts thanks to their much larger specific surface areas, more associated sorption sites, lower temperature modification, shorter interparticle diffusion distance, more tunable pore size, and different surface chemistry than other materials (Tang et al., 2014b).

Although nanomaterials are a promising resource for the remediation of heavy metal(loid) polluted sediments, few studies have been published on immobilizing/adsorbing heavy metal(loid)s by utilizing nanomaterials for sediment remediation.

Thanks to their size nanomaterials have been shown to possess distinctive chemical, catalytic, electronic, magnetic, mechanical, and optical properties. This variety of properties makes them useful in a variety of domestic and industrial applications, ranging from enhanced drug delivery to new methods for the treatment of contaminated water for this reason, they are among the most studied materials of the last 15 years. (Crane & Scott, 2012)

In recent years, few studies have been conducted in the field of sediment remediation with nanomaterials. Nanomaterials have higher reactivity and sorption abilities to remediate sediments contaminated than the same materials at normal sizes, which were used for soil/solid waste remediation originally (Peng et al., 2018b).

The more material dimension decreases, the more the atoms lying on the external surface increase. In this way, they increase their interaction with other atoms, molecules, and complexes to achieve charge stabilization. Additionally, their minuscule size allows nanoparticles to be incorporated within aqueous suspensions and behave as a colloid. (Crane & Scott, 2012)

One of the main advantages of the use of nanomaterials is that they can be synthesized starting from a wide variety of raw materials by applying biological, physical, or chemical methods. Two different chemical synthetic approaches can be identified depending on the size of the raw material: (i) the Top-down approach starts from bulk material to create correspondingly smaller structures using finer tools; and (ii) the Bottom-up approach assembles materials from the nanoscopic scale, such as molecules and atoms to form larger structures (Biswas et al., 2012). Both approaches are sustainable because they minimize the addition of chemicals and reduce the amount of material needed in the clean-up process. The latter approach in particular allows a faster degradation and stabilization of contaminants, reducing the time frame and even the costs of the process. Hence, the use of nanomaterials for environmental remediation is more effective if compared to conventional remediation approaches since nanometric materials show a high surface-area-to-volume ratio, high reactivity, and a target-specific ability to capture toxic compounds(Guerra et al., 2018). In this way, extending the range of available in situ remediation technologies can be possible.

The main characteristics required for particles of in-situ remediations of polluted water are: (i) high reactivity for contaminant removal; (ii) enough

mobility to the presence of porous media; (iii) sufficient reactive longevity; and (iv) low toxicity.

All the studies conducted on nanomaterials demonstrate that they are effective in stabilizing/adsorbing heavy metal(loid)s, thereby decreasing the mobility and bioavailability of metal(loid) ions. Unfortunately, heavy metals cannot be degraded into non-toxic substances in sediments, but they can be immobilized/passivized by adding different amendments to the sediments.

In today's scientific literature, the most interesting and most effective materials are nano zero-valent iron, nanoapatite, carbon nanotubes, electrospun nanofibers and cellulose nanostructured sponges.

### *3.1 Nano Zero-valent iron*

Nano Zero-valent iron (nZVI) nanomaterials have a core-shell structure that consists of a metallic iron core and the shell is made by a layer of iron oxide, which is naturally generated during the nZVI synthesis. (Crane & Scott, 2012) These characteristics make it a good material for treating heavy metal and chlorinated organic solvent contaminants lying in groundwater and soil. (Zhang, 2003)

The strengths of the structural properties of nZVI are the size and the surface area that can be modulated by the synthesis conditions. The particles of nZVI usually have a spherical dimension with a range from 10 to 100 nm; the smaller the particle size, the higher the surface area to volume ratio will be, resulting in higher surface reactivity (Yirsaw et al., 2016).

The principal mechanism by which nZVI removes contaminants (especially metalloids) from water and soils is the chemical reduction that requires contaminants to be adsorbed nearby (electronic range) to the iron surface. Removal generally occurs via the reductive degradation of the chemical, i.e. the contaminant is physically destroyed for the treatment of organic contaminants, such as chlorinated organics and polychlorinated biphenyls. (Crane & Scott, 2012)

In short, for in situ remediation heavy metals contaminants are trapped (thanks to the limited mobility of bare nZVI (Yirsaw et al., 2016)) without

being neither destroyed nor extracted from the system. (Crane & Scott, 2012) As demonstrated by (Fajardo et al., 2012), using a dose of nanoparticles equal to 34 mg/g soil increased its capacity to immobilize lead by 25%; a similarly significant reduction is observed in the extractable Zn fraction (20%) after the soil treatment with iron nanoparticles. The use of NZVI particles has resulted in a powerful tool to efficiently immobilize the heavy metals assayed, Pb and Zn.

nZVI can be modified with a variety of elements. (Zhu et al., 2016) synthesized nZVI/Cu materials that result uniforms, with an average particle size of 20–50 nm. The study indicated that nZVI/Cu works fine to remove chromium and other contaminants in polluted soils.

(Chen et al., 2016) evaluated nano-zero-valent iron/activated carbon (nZVI/AC) composite for its effectiveness in the stabilization of Cu, Pb, Cd, and Cr in dredged river sediment. These heavy metals were successfully stabilized by the addition of nZVI/AC. Increasing the dosage of nZVI/AC there was a general improvement in stabilization especially for Cu, Pb, and Cd.

(Su et al., 2016), (Dong et al., 2017) and (Qian et al., 2022) have studied the effectiveness of a biochar-supported nanoscale zero-valent iron (nZVI@BC) material. (Su et al., 2016) have compared the stability and mobility of nZVI@BC and bare-nZVI through sedimentation tests and column experiments. Experiments indicate that nZVI@BC had better stability and mobility than bare-nZVI. This study indicated that nZVI@BC might be used for the in-situ remediation of Cr(VI)- contaminated soil.

(Dong et al., 2017) investigated the feasibility of nZVI supported by the various modified biochars (HCl-BC, KOH-BC, and $H_2O_2$-BC) for the Cr(VI) removal. The treatment of biochars with HCl gave a good response in terms of the capacity of removal of Cr(VI) thanks to the larger surface area and lower surface negative charge of HCl-BC. Another important role is played by the mass ratio of nZVI to HCl-BC in the particle dispersion and in the Cr(VI) removal; the mass ratio of nZVI/HCl-BC at 1:1 appeared to give the best

performance. Considering the biochar as ready-to-use and cost-efficient even if modified, nZVI@HCl-BC use can be successful in environmental remediation to remove Cr(VI) from water. Furthermore, the insoluble reaction products of Cr(III) hydroxides or Cr(III)/Fe(III) hydroxides cover the surface of HCl-BC, making easier and more direct the chromium and nZVI removal from water and eliminating potential secondary pollution issues caused by the reaction products.

(Qian et al., 2022) compare the immobilization performance of BC, nZVI, and BC-nZVI behaviour with Cd and Pb. They found that 86.49% of Cd was adsorbed by BC-nZVI and it was better than the other two adsorbent materials. Pb has the same behavior as Cd, the immobilization rate is 80.14% using BC-nZVI.

Another material used to modify the properties of nZVI is Sulphur. Sulfide-modified nanoscale zerovalent iron (S-nZVI) is a very interesting material because it's easy to produce and has high reactivity with organic pollutants (Su et al., 2015). On the other hand, the structure of this type of material is still poorly understood and its potential application in heavy metal remediation has not been explored, but batch tests demonstrate its cadmium (Cd) removal performance under different aqueous conditions and S-nZVI had an optimal Cd removal capacity.

The use of sodium alginate (SA)-modified nanoscale zero-valent iron (nZVI) showed in studies conducted by (Huang et al., 2016) that play a constructive role in the remediation of cadmium (Cd) contaminated river sediments or rather that the addition of SAnZVI immobilize Cd in polluted sediments by reducing his bioavailability.

In light of all these studies conducted, it is possible to state that although nZVI is already widely commercialized, the experimental data available to us are mostly derived from laboratory research activities. This is also related to the scepticism that induces nanomaterials as a means of remediation in the environmental field.

It is still ongoing the evaluation of toxicity of the Fe-containing nanomaterials remains an object of permanent research and polemics. (Kharisov et al., 2012)

In the last years, nano zero-valent iron (nZVI) has shown good effectiveness for environmental remediation for a wide variety of organic and inorganic contaminants present in soils. (Calderon & Fullana, 2015)

This material is investigated as a new technology that can be used as a granular form for in situ remediation. The goal is improving the remediation efficiency thanks to the use of nZVI, seen as a promising option for the treatment of source zones (Taghavy et al., 2010).

Recently, this technology has achieved commercial status in many countries around the world, but not yet universally accepted, as the data collected brings up discrepancies given by the testing parameters chosen. (Crane & Scott, 2012).

In addition, a concern also emerges for what the consequences of using this nanomaterial might be. The effects that the use of those materials can have on the environment are still unknown.

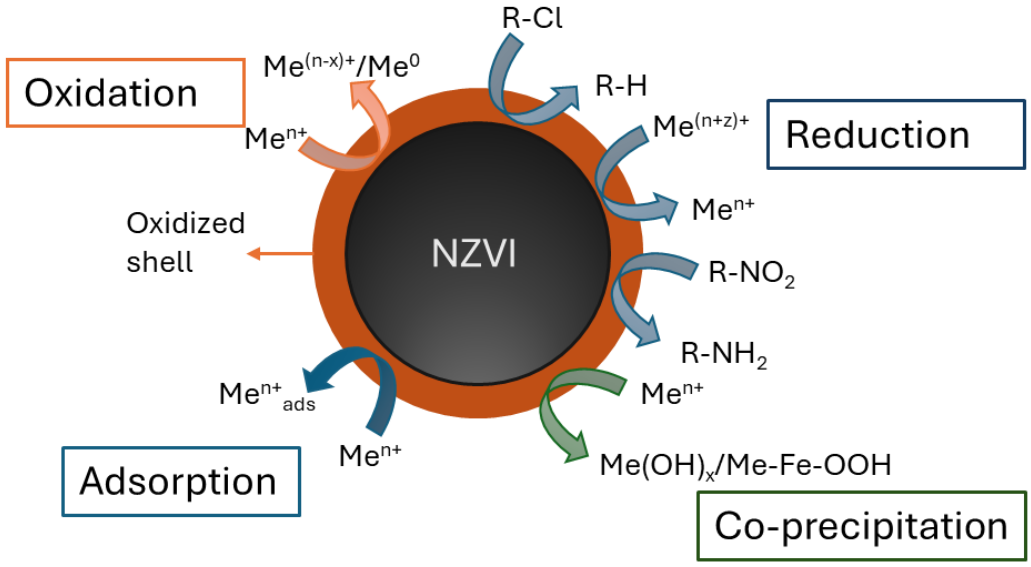


Fig. 3.1 – Reaction of nano zero-valent iron with metalloid.

### *3.2 Nano apatite*

The biggest advantages of mineral apatite are that it is cheap and effective for the remediation of contaminated sites due to its ready availability. At the same time, however, it has limitations in its ability to immobilize $Pb^{2+}$, and its low efficacy in immobilizing $Cd^{2+}$, $Co^{2+}$, $Cu^{2+}$, $Mn^{2+}$, $Ni^{2+}$, and $Zn^{2+}$ must be considered. (Qian et al., 2009)

In recent times, nanohydroxyapatite (nHAp) has been widely applied for the remediation of contaminated soil and purification of wastewater polluted with heavy metals for its strong ability to fix these contaminants. (Silva et al., 2017)

The advantages of using nanohydroxyapatite lie in the size of the particles that were under 200nm and in the fact the surface area to volume ratio is high. (Liu & Zhao, 2013)

The potential of the hydroxyapatite nanoparticles to remove copper ions from aqueous solutions was studied under different experimental conditions. Maximum adsorption capacity 70.92 mg/g of copper ions on hydroxyapatite nanoparticles. (Joshi & Manocha, 2017a)

To improve the efficiency of the nHAp many researchers try to add some additives.

To a poor crystalline chlorapatite (Liu & Zhao, 2013) added calcium phosphate nanoparticles obtaining ($Ca_5(PO_4)_3Cl$), a perfect material for in situ immobilization of Pb(II) in contaminated soil. This type of material has also potential applications for the remediation of other hazardous heavy metals and radioactive nuclides such as Cu, Cd, Zn, and U.

Another interesting addition is Lactonic Solphorolipid (LS) to the system nano-chloroapatite. (Deng & Zhan, 2023) compared LS, nClAP, and LS-nClAP and found that due to the presence of hydroxyl and carboxyl groups, the LS-nClAP system performs best in Cd adsorption (93.25%).

Even (Ylng Ma et al., 1993) have synthesized nanocrystalline calcium hydroxyapatite (Hydroxyapatite [$Ca_{10}(P0_4)_6(OH)_2$). Their experiments

showed that Pb was immobilized by the dissolution of hydroxyapatite and precipitation of hydroxypyromorphite [$Pb_{10}(P0_4)_6(OH)_2$].

(Mohammad et al., 2017) have developed and tested hydroxyapatite nanorods (nHAp) and hydroxyapatite/chitosan nanocomposite (nHApCs) as potential sorbents for the removal of lead ions from aqueous lead-containing solutions in a batch adsorption experiment. This study found the effectiveness of nHAp and nHApCs sorbents for the removal of $Pb^{2+}$ ions from aqueous lead-containing solutions for use in wastewater treatments.

(Feng et al., 2010) have studied Magnetic hydroxyapatite nanoparticles (MNHAP) adsorbents used for the removal of $Cd^{2+}$ and $Zn^{2+}$ from aqueous solutions. The results revealed that the most prominent advantage of the prepared MNHAP adsorbents consisted of their separation convenience compared to the other adsorbents.

Another class of materials studied is Magnetic chlorapatite nanoparticles (MNCLAP) by (Keochaiyom et al., 2017) that were used as adsorbents to remove $Zn^{2+}$, $Cd^{2+}$ and $Pb^{2+}$ from aqueous solutions. Experimental results revealed that the prepared MNCLAP combined both the properties of chlorapatite and magnetic material and it showed remarkable advantages in heavy metal removal from aqueous solutions. For the first time, the combination of both properties of chlorapatite and magnetic material showed remarkable advantages in heavy metal removal from aqueous solutions.

(Wan et al., 2018) successfully synthesized Rhamnolipid stabilized nClAP for Pb and Cd immobilization in polluted sediment. Rha-nClAP was shown to be more effective than ClAP in precipitation or adsorption processes. This phenomenon could be related to the surface charge of the amendments a higher zeta potential could enhance metal mobilization through electrostatic stabilization. The conclusion that can be reached is that Rha acted as an eluent for metal release from the sediment while ClAP played as a metal precipitation agent, thus greatly improving the metal stabilization efficiency.

Another alternative to immobilize Pb in contaminated sediment is biochar-supported nano-chlorapatite (BC-nClAP) (Huang et al., 2018b). It was found that BC-nClAP can transform Pb effectively from a labile fraction into a stable fraction with a maximum transformation efficiency increasing to 94.1% after 30 days of treatment, and the stabilization efficiency of the toxicity characteristic leaching procedure reached 100% only after 16 days of treatment.

Biochar-supported nano-hydroxyapatite (nHA@BC) material was used in the in-situ remediation of lead-contaminated soil (Yang et al., 2016a) and this material showed a very good performance in mobility rather than immobilization rate of Pb in the soil.

Another interesting material is the addition of BC to the nano-hydroxyapatite. (Ahmed et al., 2022) point out that the addition of BC to nano-hydroxyapatite adds -OH and -COOH groups on the BC surface which is already a good adsorbent for Pb. Thanks to the ion exchange mechanism there is the surface complexation with Pb2+ and -OH and -COOH groups. The adsorption capacity of this material is very high and equal to 191.76 mg/g.

(Wan et al., 2016) studied synthesized nano-chlorapatite by using sodium dodecyl sulfate (SDS) as a stabilizer (SDS-nClAP). Experimental data suggested that SDS-nClAP was effective in transforming labile Pb to a stable fraction. The increase of available phosphorus in both SDS-nClAP and ClAP-treated sediment samples verified the dissolution-precipitation mechanism involved in Pb immobilization.

Even simple nanohydroxyapatite turns out to be effective for most metals commonly found within sediments. The comparison all studies showed that it achieves efficiency in immobilizing Pb up to 100% (Huang et al., 2018c, 2018a; Yang et al., 2016b); other metals on which it is particularly effective, with up to 90%, are Zn and Cu; even with Ni it has high efficiency, around 70/80% (Mobasherpour et al., 2011); on the other hand, for Cd, Fe, and Mn, the percentages are below 50% (Feng et al., 2010; He et al., 2013; Joshi &

Manocha, 2017b; Keochaiyom et al., 2017; Mobasherpour et al., 2012; Qian et al., 2009; Shin & Kim, 2016; Silva et al., 2017; Wan et al., 2018; Zhang et al., 2010).

In all the studies conducted, on different matrices (water, soil, and sediments) the tests stopped at the laboratory scale or at most at benchtop reactors.

From the point of view of environmental sustainability, this class of materials, unfortunately, has two serious flaws nano-hydroxyapatite cannot be reused multiple times, nor can it be synthesized using non-virgin materials (waste or recovered materials).

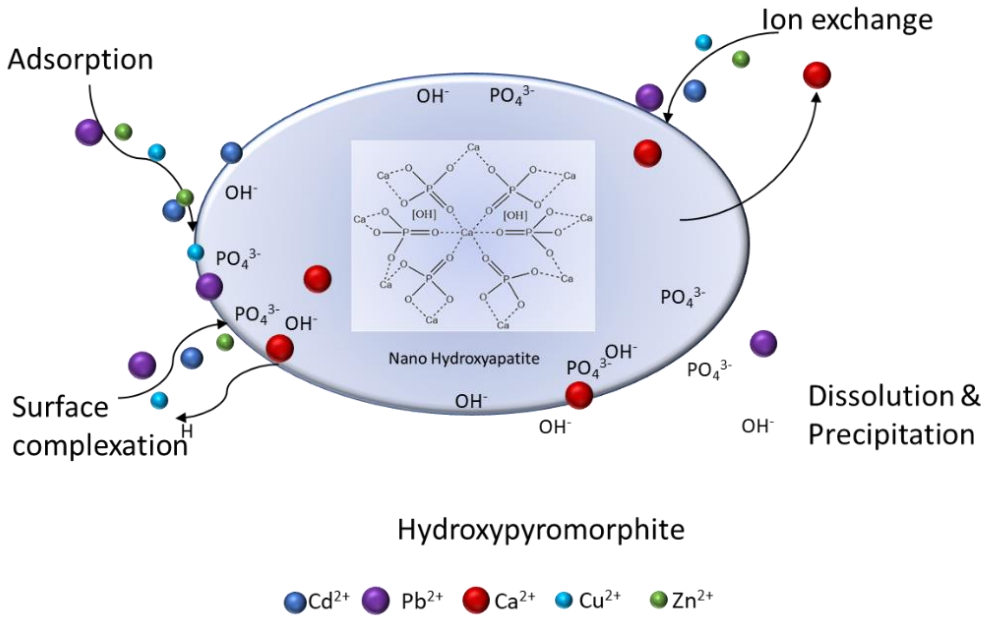


Fig. 3.2 - Structure of nano hydroxyapatite and reactions with metalloid.

### *3.3 Carbon nanotubes*

The carbon nanotubes (CNTs) are a member of the fullerene structural family and they are considered good adsorbent materials, especially for the removal of heavy metals (lead, chromium, cadmium, arsenic, copper, zinc, and nickel) from water, soil, and sediments. Their

efficacy is due to the physical adsorption, electrostatic interaction, surface complexation, and chemical interaction between the surface functional groups and the metal ions (Ihsanullah et al., 2016). All these mechanisms take place thanks to the typical structural properties of nanomaterials such as large surface area and restrained aggregation property (Liang et al., 2015).

Another winning strategy that enhances the already good properties of this material is the addition of other materials such as alumina or the variation of the structure making them multi-walled or biochar-like.

Multi-wall carbon nanotubes were applied for Pb(II) and Ni(II) ion removal from paint, battery and electroplating wastewater (Egbosiuba et al., 2021). They studied the behavior of different nanosized materials from 5 to 15 nm and from 16 to 25 nm. They demonstrated excellent adsorption of Pb(II) and Ni(II) ions, particularly, MWCNTs5-15 nm possessed a high adsorption capacity of 215.38 ± 0.03 mg/g for Pb(II) and 230.78 ± 0.01 mg/g for Ni(II). Again, the maximum adsorption capacity of 201.35 ± 0.02 and 206.40 ± 0.02 mg/g was achieved for Pb(II) and Ni(II) using MWCNTs16-25 nm.

A magnetic multi-wall carbon nanotube (MMWCNT) nanocomposite was synthesized and used as an adsorbent for the removal of cationic dyes from aqueous solutions by (Gong et al., 2009). The MMWCNT nanocomposite was composed of commercial multi-wall carbon nanotubes and iron oxide nanoparticles. Adsorption characteristics of the MMWCNT nanocomposite adsorbent were examined using methylene blue, neutral red, and brilliant cresyl blue as adsorbates.

(Song et al., 2017) have studied the adsorbent behaviour of multi-walled carbon nanotubes (MWCNTs) in in-situ remediation for sediments contaminated by cadmium and phenanthrene. Adsorption experiments indicated that MWCNTs showed a much better adsorption performance towards phenanthrene and Cd(II) compared with the sediments. The in situ remediation with MWCNTs could distinctly decrease the aqueous concentrations of phenanthrene and Cd(II) released from the sediments,

reducing environmental risk towards overlying water. Also (Mubarak et al., 2016) studied multi-walled carbon nanotubes (MCNTs) and tested them for the removal of Zn(II) from wastewater. The ideal conditions have been set up to reach 99.9 % of Zn(II) efficiency through these tests. Hence, MCNTs serve an important role in the removal of heavy metals from wastewater.

(Que et al., 2019)'s study showed that the addition of rice husk biochar (RHB) and activated carbon (AC) to CNTs was successful for the immobilization of heavy metal Cu. Heavy-metal contaminated sediments were immobilized by RHB and AC with an additional amount of 2%, 5%, and 10% (w/w). From the experimental data emerges that AC was more effective than RHB on Cu immobilization in the sediment, due to the strong specific surface area and pore structure of AC. Meanwhile, AC is more expensive (~$3.70/kg) and RHB (~$0.30/kg) are less costly. Compared to the effect of AC and RHB on the Cu immobilization and microbial community, the RHB would be a low-cost and environmentally friendly material for heavy-metal contaminated site remediation.

Another change made to CNTs is the addition of alumina onto the surface of multi-wall carbon nanotubes (MWCNTs), studied for simultaneous removal of cadmium ion (Cd(II) ion) and trichloroethylene (TCE) (Liang et al., 2015). The main mechanism of absorption of Al2O3/MWCNTs involving Cd(II) ion and TCE is the electrostatic interaction. There are, however, interactions between hydrogen bonds and protonation or hydroxylation of $Al_2O_3$. The maximum adsorption capacities of $Al_2O_3$/MWCNTs for TCE and Cd(II) ion were 19.84 mg/g and 27.21 mg/g, respectively, which were higher than that of $Al_2O_3$, MWCNTs, and the functionalized MWCNTs. The results suggested that the Al2O3/MWCNTs could be considered as an effective and promising adsorbent for the simultaneous removal of Cd(II) ion and TCE from groundwater.

On the other hand, unmodified carbon nanotubes were found to be effective for the adsorption of pollutants such as heavy metals and organic dyes. Analysing these data in detail shows that Cd is the most studied pollutant

with a maximum adsorption capacity of 27.21 mg/g (Li et al., 2003; Liang et al., 2015; Song et al., 2017; Sun et al., 2015); another fairly studied contaminant is Cu with a maximum adsorption capacity of 24.49 mg/g (Que et al., 2019); Pb and Zn are relatively poorly studied with an adsorption capacity of 97.08 mg/g and 1665 mg/g, respectively ((Li et al., 2003; Mubarak et al., 2016); Other types of contaminates towards which it is effective are Cr, As, Hg, Ni, (Ihsanullah et al., 2016), Cationic dyes (es Methylene blue, neutral red and brilliant cresyl blue) (Gong et al., 2009), Dichlorodiphenyltrichlohethane and Hexachlorocyclohexane (Zhang et al., 2017).

(Chen et al., 2021) added to MWCNTs an Ionic Liquid (IL) to implement the adsorption capacity. The loading way of IL into MWCNTs by ultrasonic-assisted impregnation has been studied from the perspective of the initial concentration of $[C_4Bth][PF_6]$, the carbon nanotube size, and loading time. The load capacity reached 40 mg/g using MWCNTs with a diameter of 10 e 20 nm after 12 h. The adsorption capacity for organic molecules such as tetracyclines (TCs) is about 99.35 % in only 3 hours. IL-MWCNTs have good adsorption capacity for metal ions, especially for $Cr^{6+}$ and $Cu^{2+}$, which are about 96% and 98% respectively.

One of the main obstacles to the use of CNTs is the high cost, even though in laboratory tests they have shown a higher adsorption capacity than many traditional adsorbents. (Ihsanullah et al., 2016).

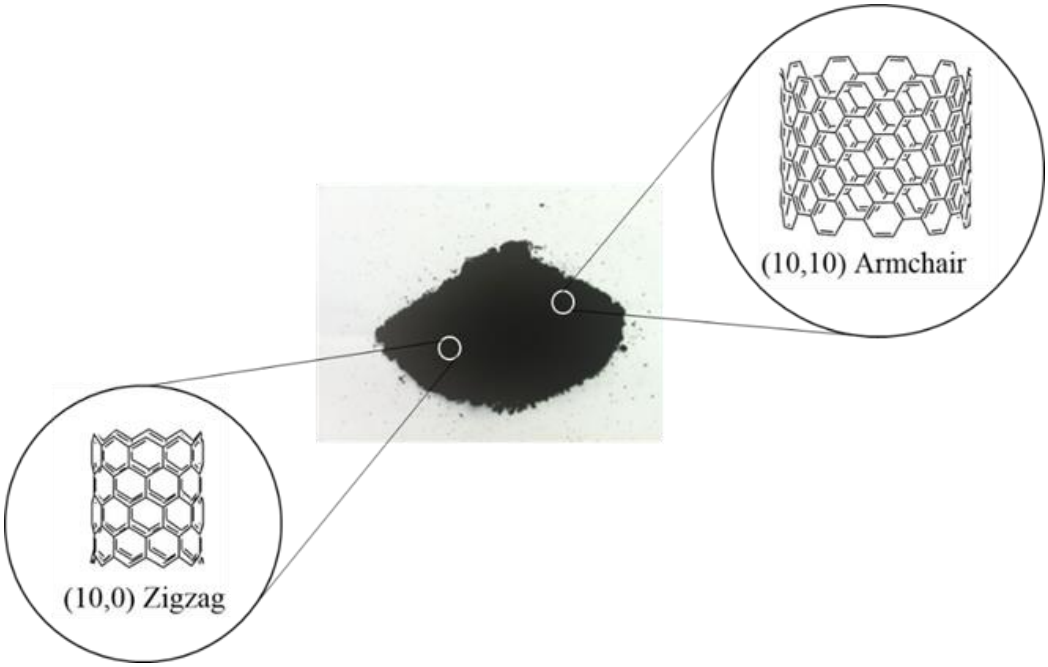


Fig. 3.3 - Structure of carbon nanotubes.

### *3.4 Electrospun nanofibers*

Electrospinning is a very versatile technology. The major applications of this technology are: tissue engineering, biosensors, filtration, wound dressings, drug delivery, and enzyme immobilization. Fibers of a nanoscale size are created through the application of an electric field between the needle of the syringe containing the polymeric solution and the collector. The distance between the fibers that compose those mats is below 1 μm. This offers many advantages like the high surface area to volume ratio, tunable porosity, and the ability to manipulate nanofiber composition to get desired properties and function (Bhardwaj & Kundu, 2010).

A review of the literature on these mats used in the field of environmental remediation revealed mainly ten types of mats.

The first type of nanofibers studied are water-stable PVA/PAA nanofibers evaluated for their performance in lead (Pb(II)) and Cadmium

(Cd(II)) removal from water in a batch experiment. Although the absorption of Pb(II) and Cd(II) occurs spontaneously, the PVA/PAA nanofibers showed a pH-dependent behaviour for heavy metal removal, and its adsorption capacities for Pb(II) and Cd(II) could reach as high as 159 and 102 mg/g, respectively. Analysis suggested that a Pb(II) cation was chelated with three carboxyl groups on the nanofibers (Zhang et al., 2019).

Another possibility is to immobilize zerovalent iron nanoparticles (ZVI NPs) into electrospun polymer nanofibrous mats. The produced ZVI NP-containing polymer nanofibrous mats exhibit a superior capability to decolourize acid fuchsine solution, a model dye in wastewater of the printing and dyeing industry, and the decolouration percentage approaches 95.8% within 40 min. (Xiao et al., 2009)

Also titanium dioxide can be immobilized on PVA/PAA nanofibers, but the problem with titanium dioxide is that it needs UV or visible light for photocatalysis to take place. (Deb et al., 2018)

(Yin et al., 2020) prepared a novel polyvinyl alcohol (PVA)/polyacrylic acid (PAA)/MXene fiber membrane by electrospinning. PVA/PAA/ MXene@PdNPs composite nanofiber membranes have been subjected to heat treatment and subsequent modification with Pd nanoparticles. The composite nanofiber membrane exhibits high specific surface area, excellent catalytic performance, and cycle stability for 4-nitrophenol (4-NP) and 2-nitrophenol (2-NA), providing a new strategy for the study of catalytic composite materials related to the degradation of wastewater.

Another simple and novel magnetic α-Fe2O3 nanofibers were synthesized by electrospinning a solution of polyvinyl alcohol (PVA) and $Fe(NO_3)_3$* $9H_2O$ composite nanofibers. Under the optimum conditions, these nanostructures were used for the effective degradation and decolourization of methyl orange (MO) in an aqueous solution, with a decolourization efficiency >99% in a short period of 10 min. The developed process was successfully applied for the degradation and decolourization of MO using

magnetic a-$Fe_2O_3$ nanofibers as a catalyst in wastewater samples. (Ghasemi et al., 2015)

(Xu et al., 2012) synthesized a vinyl-modified mesoporous poly(acrylic acid)/$SiO_2$ (PAA/$SiO_2$) composite nanofiber membranes by sol–gel/electrospinning process. This type of electrospun membrane exhibited a high adsorption capacity of malachite green with an adsorption capacity of 220.49 mg/g.

(Teng et al., 2011) synthesized a mesoporous polyvinyl alcohol (PVA)/$SiO_2$ composite nanofiber membrane functionalized with cyclodextrin groups by sol‑gel/electrospinning process. This type of nanofibers demonstrated an adsorption capacity for the indigo carmine dye of 495 mg/g due to the presence of cyclodextrin groups.

Another additive for electrospun polyvinyl alcohol (PVA) nanofibers is nanozeolite nanocomposite (NaX) which forms a novel adsorbent electrospun polyvinyl alcohol (PVA)/NaX nanozeolite nanocomposite nanofibers. The adsorption tests showed that the affinity of PVA/zeolite nanofibrous adsorbent for $Cd^{2+}$ ions sorption was higher than that of $Ni^{2+}$ ions sorption with an adsorption capacity of 838.7 mg/ and 342.8 mg/g, respectively. (Rad et al., 2014)

By using chitosan solution with Pb(II) as a template and glutaraldehyde as a crosslinker it is possible to obtain lead-ion imprinted crosslinked electro-spun chitosan nanofiber mats. The Pb(II) ion adsorption capacity of the as-prepared chitosan nanofiber adsorbents can reach 577 mg/g at the optimum pH = 6. These types of nanofibers can be regenerated under EDTA and still have an equilibrium adsorption capacity of 359 mg/g for the second Pb(II) ion adsorption. In addition, the as-prepared chitosan nanofiber adsorbents also show a good adsorption capacity for other heavy metal ions such as Cu(II), Cd(II), and Ni(II) ions. These results indicate that the chitosan nanofiber mats prepared through a combined technique of ion-imprinting and electrospinning are promising adsorbents to remove the heavy metal ions from water. (Li et al., 2013)

A novel Pb(II) ion-imprinted chelating nanofibers (nIIP), synthesized by combining electrospinning with surface ion imprinting technique, was synthesized and studied by (Tong et al., 2015). These nanofibers have an adsorbent capacity that is higher if they coexist with Pb(II) in the presence of competitive ions in an aqueous solution, and it is the potential to be applied for recovering metals from heavy metal polluted industrial wastewater such as Pb(II)/Cd(II), Pb(II)/Ni(II), and Pb(II)/Cu(II) polluted wastewater. Besides, a forty adsorption/desorption cycles revealed that nIIP was a promising recyclable adsorbent.

A novel design strategy for sorbent material is to make a nonporous core of $SiO_2$ nanofiber and a mesoporous shell (denoted as $nSiO_2@mSiO_2$ (‘‘n’’ means ‘‘nonporous’’ and ‘‘m’’ means ‘‘mesoporous’’)). This type of fiber showed both high sorption capacity and separability. With a large specific surface area and long fibrous morphology, the $nSiO_2@mSiO_2$ fiber and its thiol-functionalized counterpart exhibit impressive performance in the removal of $Pb^{2+}$ and $Cd^{2+}$ from water. (Ma et al., 2011).

(Lee et al., 2013) developed rhodamine-loaded nanofibrous membranes for the removal of heavy metal ions. All electrospun nanofibrous membranes exhibit good Ag (I) and Pb (II) ion uptake capabilities. The metal uptake of nanofibrous membranes increased with the initial metal ion concentrations and decreased with the filtering rate of the solutions.

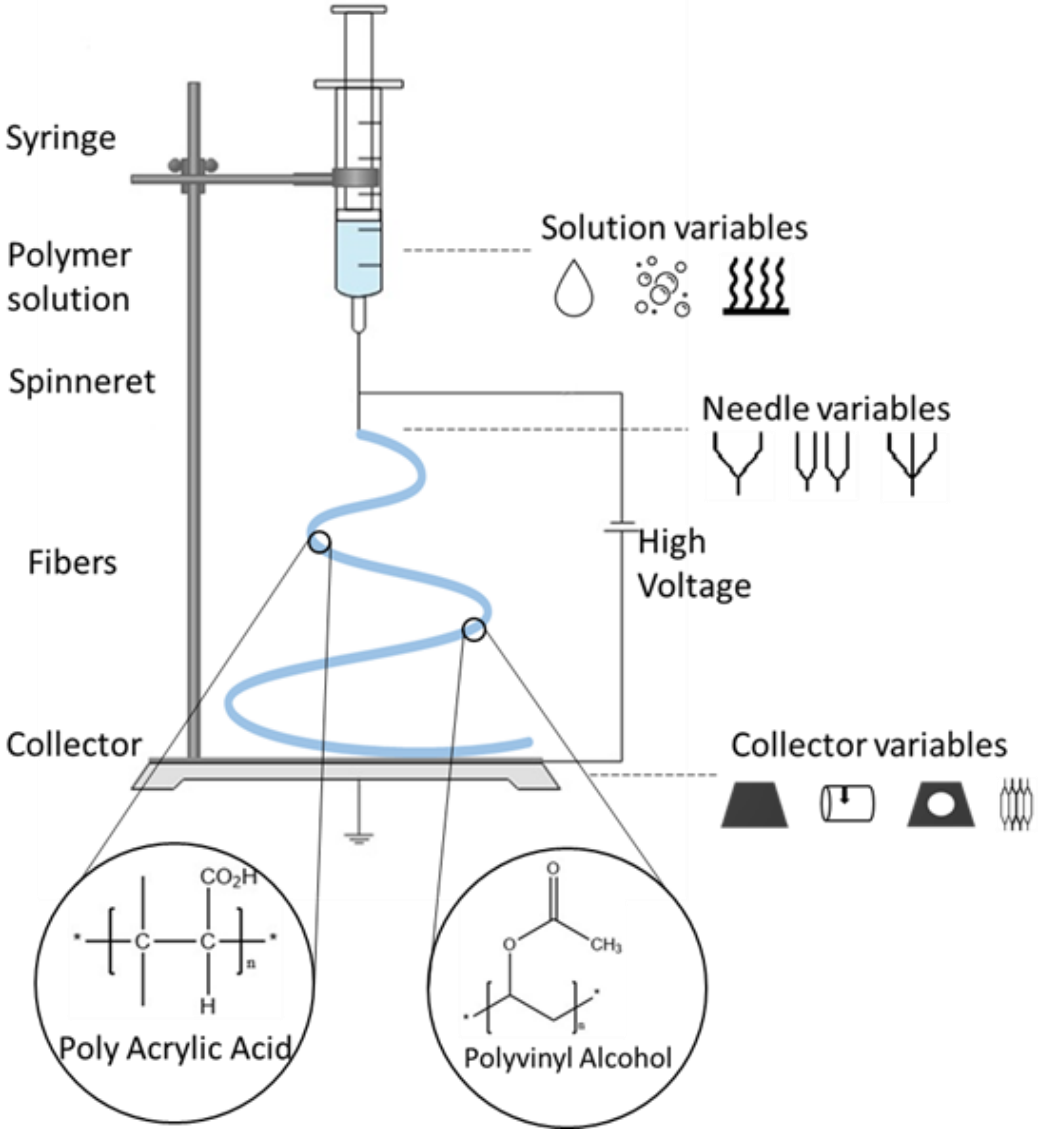


Fig. 3.4 – An example of how Electrospinning experimental apparatus works.

### *3.5 Cellulose-based nanomaterials*

The cellulose-based nanostructured sponge (CNS) is the latest and most innovative material that winks at the circular economy and the concept of sustainability is. The starting material is cellulose which can be obtained

from waste materials such as medical cotton, agricultural waste, etc.. Appropriate branching agents are added to the cellulose which gives it a nano-sized sponge-like structure. The synthesis process consists mainly of two steps and is economical. Although it is an extremely recent material, the effectiveness demonstrated in laboratory tests led to consider that is a very promising material for environmental remediation. Therefore, there are already the first studies for the development of a process suitable for production on an industrial scale. This material has a high specific surface area, a sponge-like structure, good mechanical stability in water, and shape-memory capability (Qiao et al., 2020; Melone et al., 2015a). The effectiveness of these materials in blocking and degrading contaminants, both heavy metals, and organics, is due to the presence of carboxyl groups on the outer surface. These groups are derived from the presence of the branching agents used, typically b-PEI and carboxylates.(Liu et al., 2017; Riva et al., 2021; Fiorati et al., 2017; Jin et al., 2017)

CNSs exhibit high performances in removing a wide range of heavy metal ions, i.e. Zn(II), Cd(II), Cr(III), Hg(II), Ni(II), and Cu(II) and it was tested in artificial seawater (Liberatori et al., 2020). (Melone et al., 2015a) also tested the adsorption capability of bPEI TOCNF sponges for different organic pollutants (p-nitrophenol, 2,4,5-trichlorophenol, and amoxicillin) and heavy metal ion pollutants (Cu, Co, Ni, Cd) for water decontamination.

Crosslinking reinforced flexible cellulose nanofiber-supported cryogel prepared by chemical crosslinking method using c-glycidoxypropyltrimethoxysilane (GPTMS) and branched polyethyleneimine (PEI), are effective for Cu(II) removal from aqueous solutions (Cheng et al., 2018).

Nanostructured cellulose sponges were tested in artificial seawater contaminated by $ZnCl_2$ and the cellular and tissue responses of marine mussel Mytilus galloprovincialis were measured before and after CNS treatment. The ecotoxicological evaluation confirmed the ability of CNS to remove Zn from ASW by showing a full recovery of Zn-induced toxicological

responses to the levels of mussels exposed to ASW only (controls). The proposed effect-based approach was thus proven to be useful in further supporting the environmental relevance of CNS' efficacy in heavy metal removal from seawater and their eco-safe application by linking ecotoxicological and chemical information (Liberatori et al., 2020)

(Tang et al., 2019) have developed a mussel-inspired coating strategy to introduce polydopamine onto the surface of CNFs, which were cross-linked with polyethyleneimine (PEI) to form the aerogels. This synthesis strategy is another step toward sustainability as the synthetic procedure was optimized to achieve a minimal consumption of raw materials to produce a robust porous structure while maintaining characteristic properties like low density, high porosity, and shape recovery in air and water. This class of materials has been shown to be effective for two representative contaminants, Cu(II) and Methyl orange (MO).

(Deng et al., 2016) have been synthesized and tested hyperbranched polyethyleneimine (HPEI) modified cellulose fiber (CellMW-HPEI) as an effective biosorbent for the removal of inorganic arsenic. On the modified fiber surface, the high density of amine groups probably enhanced the adsorption of arsenic ions due to electrostatic attraction and surface complexation in the binding process.

The common feature of these different synthesis methods with different branchers is the availability of carboxyl and amino groups on the surface of the final material. (Liu et al., 2017; Ge et al., 2016)

The two main advantages of this class of material are sustainability and reusability. It's sustainable because, as mentioned above, the raw material can be recovered from materials considered waste, such as medical cotton, agriculture waste, etc. The reusability has been tested by regeneration tests: after the first use, the material has been regenerated through an acid solution. Then it can be successfully reused several times (Riva et al., 2020).

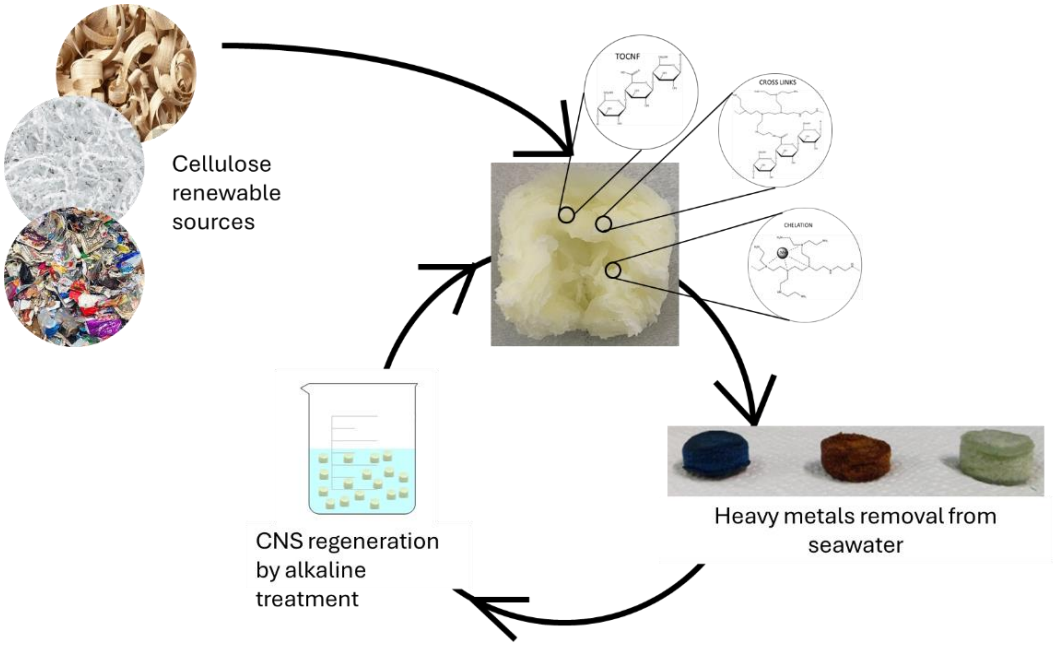


Fig. 3.5 - characteristic of TOCNF, TEMPO (2,2,6,6-tetramethylpiperidine 1-oxyl free radical)-oxidized cellulose nanofiber.

# 4. RESEARCH PURPOSE

The PhD thesis was elaborated thanks to a National Operative Program of Research and Innovation -innovative industrial research PhD- for the years from 2014 to 2020. The goal of this project is to connect university research with the real needs of the industry.

Contaminated sediments represent a huge problem for all port areas of the world. Contaminants are released in the overlayer water becoming available for benthic organisms and subsequently included in aquatic food chains. The development of new technologies for the remediation of contaminated marine sediments is therefore impellent. One of the most sustainable options in terms of efficacy, durability, and economy is represented by the in-situ capping technology, based on the physical covering of the contaminated site.

The aim of this PhD thesis is the individuation of innovative materials that can be applied as a "reactive" capping layer and, in particular, for the reactive core mat. From an experimental point of view, it was developed a synthetic protocol for the obtainment of a cellulose (Cls)-based material also adaptable to chitin as the starting biopolymer. Furthermore, it investigated the adsorption properties of these functionalized materials with organic molecules and heavy metals to ascertain their potential for environmental remediation.

These two scopes needed a detailed experimental laboratory plan schematized in the following points:

- Scrutinizing the best synthesis protocol in terms of reproducibility at laboratory scale to obtain a Cls-based material;
- Individuation of the best way to obtain a micro or nanostructured material comparing two different techniques (freeze-drying (Fr) and Soxhlet extractor (Sxl));
- Implementation of the synthesis protocol to chitin as the starting material;

- Scale-up of the synthetic protocol aiming at future industrial production of the material;
- Test the material in adsorption experiments with organic dyes and heavy metals as examples of common sediment pollutants;
- Implement an LCA study to investigate the environmental impact of all the previous experimental steps.

# 5. EXPERIMENTAL PLAN

## *5.1 Introduction*

To achieve the results described above, it was necessary to define an experimental plan in the Chemistry and Environmental technology laboratories.

The experimentation was divided into five phases:

In the first phase, a synthesis protocol was developed to produce Cls-based materials. During this phase protocol found in the literature was adapted to our laboratory's instruments and technologies. Thanks to preliminary tests, the best way to obtain the material is weighted.

In the second phase, the protocol developed was adapted to obtain Chn-based material.

In the third phase, it was planned a scale-up of the materials production of the materials.

In the fourth phase, the two materials were tested to study their behaviour with organic dyes and inorganic compounds.

Finally, in the fifth phase, all the results were analysed with LCA tool to study the environmental impacts of the materials production processes.

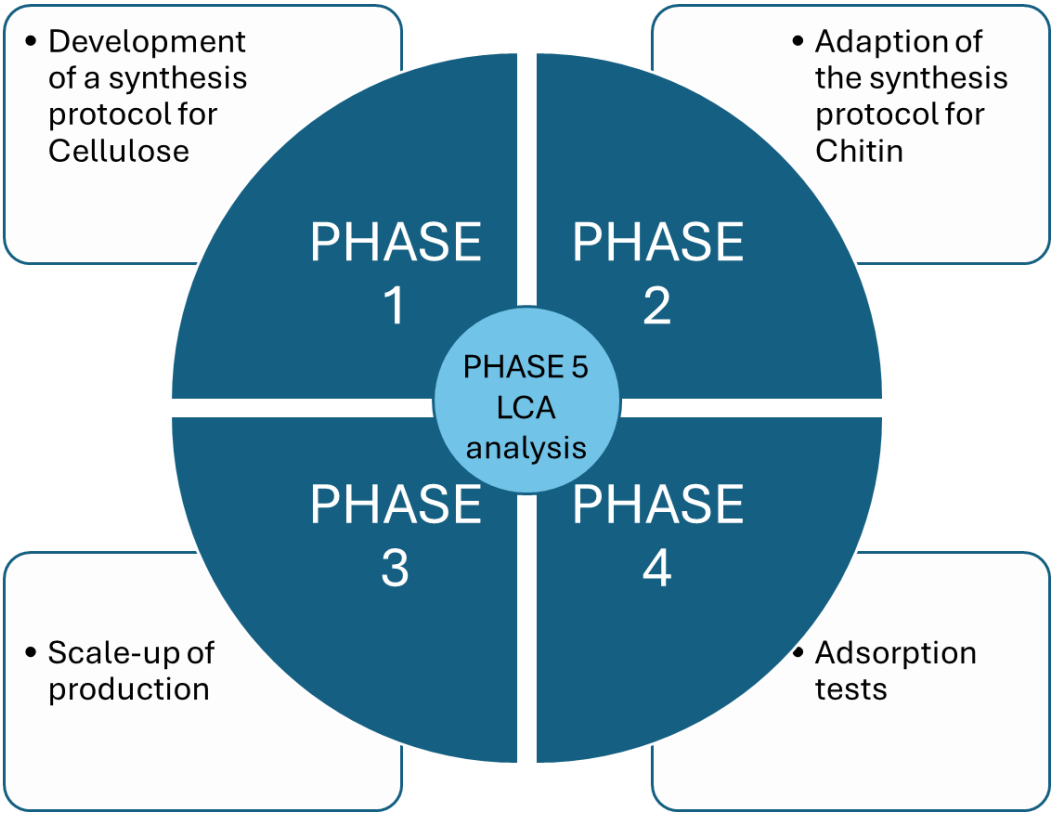


Fig. 5.1- Scheme of the experimental plan.

### *5.2 Synthesis protocol*

The first synthesis protocol reproduced in our laboratory was adapted from (Melone et al., 2015b).

The synthesis seemed to be easy and it was conducted at room temperature and atmospheric pressure. This protocol could be divided into 3 phases: first, the cellulose is oxidized in basic condition, after it is acidified to obtain the nanofiber and finally was added the brancher to obtain the final structure. All the passages were followed and adapted to our laboratory.

The way to obtain the aerogel was investigated. Different techniques (Fr and Sxl) and solvents used for Sxl (Ac, Me and Et) were compared. Thus the best way to obtain the material could be known (Fig. 5.2).

Once identified the best protocol to obtain the material, it was decided to change the starting material, the cellulose, with the chitin. Chitin is a polymer with a structure very similar to cellulose and it is the second most abundant polymer. The oxidative protocol of the chitin was investigated by other researchers, but without the same results of the cellulose in terms of yield. The objective was to find the best condition to obtain the maximum oxidation possible and after that investigate the possibility of adding the same brancher of the cellulose to obtain an aerogel-like material too.

With the ultimate goal of using these materials in the real field, a first production scale-up protocol was devised. The first step was to double the quantities of the reagents keeping the stoichiometric ratios identified as optimal fixed. Verified the feasibility of this procedure the quantities were increased four times than the starting quantities. Also in this case the stoichiometric ratios were fixed. The hope is that the final yield is related to the increase in the starting materials.

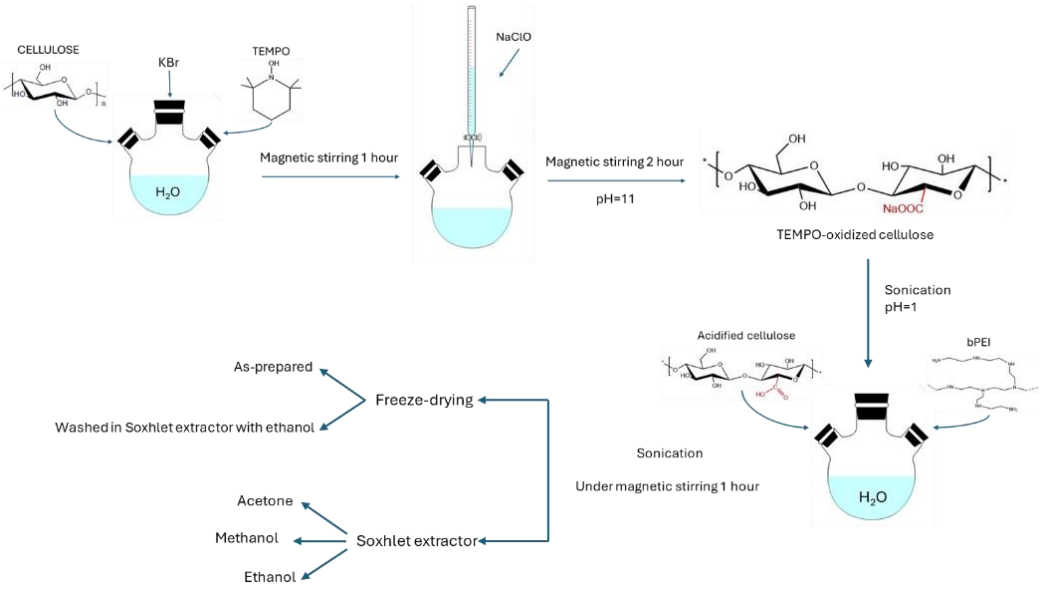


Fig. 5.2 - Scheme of the possible production of Cls-based materials.

### *5.3 Tests on materials*

To know which could be the best materials between the different ways of production, they are tested with adsorption experiments.
All the synthesized materials were tested with organic dyes and only the better performers were also tested with heavy metals.
For the tests with organic dyes were chosen three molecules: Methylene blue (MB), 4-nitrophenol (4Nph) and 4-nitrobenzaldehyde (4NBAld). Each molecule was tested with Cls-based material obtained with Fr, Cls-based material obtained with Fr and washed with Sxl using Et as solvent, Cls-based material obtained with Sxl using Ac, Me and Et as solvent and Chn-based material obtained with Sxl using Et as solvent.
In this phase, the adsorption kinetics was investigated. The experiments were conducted for 24 hours, using 10 ml of monocontaminated solution and 100 mg of adsorbent materials.

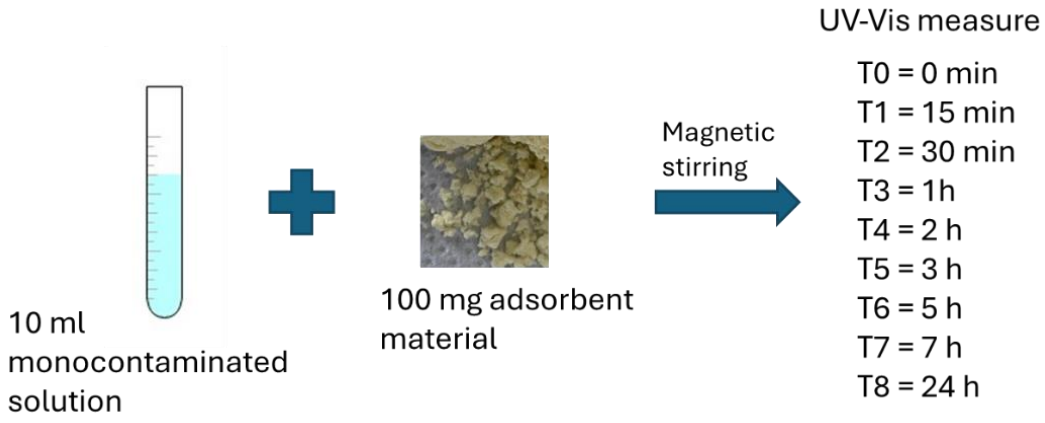


Fig. 5.3 - Scheme of organic dyes adsorption experiments.

Only the Cls-based material that gave the best results with organic dyes and Chn-based material were tested with heavy metals. In this case, it was not investigated the kinetics because it seemed to be too slow. The

maximum adsorption capacity of up to 24 hours was measured for eight different concentrations (from 0.5 ppb to 150 ppb).
Thanks to these tests it could be possible to assert if these materials could be a valid alternative to material adopted nowadays.

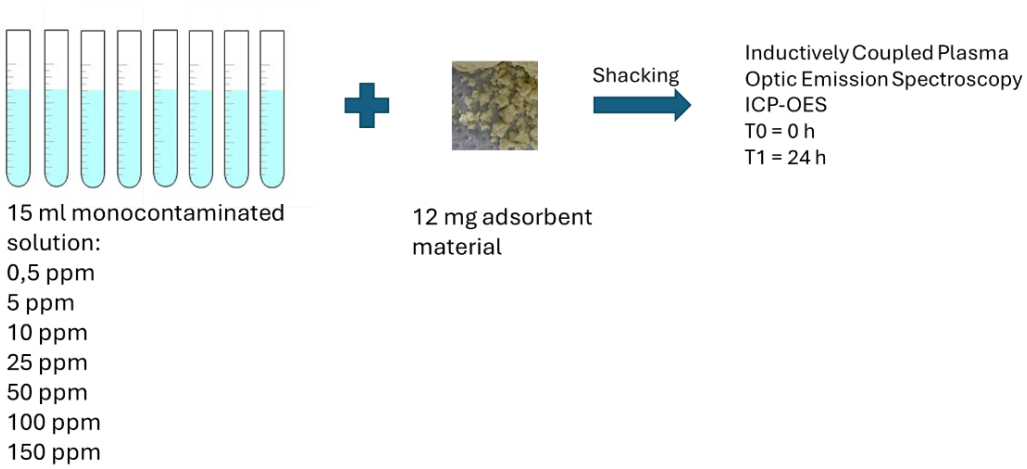


Fig. 5.4 - Scheme of heavy metal adsorption tests.

### *5.4 Environmental impact*

With the search for new materials for remediation also comes the question of whether they are sustainable, both in production and use. Life Cycle Assessment is the perfect tool for investigating and answering these questions.
The experimental plan was concluded with an LCA analysis to investigate which are the environmental impact of the different ways to obtain the Cls-based material, the synthesis protocol for the Chn-based material and a comparison between all.
It is also useful to investigate which components of the production process that have a high impact on the environment. In this way, it is possible during the scale-up phase to improve a more sustainable way of obtaining the materials. It is not certain that a linear scale-up of reagents or energy used

will correspond to a linear scale-up of the impacts. Another factor to consider is that the energy used will not increase linearly with the increasing quantities of the reagents.

The environmental impact of adsorption process, depending on the maximum adsorption capacity of contaminants, is also an interesting fact to analyse for a complete analysis.

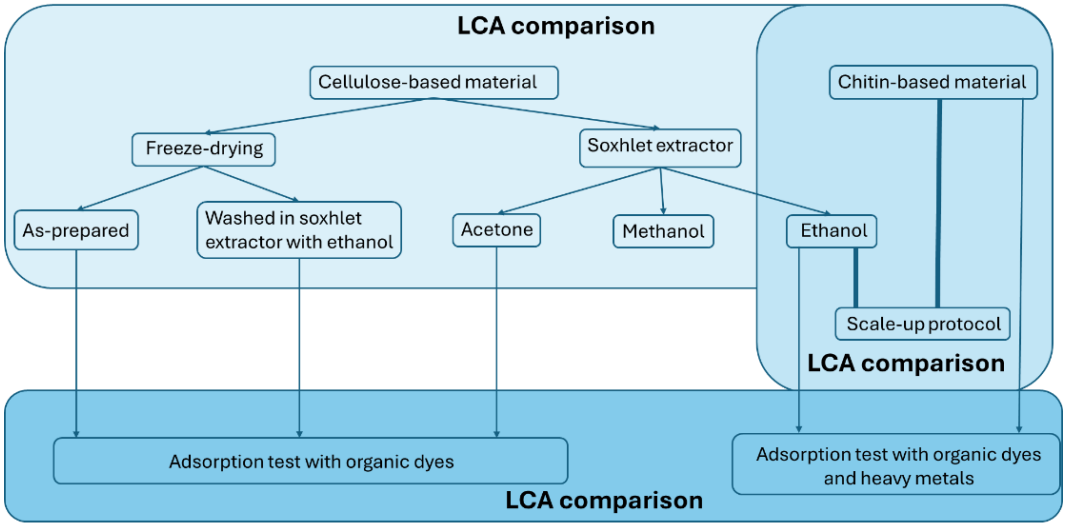


Fig. 5.5 - Scheme of Life Cycle Assessment comparison.

# 6. SYNTHESIS OF NEW SUSTAINABLE BIO-BASED MATERIALS

## *6.1 Cellulose-based material*

Cellulose is the most abundant biopolymer in Earth. It is colourless, odourless, tasteless, nontoxic and exhibits interesting properties such as good mechanical strength, biocompatibility, hydrophilicity and high sorption capacity. Moreover, it is insoluble both in water and in most organic solvents. (Riva et al., 2021) Cellulose can be extracted by primary vegetable sources (mainly cotton) or recovered by agricultural, food, municipal and industrial biowastes (including paper, carton and wood from demolition sites).

The synthesis protocol adopted in our laboratory was previously reported by (Melone et al., 2015a). The synthetic protocol can conceptually be divided into three different steps: oxidation, acidification and addition of a branching agent. The commercially available cellulose microcrystalline powder was oxidized with NaClO (10-15% w/w) in the presence of KBr and the radicalic initiator 2,2,6,6 tetramethylpiperidinyloxyl (TEMPO) in deionized water (fig. 6.1). The mixture was then acidified with HCl (37% v/v) to protonate the formed carboxylate moieties and the final step consisted in the addition of branched polyethyleneimine (bPEI, average molecular weight = 25.0 kDa). The final mixture was frozen overnight to induce the formation of entrapped ice crystals affording the sponge-like consistency to the resulting material.

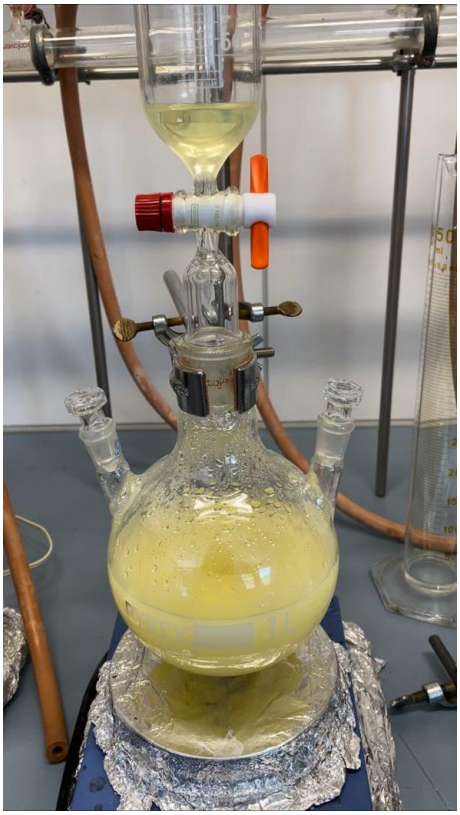

Fig. 6.1 - Photograph of the reaction apparatus used for the cellulose oxidation during the dropwise NaClO addition.

In order to remove the entrapped water and obtain the aerogel, three methods were tested and compared: the use of the Fr method, the Soxhlet extraction with an appropriate solvent or these two methods combined in sequence.

Freeze-drying is a technological process that allows the removal of water from an organic substance with the least possible deterioration of the substance's structure and components (fig.6.2). The principle of the method involves the application of heat to the frozen material kept in a vacuum. Water contained in the sample and segregated in the form of ice is directly removed as vapour by sublimation, working with pressure values

corresponding to the triple point of water (T = 0.01 °C, P = 6.10 mbar). The extracted aqueous vapour is captured by the vacuum pump. Therefore, the process is conducted under carefully controlled temperature and pressure conditions to avoid damage to the material structure so that the original matrix is almost perfectly restorable when rehydration is desired at the time of use.

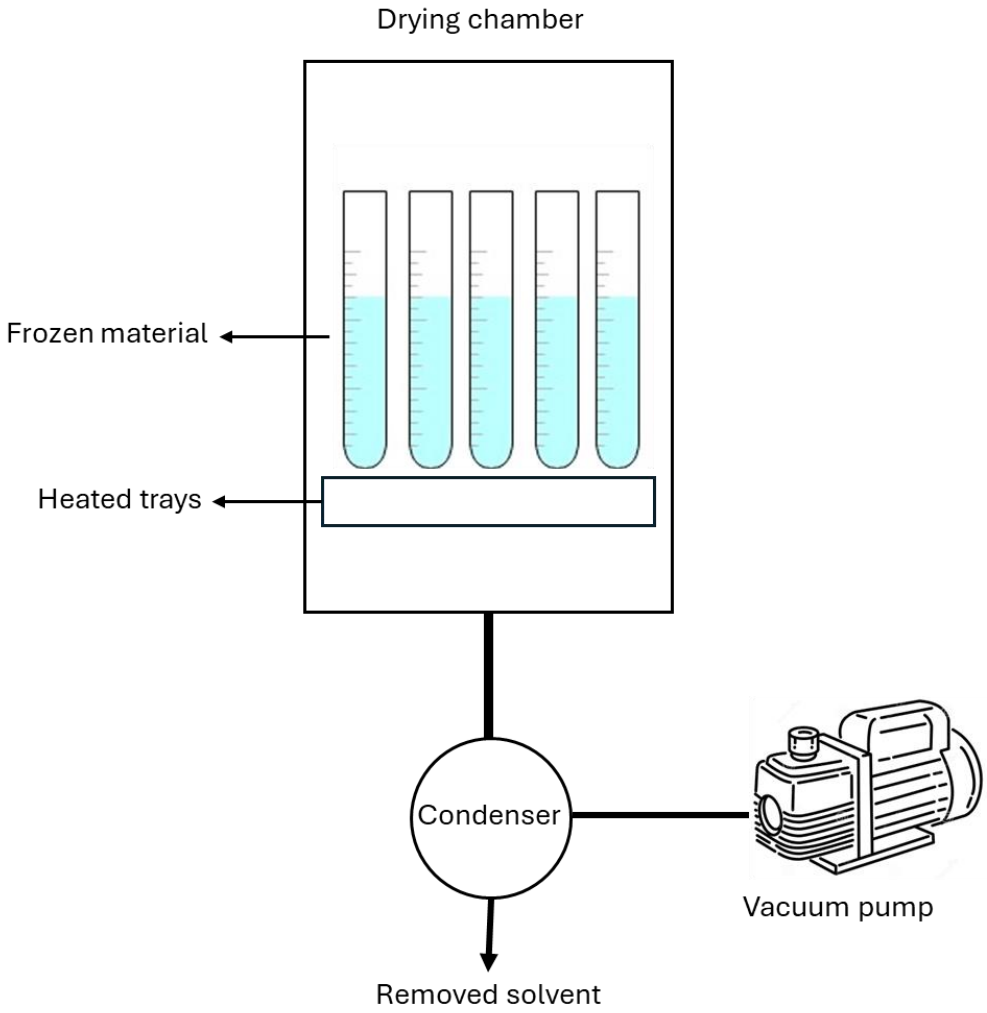


Fig. 6.2 – Freeze- drying mechanism.

However, the process needs for previously freezing the samples with liquid nitrogen, before placing them in the freeze-dryer and leaving them for 48 hours. The samples were then dried in the oven for about 16 hours and then the samples were washed for 24 hours with Et in the Sxl to remove all the excess bPEI. The whole procedure therefore took a total time of about 90 hours.

A Sxl has three main sections: a percolator (boiler and reflux) which circulates the solvent, a thimble (usually made of thick filter paper) which retains the solid to be extracted, and a siphon mechanism, which periodically empties the thimble (fig 6.3).

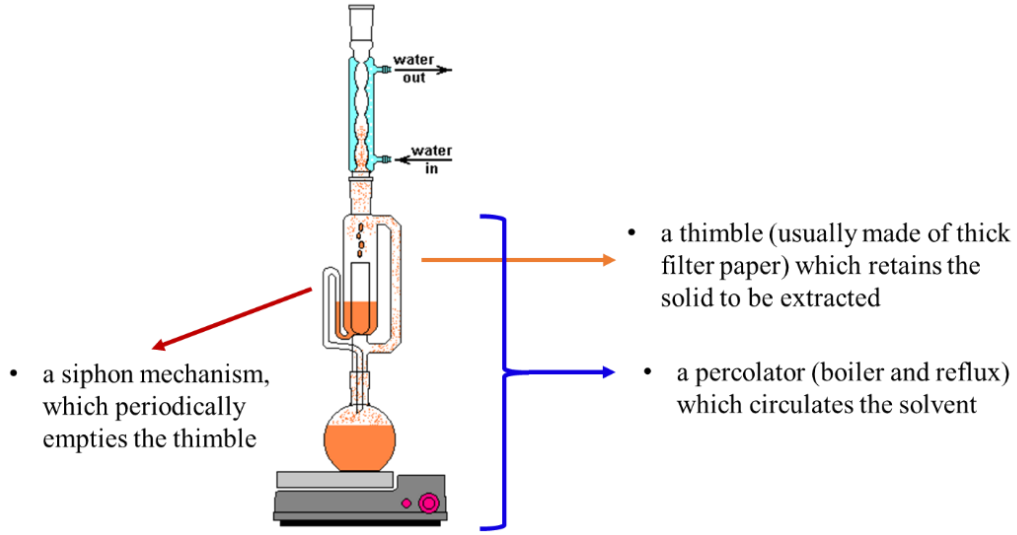


Fig. 6.3 – Sxl scheme.

The solvent is heated, and the solvent vapour rises along a distillation arm and trickles into the chamber that houses the thimbleful of solid. The condenser ensures that the solvent vapour cools and drips back into the chamber that houses the solid material. The chamber containing the solid material slowly fills with a hot solvent that will dissolve the desired part of

the mixture (impurities or unreacted substances). When the Soxhlet chamber is nearly full, it is emptied by the siphon and the solvent is returned to the distillation flask. This cycle can be repeated several times, for hours.
During each cycle, the impurities contaminating the functionalized cellulose dissolve in the solvent. In this case, water and unreacted bPEI are removed from the sample. The advantage of this system is that, instead of passing many portions of hot solvent through the sample, only one batch of the solvent is used. This is important in terms of sustainability of the entire process. The non-soluble part of the extracted solid remained in the thimble is constituted by the nanocellulose aerogel. The sample thus obtained is thermally treated in a vacuum oven at 60°C for about 2 hours.
The solvents used in the Soxhlet apparatus were Ac, Me, or Et. Being the geometry and morphology of the structure not affected by the used solvent, Et was identified as a better choice for both material performance and lower environmental impact. (Capello et al., 2007)

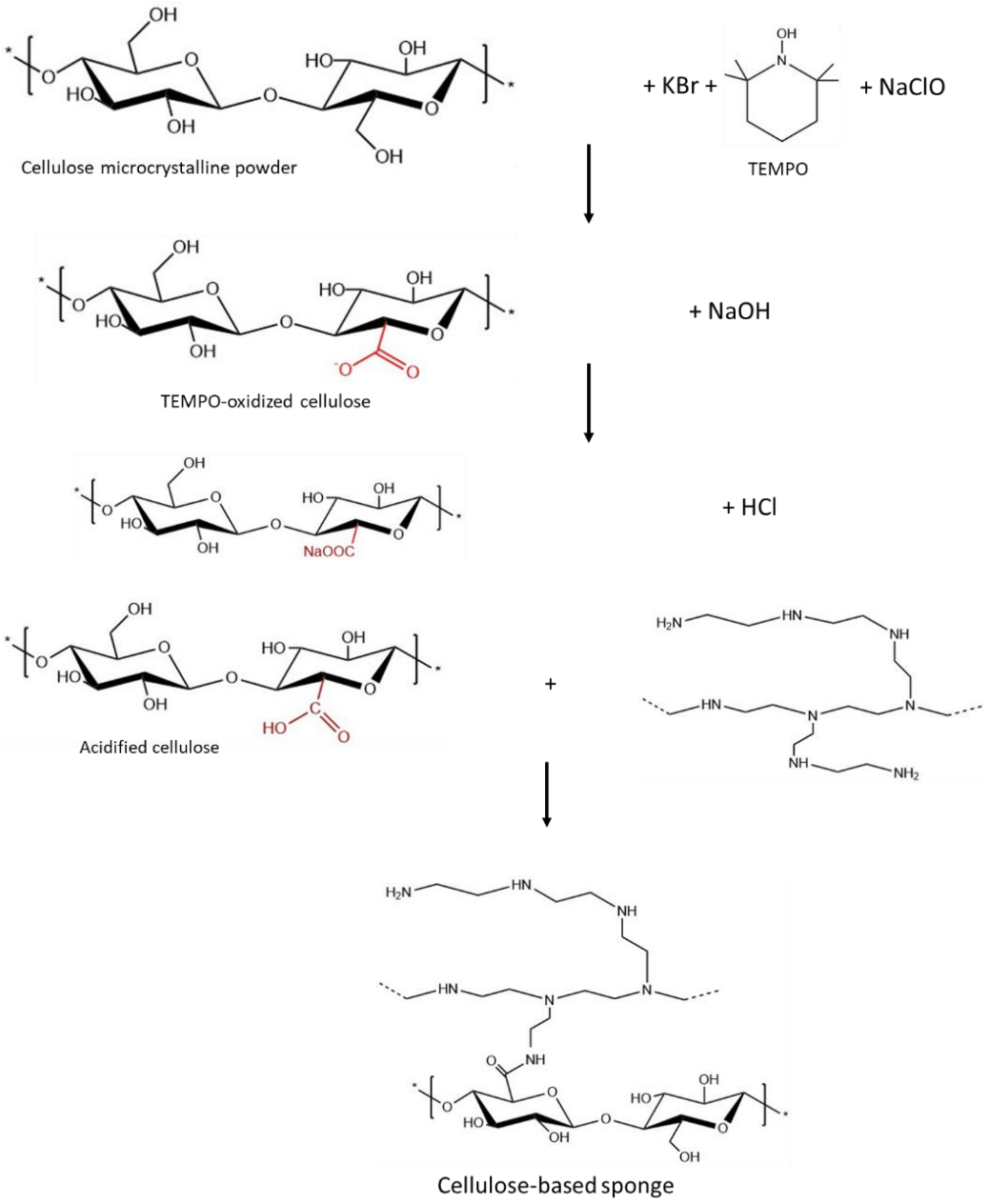


Fig. 6.4 - Scheme of the reaction to obtain a Cls-based material.

### *6.1.1 Materials and Methods*

All the reagents were purchased from Sigma Aldrich and used without further purification.

The Cls-based material has been obtained from the following sources: Cellulose microcrystalline powder ($(C_6H_{10}O_5)$n, Sigma Aldich), ), Potassium Bromide (KBr, ACS reagent, 99.0%, Sigma Aldrich), 2,2,6,6 tetramethylpiperidinyloxyl (TEMPO, 98%, Sigma Aldrich), Sodium Hypochlorite (NaClO 10-15% w/w, Sigma Aldrich), and branched Polyethylenimine (bPEI, average Mw ~25,000 by LS, average Mn ~10,000 by GPC, branched, Sigma Aldrich).

Fourier-Transform Infrared (FT-IR) Spectroscopy. The solid samples were investigated by attenuated total reflectance (ATR) FT-IR analyses on a Jasco FT/IR 4200 spectrometer equipped with a single bounce ZnSe crystal. 100 scans for each sample were collected in the 4000÷500 cm–1 spectral range with a resolution of 2 cm–1.

Scanning electron microscopy (SEM). Morphological characterizations were carried out on a field emission gun scanning electron microscope (FEG-SEM) Zeiss Σigma 300 VP (Zeiss Oberkochen, Germany). The samples were deposited on aluminum stubs coated with a pure graphite tape and sputtered with gold with a Sputter Quorum Q150 (Quorum Technologies Ltd, East Sussex, UK). Analyses were performed at 0.5 ÷ 30 kV using a 7.5 mm working distance at a 1000× magnification.

### *6.1.2 Experimental Procedures*

All syntheses were performed at room temperature under air. Cellulose microcrystalline powder (8.100 g, 50.0 mmol), potassium bromide (1.190 g, 10.0 mmol) and 2,2,6,6 tetramethylpiperidinyloxyl (TEMPO) (0.156 g, 1.0 mmol) were charged in a 3-neck flask and dispersed with deionized water (450 mL). The obtained mixture was kept under vigorous stirring with a magnetic bar until the complete dissolution of the reagents (~ 1 hour). After that, sodium hypochlorite (75 mL) was slowly added with a

dropping funnel for 30 minutes, while the pH of the resulting reaction mixture was kept constant (~ 11.0) by periodically introducing aliquots of a 0.5 M NaOH aqueous solution. After 2 hours of magnetic stirring the formation of a suspension in water of oxidized cellulose is observed, which is left for one hour to precipitate and separate the oxidized cellulose from the aqueous solution. The supernatant was eliminated, the oxidized cellulose fibres were centrifuged, and the precipitates were collected. The oxidized cellulose fibres were washed with deionized water 3 times and after that, the fibres were redispersed in 200 ml of deionized water. The suspension was sonificated in cold water for 1 hour and the suspension was acidified to pH ~ 1.0 with 3 mL of concentrated hydrochloric acid. The resulting suspension was centrifuged to remove the soluble fraction. Finally, the collected precipitates were washed six times with deionized water.

The oxidized cellulose was dispersed in deionized water (100 mL) before the addition of branched polyethyleneimine (bPEI) (8.28 g). The amount of branched polyethyleneimine is in a ratio of 2:1 of weight with oxidized cellulose fibres. The obtained solution was kept under vigorous stirring for 1 hour and subsequently sonicated for 30 minutes. The resulting mixture was poured into Soxhlet thimbles (100 mL) and refrigerated (–30 °C) overnight. Freezing is useful to give the three-dimensional structure thanks to the formation of the ice crystal.

Purification protocol. Different methods were tested and compared: the Fr method without and with the washing in the Sxl with Et to eliminate bPEI unreacted residues and the use of a Sxl with the most appropriate solvent between Ac, Me and Et.

After the first synthesis, the final liquid material obtained was divided into 4 different samples:

- The first small cellulose thimble was put in the Sxl with Ac for two hours and 30 minutes

- The second small cellulose thimble was put in the Sxl with Ac for 5 hours (the Sxl was stopped when the solvent in the chamber was transparent)
- The remaining solution was divided into 12 falcons filled with 10 ml of material. All the falcons were frozen at -30°C and freeze-dried for 48 hours. The samples are left in the oven at 80°C for 16 hours and after that, a part of them is washed with a Sxl using Et as solvent to eliminate all the bPEI unreacted.

All the samples extracted from the Sxl were dried under vacuum in an oil bath at 60°C for one hour and 30 minutes.

As it is possible to observe in the fig. 6.5 B e C there are some differences between the Cls-based material obtained with Sxl using Ac as solvent for 2 hours and 30 minutes and the Cls-based material obtained after 5 hours: the first one (fig. 6.5 B) appear more compact than the Cls-based material obtained after 5 hours (fig. 6.5 C). Another visible difference is the hardness, the first material is not simple to cut, and the second is extracted from the thimble and had the small size visible in the photo.

The synthesis was repeated and the material was placed in a Sxl using Me as solvent for 24 hours. After the drying process, the material became stiff and cut-resistant and compact. For these reasons, Me was not considered a good solvent for this kind of material. (Fig. 6.6)

Another synthesis was done using the Sxl using Et as solvent for 24 hours. Extracting the material from the thimble is already visible in the sponge-like structure before the drying process. After the drying process, the material preserves the structure and becomes less soft but easy to cut and elastic. (Fig 6.7)

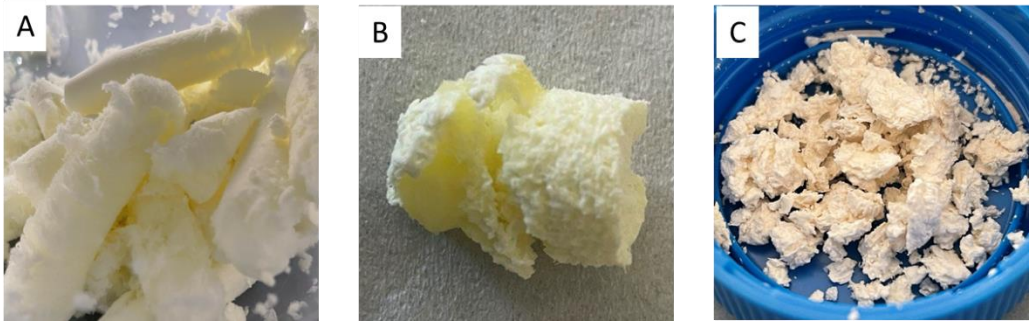


Fig. 6.5 – Cls-based material obtained with A) freeze-dried for 48 hours, B) Sxl for 2.5 hours using Ac as solvent and C) Sxl for 5 hours using Ac as solvent.

Fig. 6.6 – Cls-based material obtained with Sxl using Me as solvent.

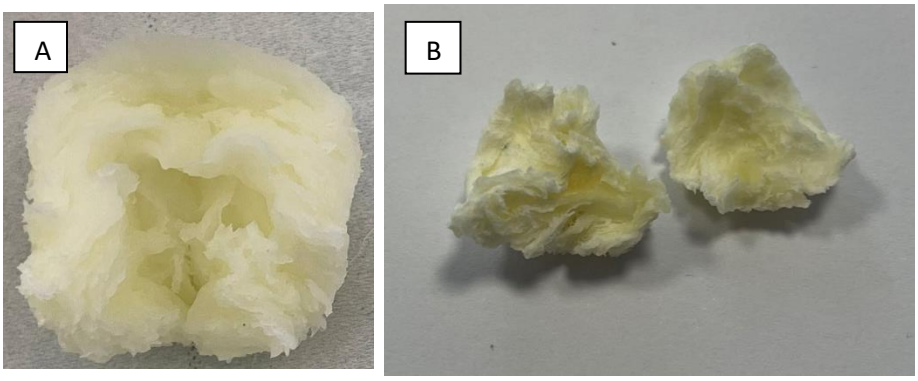


Fig. 6.7 - Cls-based material obtained with Sxl using Et as solvent: A) before the drying process and B) after the drying process.

Thanks to this set of synthesis is possible to conclude that the best protocol to adopt to obtain the material is using a Sxl using Et as solvent.

A further optimization of the morphological properties of the Cls-based sponges was attempted by changing:

- the molecular weight of the branching agent (bPEI with Mw ~ 800);
- the particle sizes of the microcrystalline cellulose (10÷100 μm).

The material obtained using bPEI with Mw ~ 800 was compact and after the Sxl and drying process had a granular aspect (Fig. 6.8). The granular appearance and absence of a sponge-like structure may be attributable to the lower ramification degree of the chosen bPEI.

The Cls-based material obtained from the cellulose with a granular size between 10 and 100 μm didn't form the structure with the brancher: its aspect after the 24 hours in the Sxl was not like a sponge, but it seemed as if the material collapsed and the brancher is not bonded with oxidized cellulose. (fig. 6.9)

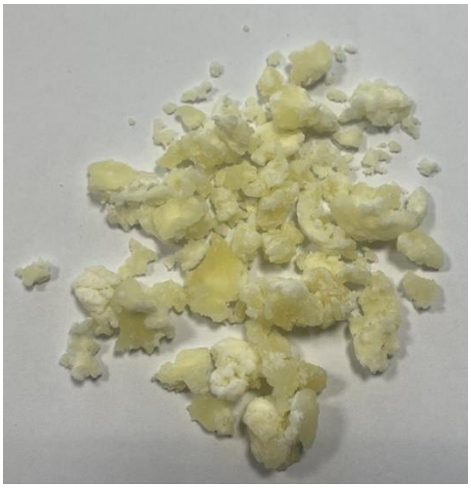

Fig. 6.8 – Cls-based material synthesised with bPEI with Mw ~ 800.

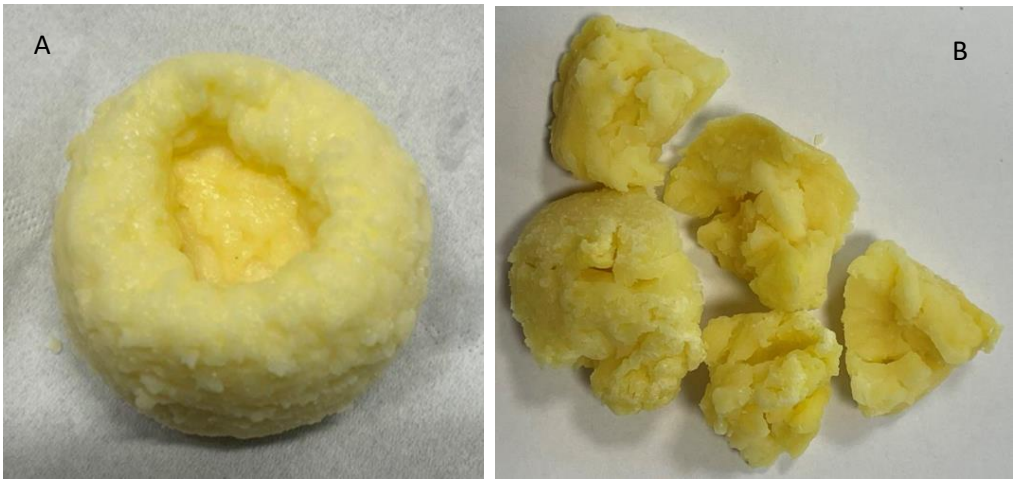


Fig. 6.9 – Cls-based material synthesised from Cls with a granular size between 10 and 100 μm: A) after Sxl and B) after drying.

### *6.1.3 Characterization*

The chemical characterization of nanostructured material in terms of the oxidation of cellulose and the subsequent creation of amine and amide groups is carried out by Attenuated Total Reflectance (ATR) infrared (IR) spectroscopy.

Fig. 6.10 shows the spectra of the cellulose microcrystalline powder, the oxidized cellulose, and the final material (bPEI-TOCNF). The IR spectrum of the oxidized cellulose clearly exhibits a peak at 1730 $cm^{-1}$ associated with the C=O stretch of the carboxylic acid moieties. In the bPEI-TOCNF spectrum, the C=O peak is shifted to 1670 $cm^{-1}$ due to the formation of amide moieties. Furthermore, the broad O-H stretching band in the wavenumber range between 3000 $cm^{-1}$ and 3700 $cm^{-1}$ overlaps the N-H stretching peak.

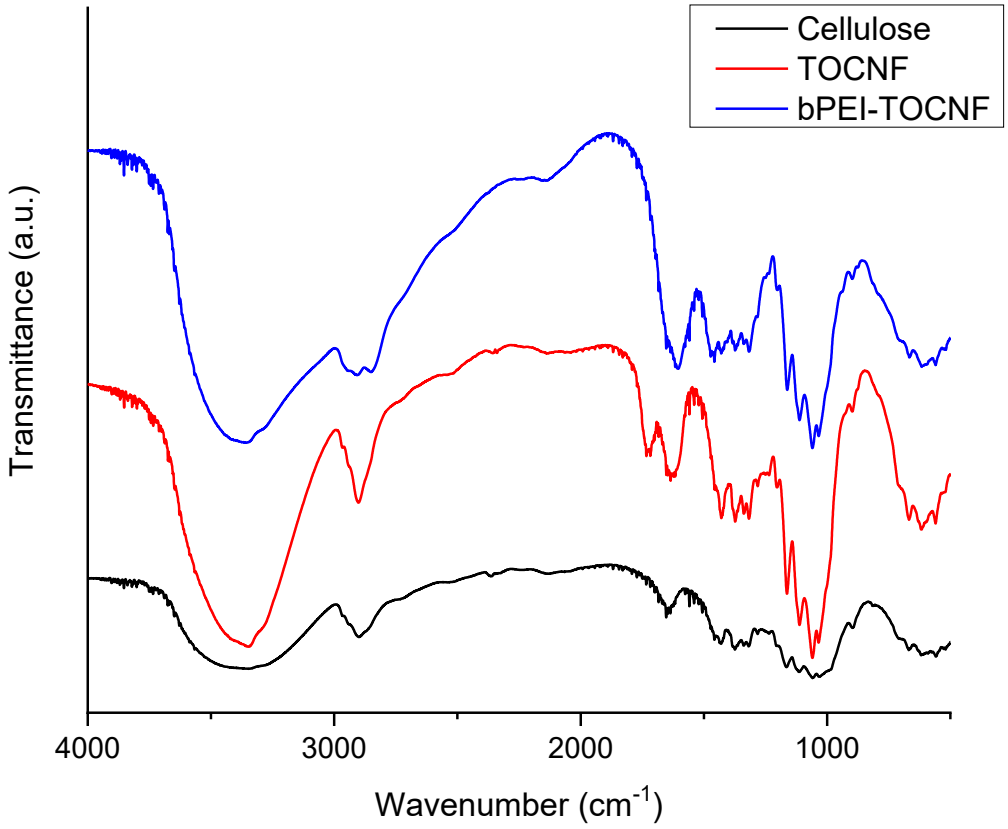


Fig 6.10 - ATR spectrum of chitin powder, oxidized chitin and finally oxidized chitin to which b-PEI has been added.

The morphological characterization of the nanostructured material was carried out by Scanning Electron Microscopy (SEM), in order to investigate the consistency of the porous structure. It was possible to study and compare the morphology of the four different materials obtained. Thanks to SEM techniques all the materials had a porous structure (fig. 6.6). There were no morphological big differences between the material obtained with freeze drying and the materials obtained with Sxl. Also the samples obtained with different solvents didn't show differences in morphology. Handling the samples it was possible to observe that the sample obtained with the Fr process was fragile, in fact when it was used for the adsorption tests under magnetic stirring it crumbled.

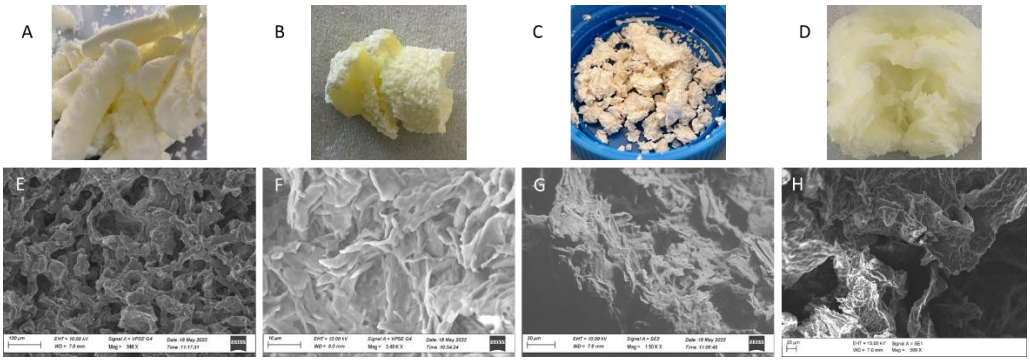


Fig. 6.11 - A) Cls-based material obtained with Fr, B) Cls-based material obtained with Sxl with Ac after 2.5 h, C) Cls-based material obtained with Sxl with Ac after 5 h, D) Cls-based material obtained with Sxl with Et, E) SEM image Cls-based material obtained with Sxl with Ac after 2.5 h, F) SEM image Cls-based material obtained with Sxl with Ac after 5 h, G) SEM image Cls-based material obtained with Sxl with Et.

The density of all the Cls-based material was calculated by weighing a cube with a side of 1 cm, with the formula

d= mass/volume.

As reported in Table 6.1, the density values of the obtained materials ranged from 0.23 to 0.31 g/cm3. Importantly, the Cls-based material obtained with Sxl using Et as solvent appear with a low density as the others two materials

(Cls-based material obtained with Fr and Cls-based material obtained with freeze drying and washed in Sxl) and as it is visible from SEM images with a lot of pore inside the structure.

Tab. 6.1 – Density of three Cls-based materials.

| **Material** | **Density (g/cm$^3$)** |
|---|---|
| Cls-based material obtained with Fr | 0.26 |
| Cls-based material obtained with Fr and washed in Sxl with Et | 0.23 |
| Cls-based material obtained with Sxl using Et as solvent | 0.31 |

### *6.2 Chitin-based material*

The Chn-based sponges were prepared by adapting the synthetic protocol optimized for the obtainment of the Cls-based analogous materials. The synthetic protocol could be divided into three different steps: oxidation, acidification and addition on a brancher. The commercially available chitin powder was oxidized with NaClO (10-15% w/w) in the presence of KBr and the radicalic initiator 2,2,6,6 tetramethylpiperidinyloxyl (TEMPO) in water. The mixture is then acidified with HCl 37% v/v and the final step is to add branched Polyethyleneimine (bPEI 25kDa). The final mixture is frozen overnight in this manner the ice crystal formed during this process gave the sponge-like structure. The frozen material is purified by a Sxl, which is the best way to remove unreacted chemicals (bPEI) and maintain the structure created during freezing. A Sxl is also a sustainable procedure because of uses the same batch of the solvent for a lot of cycles. After that, the sponge was dried under vacuum.

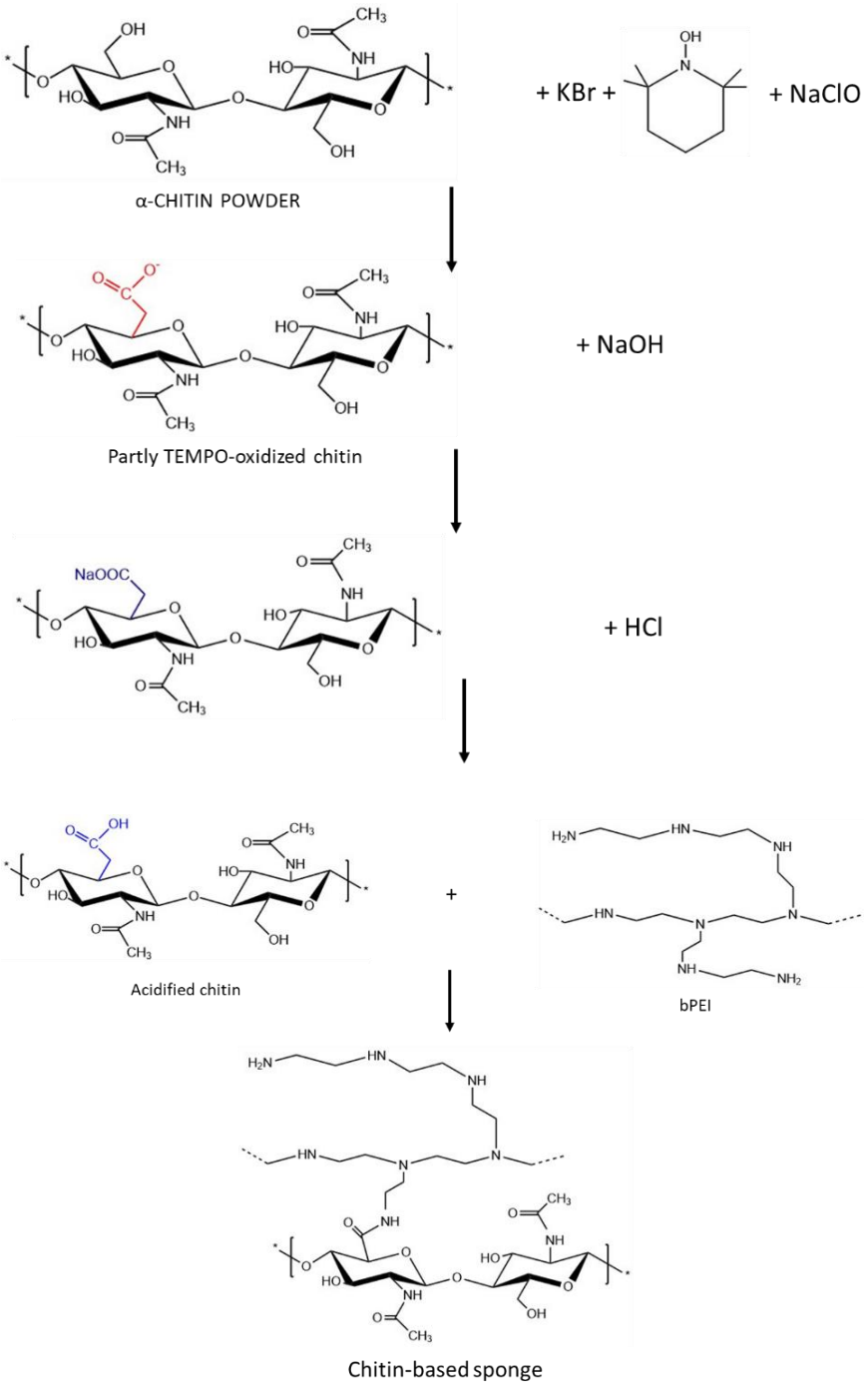


Fig. 6.12 - Scheme of the reaction to obtain a Chn-based material.

*6.2.1 Materials and Methods*

All the reagents were purchased from Sigma Aldrich and used without further purification.

The Chn-based material has been obtained from the following sources: Chitin from shrimp shell ($(C_8H_{13}NO_5)n$, Practical grade, Sigma Aldrich), Potassium Bromide (KBr, ACS reagent, 99.0%, Sigma Aldrich), 2,2,6,6 tetramethylpiperidinyloxyl (TEMPO, 98%, Sigma Aldrich), Sodium Hypochlorite (NaClO 10-15% w/w, Sigma Aldrich), and branched Polyethylenimine (bPEI, average Mw ~25,000 by LS, average Mn ~10,000 by GPC, branched, Sigma Aldrich).

Fourier-Transform Infrared (FT-IR) Spectroscopy. The solid samples were investigated by attenuated total reflectance (ATR) FT-IR analyses on a Jasco FT/IR 4200 spectrometer equipped with a single bounce ZnSe crystal. 100 scans for each sample were collected in the 4000÷400 $cm^{-1}$ spectral range with a resolution of 2 $cm^{-1}$.

Scanning electron microscopy (SEM). Morphological characterizations were carried out on a field emission gun scanning electron microscope (FEG-SEM) Zeiss Σigma 300 VP (Zeiss Oberkochen, Germany). The samples were deposited on aluminum stubs coated with a pure graphite tape and sputtered with gold with a Sputter Quorum Q150 (Quorum Technologies Ltd, East Sussex, UK). Analyses were performed at 0.5 ÷ 30 kV using a 7.5 mm working distance at a 1000× magnification.

*3.2.2 Experimental procedure*

All syntheses were performed at room temperature under air. Chitin powder from shrimp shells (8.100 g, 40.0 mmol), potassium bromide (1.190 g, 10.0 mmol) and 2,2,6,6 tetramethylpiperidinyloxyl (TEMPO) (0.156 g, 1.0 mmol) were charged in a 3-neck flask and dispersed with deionized water (450 mL). The obtained mixture was kept under vigorous stirring with a magnetic bar until the complete dissolution of the reagents (~ 1 hour). After that, sodium hypochlorite (75 mL) was slowly added with a dropping funnel

for 30 minutes, while the pH of the resulting reaction mixture was kept constant (~ 11.0) by periodically introducing aliquots of a 0.5 M NaOH aqueous solution. After 2 hours of magnetic stirring the formation of a suspension in water of oxidized chitin is observed, which is centrifuged and the supernatants are collected. The solution was acidified to pH ~ 7.0 with 5 mL of concentrated hydrochloric acid and the resulting suspension was centrifuged to remove the soluble fraction. Finally, the collected precipitates were washed three times with deionized water.

The oxidized chitin was dispersed in deionized water (120 mL) before the addition of branched polyethyleneimine (bPEI) (9.85 g). The obtained solution was kept under vigorous stirring for 1 hour and subsequently sonicated for 30 minutes. The resulting mixture was poured into Soxhlet thimbles (100 mL) and refrigerated (–30 °C) overnight.

Purification protocol. The frozen thimbles were purified with a Sxl for 24 hours using Et as solvent. The obtained sponge was dried under vacuum at 60 °C for 3 hours and stored in 50 mL vials.

After the ATR characterization of this material was observed that the signal at 1731 $cm^{-1}$ oxidized chitin at pH ~ 7.0 was not clearly visible. It was made the second synthesis where the HCl added was enough to obtain a pH ~ 1. The material was characterized by ATR and was observed that the signal at 1731 $cm^{-1}$ was clearly visible, so the oxidation happened for sure.

Another difference between the two materials is visible in the pictures (fig. 6.13 and fig. 6.14). The material obtained from the oxidation at pH ~ 7 after 24 hours in the Sxl using Et as solvent crumbled with a powdery appearance and it conserved the same appearance after the drying process.

The material obtained from the oxidation at pH ~ 1 was more compact after the Sxl while retaining its sponge-like appearance. The sponge-like appearance is maintained also after the drying process.

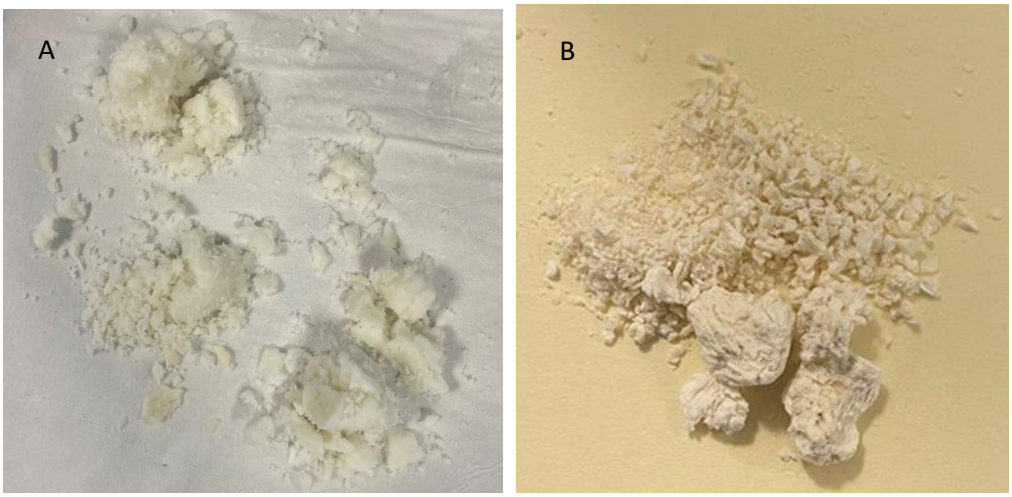


Fig. 6.13 – Chn-based material obtained with oxidation at pH ~ 7: A) after 24 hours in the Sxl using Et as solvent and B) after the drying process.

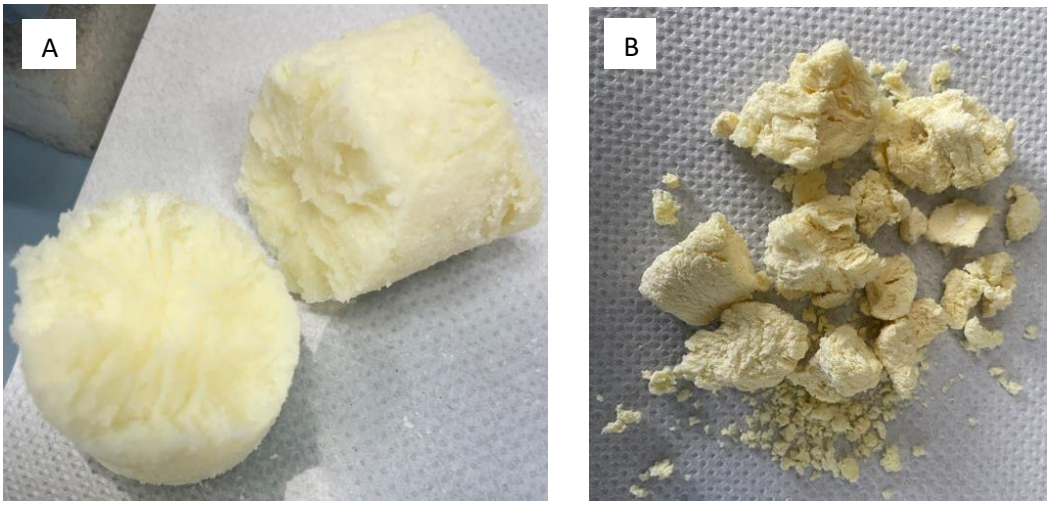


Fig. 6.14 – Chn-based material obtained with oxidation at pH ~ 1: A) after 24 hours in the Sxl using Et as solvent and B) after the drying process.

### *6.2.3 Characterization*

The purpose of this synthetic procedure is to add amide groups to the chitin structure because of their high reactivity with molecules especially

with the organic one. Although chitin is a more difficult polymer to oxidize than cellulose and preference is given to using the deacetylation reaction to obtain chitosan, oxidation allows additional amide groups to be added. The advantage of using chitin over cellulose is the presence of an amide group on each monomer, which therefore increases its reactivity with other molecules.

The chemical characterization of Chn-based material in terms of the oxidation of chitin and the subsequent creation of amine and amide groups is carried out by Attenuated Total Reflectance (ATR).

Fig. 6.15 shows the main steps of the synthesis procedure: the spectra of the chitin powder, the oxidized chitin, and the final material (bPEI-TOChNF). The IR spectrum of the oxidized chitin clearly exhibits a peak at 1731 $cm^{-1}$ associated with the C=O stretch of the carboxylic acid moieties. In fig. 6.16 is possible to appreciate the difference between the chitin oxidized with a pH equal to 7 (in black) where the signal is very small and the chitin oxidized with a pH equal to 1 where the peak is more visible. In the spectrum of the final Chn-based material, the C=O peak is shifted to 1625 $cm^{-1}$ due to the formation of amide moieties. Furthermore, the broad O-H stretching band in the wavenumber range between 3000 $cm^{-1}$ and 3700 $cm^{-1}$ overlaps the N-H stretching peak.

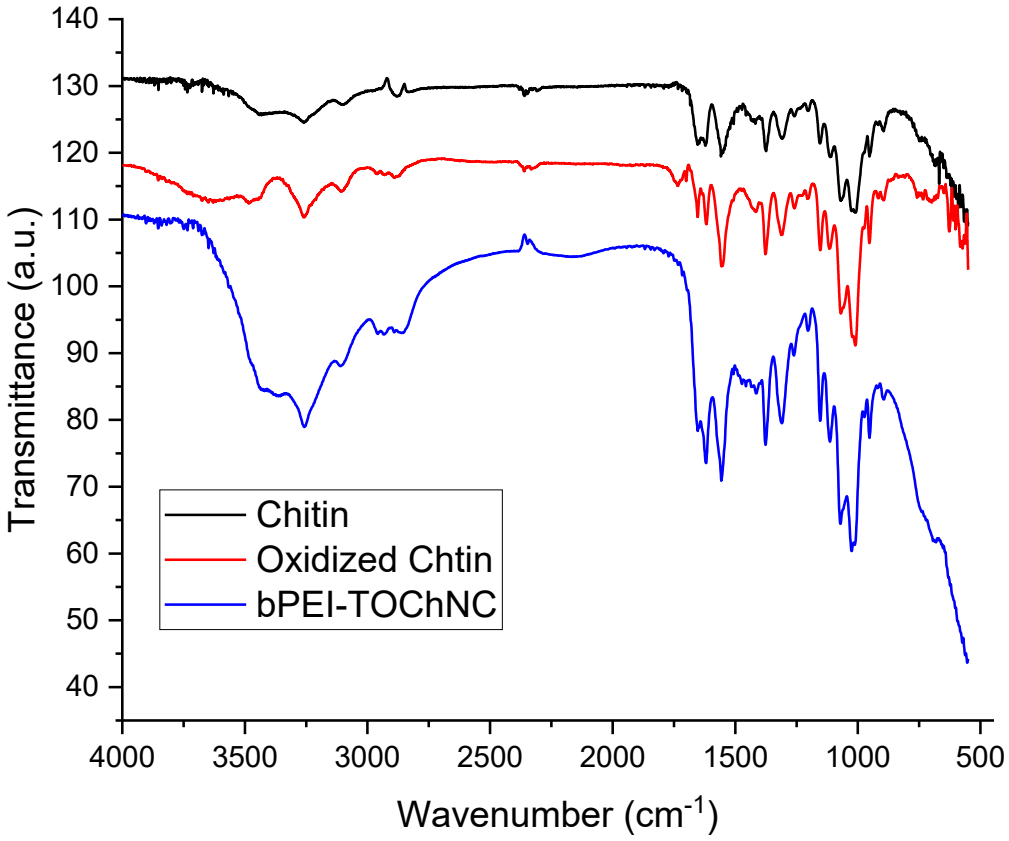


Fig. 6.15 - ATR spectrum of chitin powder, oxidized chitin and finally oxidized chitin to which b-PEI has been added.

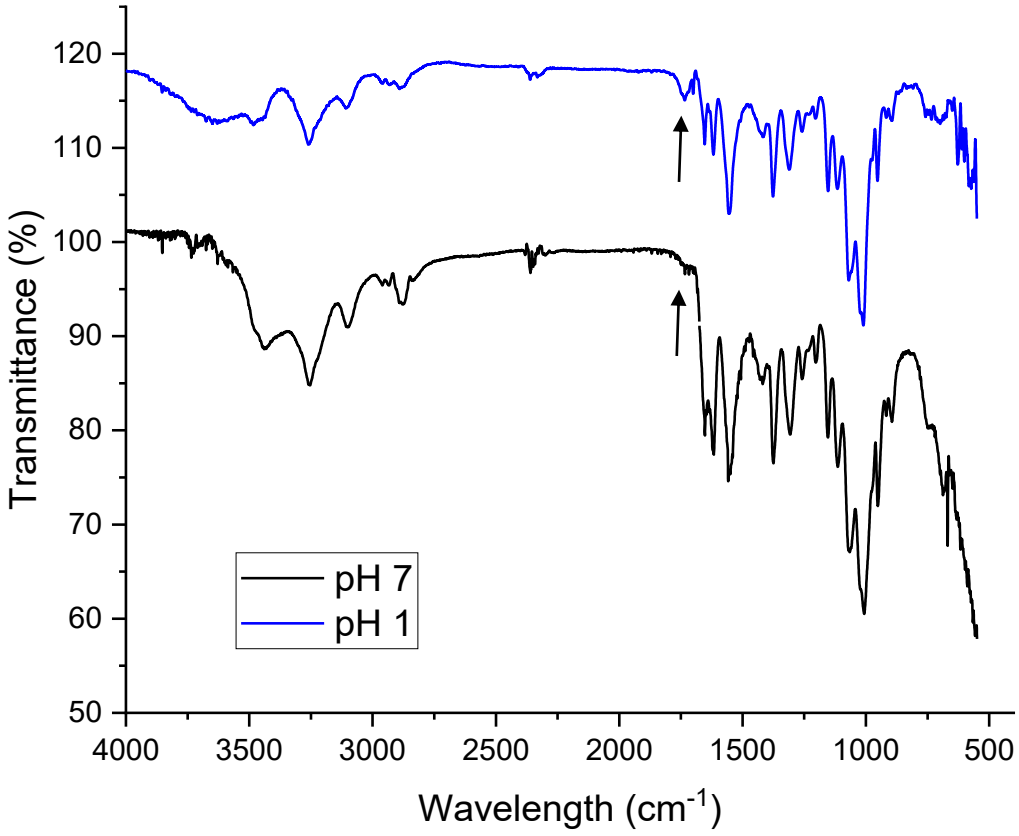


Fig. 6.16 - ATR spectrum of oxidized chitin at pH ~ 7 and oxidized chitin at pH ~ 1.

The morphological characterization of the nanostructured material investigating the pore distribution and how the structure looks is carried out by Scanning Electron Microscopy (SEM). The morphology of this material was found to be extremely porous, and therefore the SEM images made it possible to confirm the hypotheses made simply by observing the ratio of weight to the volume occupied.

The density of this material was calculated on a small cube with a volume equal to 1 $cm^3$. The density is calculated with the formula

d= mass/volume.

Tab. 6.2 – Density of the Chn-based materials oxidized with different pH values.

| **Material** | **Density (g/cm³)** |
|---|---|
| Chn-based material obtained by pH ~ 7 | 0.49 |
| Chn-based material obtained by pH ~ 1 | 0.15 |

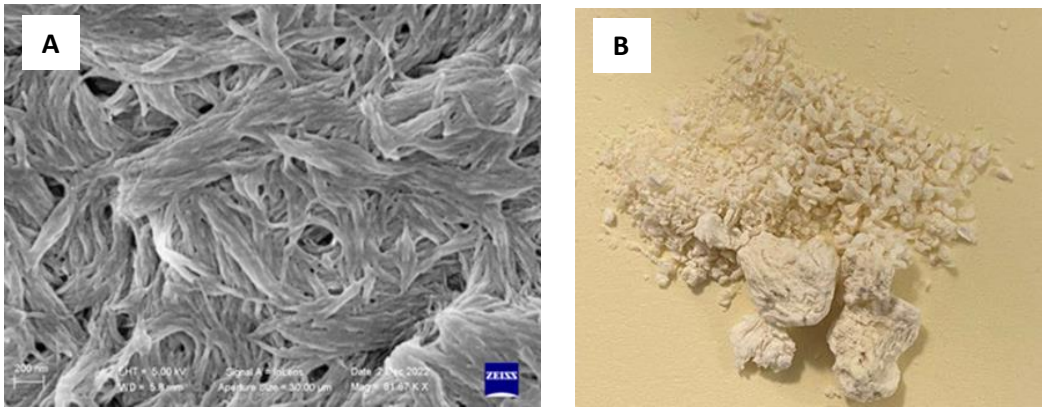


Fig. 6.17 – Chn-based material obtained with pH ~ 7: A) SEM image, B) appearance of the material immediately after the drying step.

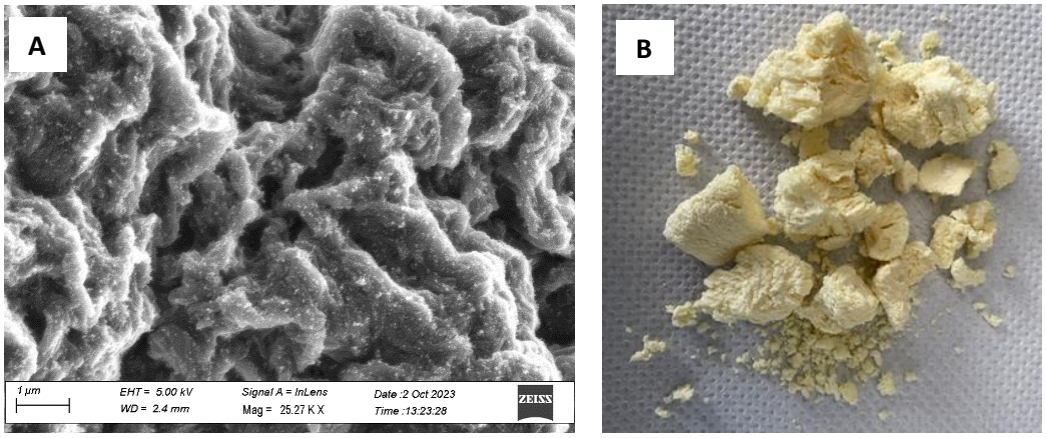


Fig. 6.18 – Chn-based material obtained with pH ~ 1: A) SEM image, B) appearance of the material immediately after the drying step.

### *6.3 Scale-up protocol of the synthesis process*

The experimentation aim is to obtain new materials which can be used for environmental remediation. For this reason, the production of these materials must be implemented to the point of moving from laboratory to industrial-scale production.

The quantities of all the reagents were increased two times and four times and it was observed whether the quantities of final materials grew proportionally to the increase in reactants. This phase started with the synthesis using doubled quantities of reagents. The Cls-based material was the first material produced. The first synthesis failed, there wasn't the ramification after the Sxl. The material appeared as if it had collapsed on itself. A second synthesis was done and it was successful, but the final quantity of the material obtained wasn't double that of the first synthesis.

The Chn-based material obtained with the synthesis with pH ~ 1 was scaled up successfully. The quantity of the Chn-based material obtained was 3 times bigger than the quantity obtained with the first synthesis.

The last part of the scale-up was with all the reagents quantities multiplied by 4. The first synthesis was for the Cls-based material which was not successful because the cellulose oxidized didn't branched with the bPEI. It is possible to state that the synthesis protocol cannot be scaled up by increasing the reagents while leaving the molar ratios between them unchanged.

The synthesis of the chitin was successfully done and the Chn-based material obtained was 10 times more than that obtained with the first synthesis.

In fig. 6.19 is possible to observe the opposite trend that the scale-up of the cellulose and the scale-up of the chitin had. It seems that the maximum yield for the chitin is obtained with the quantity multiplied by four, although the molar ratio of the reagents is always kept constant. The Cls-based material

behaves oppositely to Chn-based material, so it is not possible to scale-up the material keeping constant the molar ratio between the reagents.

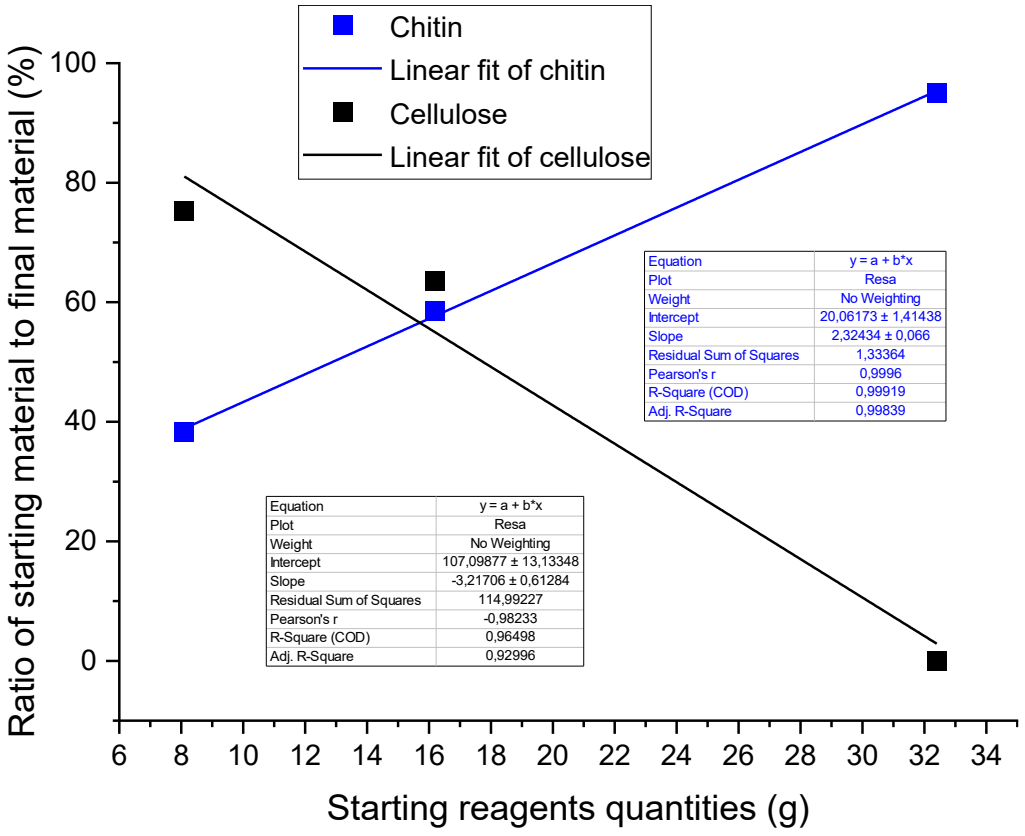


Fig. 6.19 – Increment of the quantity of Cls-based material and Chn-based material product, with the same quantity of starting material (Cls and Chn) in the scale-up production.

It can be concluded that the Chn-based material is better than the Cls-based material in the simplicity of scaling up production while keeping the synthesis protocol unchanged. Another fact in favour of scaling up the Chn-based material is the percentage increase in the ratio of chitin used as a starting point to the final product obtained, which rises from 38% to 95%.

the Chn-based material is therefore an ideal candidate for scaling up production from laboratory to industrial scale.

# 7. ADSORPTION TESTS

After the development of the synthetic protocol and the fulfilment of the chemical and morphological characterization on the corresponding materials, they were subjected to adsorption tests with organic molecules and heavy metals simulating a pollution condition. The tests were conducted on a lab scale to study the potential of these materials as adsorbents through the evaluation of the adsorption kinetics for organic compounds and the maximum adsorption capacity for heavy metals. As a general behaviour, adsorption of organic molecules is more difficult because of their dimensions and different interactions with the adsorbent materials. Finally, bench-scale experiments were conducted to study which could be the behaviour of these materials in a real scenario.

## *7.1 Organic dyes*

In order to evaluate the kinetics of the adsorption tests with organic compounds, it was employed the Lambert-Beer's law of the absorption spectroscopy, that is based on the correlation between the quantity of the light absorbed by a chemical species and its concentration. In the following paragraph, it is reported the theory at the basis of absorption spectroscopy and the relevant technical aspects.

### *7.1.1 Absorption Spectroscopy*

Fig. 7.1 shows a radiation beam before and after its passage through *a* solution of thickness *b* (cm) and concentration *c* (mg/L) of an absorbing species. Because of the interaction between the photons and the absorbing particles, the power of the beam is attenuated from $P_0$ to P. The transmittance T of the solution is thus the fraction of incident radiation transmitted by the solution:

$$T = \frac{P}{P_0} \qquad (7.1)$$

while the absorbance A of a solution is defined by the equation:

$$A = -\log_{10} T = \log {}^{P_0}/_{P} \qquad (7.2)$$

Therefore, the absorbance of a solution increases as the attenuation of the beam increases.

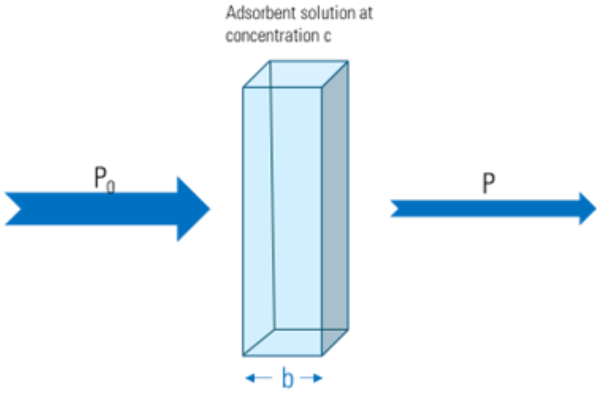


Fig. 7.1. Scheme of the Lambert-Beer Law.

According to the Lambert-Beer's Law, absorbance is directly proportional to the length of the path *b* through the solution and the concentration *c* of the absorbing species. The quantitative relationship is:

$$A = abc \qquad (7.3)$$

where *a* is a constant of proportionality called absorptivity and is typical for each chemical species. The modulus of a will depend on the units used for b and c. Usually, b is expressed in centimetres and c in grams/litre and the absorptivity therefore has the units L $g^{-1}$ $cm^{-1}$.
When in Equation 7.3 the concentration is expressed in moles/litre and the cell length is in centimetres, the absorptivity is called the molar absorptivity and is denoted by the symbol ε. Therefore, when b is in centimetres c is in moles/litre:

$$A=\varepsilon bc \qquad (7.4)$$

where ϵ units are L $mol^{-1}$ $cm^{-1}$.

Transmittance and absorbance cannot be measured, at least as defined by Equations 7.1 and 7.2, because the analyte solution must be contained in a transparent vessel, or cell. As the figure shows, there is reflection at both the air/wall and wall/solution interfaces. The resulting beam attenuation is considerable, where about 8.5 per cent of a yellow light beam is lost by reflection upon passing through a glass cell containing water. Beam attenuation can also be due to scattering by large molecules and sometimes absorption by the walls of the container. To account for these effects, the power of the beam transmitted by the analyte solution is usually compared with that of the beam transmitted by an identical cell containing only the solvent. This gives an experimental absorbance that is very close to the true absorbance:

$$A=\log P_{solvente}/P_{soluzione} \sim \log P/P_0 \qquad (7.5)$$

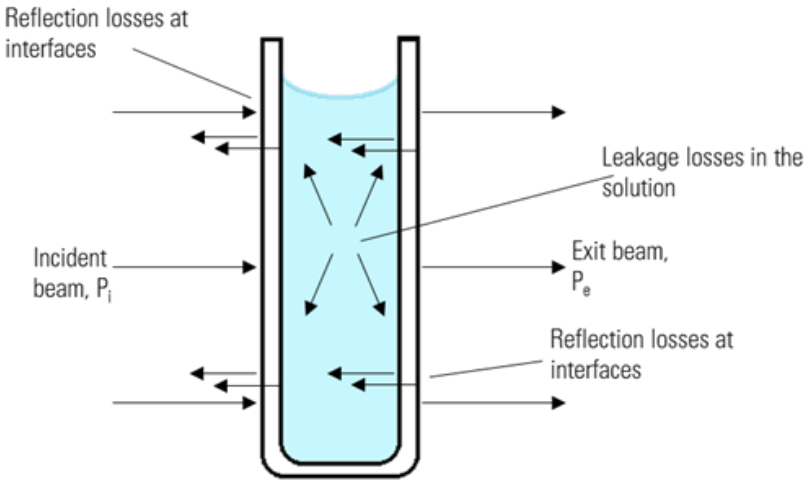


Fig. 7.2. Scheme of all the process reflection and scattering loss.

Equations 7.3 and 7.4 are two statements of Beer's law and these relationships can be rationalised as follows. Let us consider the piece of absorbent material (solid, liquid or gaseous) shown in fig. 7.3.

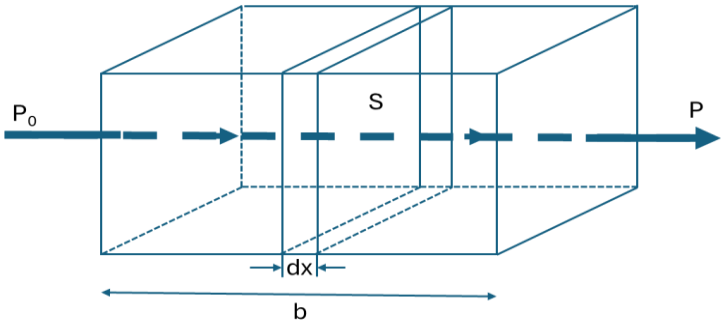


Fig. 7.3. Scheme for the mathematic demonstration.

A beam of parallel monochromatic radiation of power $P_0$ encounters the workpiece perpendicularly to the surface; after passing through a thickness b of the material, which contains n absorbing particles (atoms, ions or molecules), the power of the beam is reduced to P as a result of absorption. Let now consider a cross-section of the piece, of area S and infinitesimal thickness dx and containing dn absorbing particles. Imagine that each particle has a surface on which photon capture occurs, i.e. when a photon arrives on one of these areas, absorption occurs immediately. The total area projected, within the section, by these capturing surfaces is defined as dS; the ratio of the capturing area to the total area is then dS/S and represents in statistical terms the probability of photon capture within the section.
The power of the beam entering the section, $P_X$, is proportional to the number of photons per square centimetre per second, and $dP_x$ represents the amount lost per second within the section; the fraction absorbed is $-dP_X$ /PX and this ratio coincides with the average probability of capture (the minus sign indicates that P decreases):

$$-\frac{dP_x}{P_x} = \frac{dS}{S} \qquad (7.6)$$

Since dS is the sum of the catch areas of the particles within the section, it must be proportional to the number of particles:

$$dS = \alpha dn \qquad (7.7)$$

where dn is the number of particles and α is a proportionality constant, which can be called the capture cross-section. Combining equations 7.5 and 7.6 and integrating between 0 and n, we obtain:

$$-\int_{P_0}^{P} \frac{dP_x}{P_x} = \int_0^n \frac{\alpha dn}{S} \qquad (7.8)$$

That by

$$-\ln \frac{P}{P_0} = \frac{\alpha n}{S} \qquad (7.9)$$

Converting to base 10 logarithms and inverting the fraction to change the sign, we have:

$$\log \frac{P_0}{P} = \frac{\alpha n}{2.303S} \qquad (7.10)$$

where n is the total number of particles in the block shown in the figure. The area S of the cross-section can be expressed in terms of the volume V in cm and the length b in cm of the block:

$$S = \frac{V}{b} \qquad (7.11)$$

Substituting this quantity into equation 6.10 gives:

$$\log \frac{P_0}{P} = \frac{\alpha n b}{2.303V} \qquad (7.12)$$

Note that n/V has the units of a concentration (number of particles per cubic centimetre) and is immediately convertible to moles per litre. The number of moles is given by:

$$number\ of\ moli = \frac{n\ \cancel{particles}}{6.02x10^{23}\ \cancel{particles}/mol} \quad (7.13)$$

and c in mol/L is given by:

$$c = \frac{n}{6{,}02x10^{23}}\ mol\ x\ \frac{1000\ \cancel{cm^3}/L}{V\cancel{cm^3}} = \frac{1000\ n}{6.02\ x\ 10^{23}V}\ mol/L \quad (7.14)$$

Combining this relationship with equation 7.11 gives:

$$\log\frac{P_0}{P} = \frac{6.02x10^{23}\alpha bc}{2.303\ x\ 1000} \quad (7.15)$$

All the constants in this equation can finally be combined into a single term ε:

$$\log\frac{P_0}{P} = \varepsilon bc = A \quad (7.16)$$

Beer's law satisfactorily describes absorption only by dilute solutions and, in this sense, it is a limiting law. At high concentrations, (usually M > 0.01) the average distance between the species responsible for absorption decreases to the extent that each species influences the charge distribution of its neighbours.

### *7.1.2 Results*

The molecules chosen for the experiments were: MB, 4NBAld and 4Nph, all soluble in water. These three molecules have been chosen because we tried to test the materials obtained in conditions as much as similar to real scenarios. In fact, 4Nph is a typical persistent organic pollutant and its use is ubiquitous to manufacture drugs, fungicides, insecticides, and dyes. To evaluate the impact of the -OH group, it was established a comparison with

the corresponding 4NBAld dye, while the condensed structure of MB resembles that of PAHs.

The corresponding absorption spectra are reported in Fig 7.4.

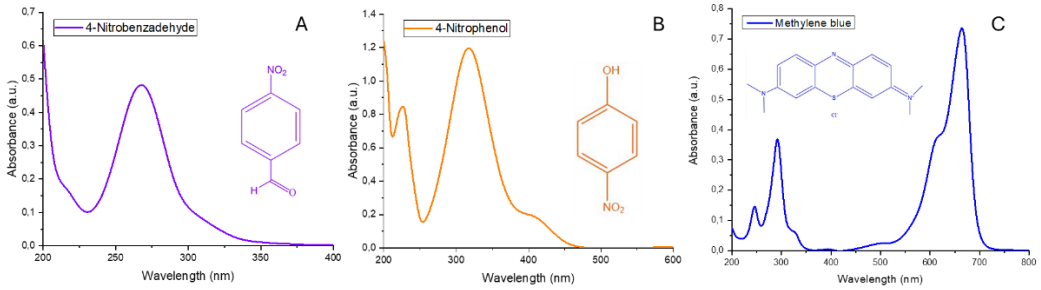


Fig. 7.4. A) Molecule and UV-Vis spectrum of 4NBAld ($10^{-4}$ M), B) Molecule and UV-Vis spectrum of 4Nph ($1.2*10^{-4}$ M), C) Molecule and UV-Vis spectrum of MB ($10^{-3}$ M).

Another important observation to make about 4Nph is that its spectrum varies with the pH. In fact, at acidic pH (~ 1) the peak is at 317 nm at basic pH (in the form of phenate ion, pH~ 12.4) the peak recorded is at 400 nm, while at an intermediate pH (~8.4) the peak recorded is the convolution of its signals. The reason for this behaviour is that the 4Nph is a pH indicator, in fact the solution at basic pH is yellow and the solution at acid pH is transparent. (Gheitasi Zarooni et al., 2020) reported how the behaviour of the 4Nph changes with the pH in the Uv-Vis spectrum as a consequence of the formation of the basic form as phenate ion.

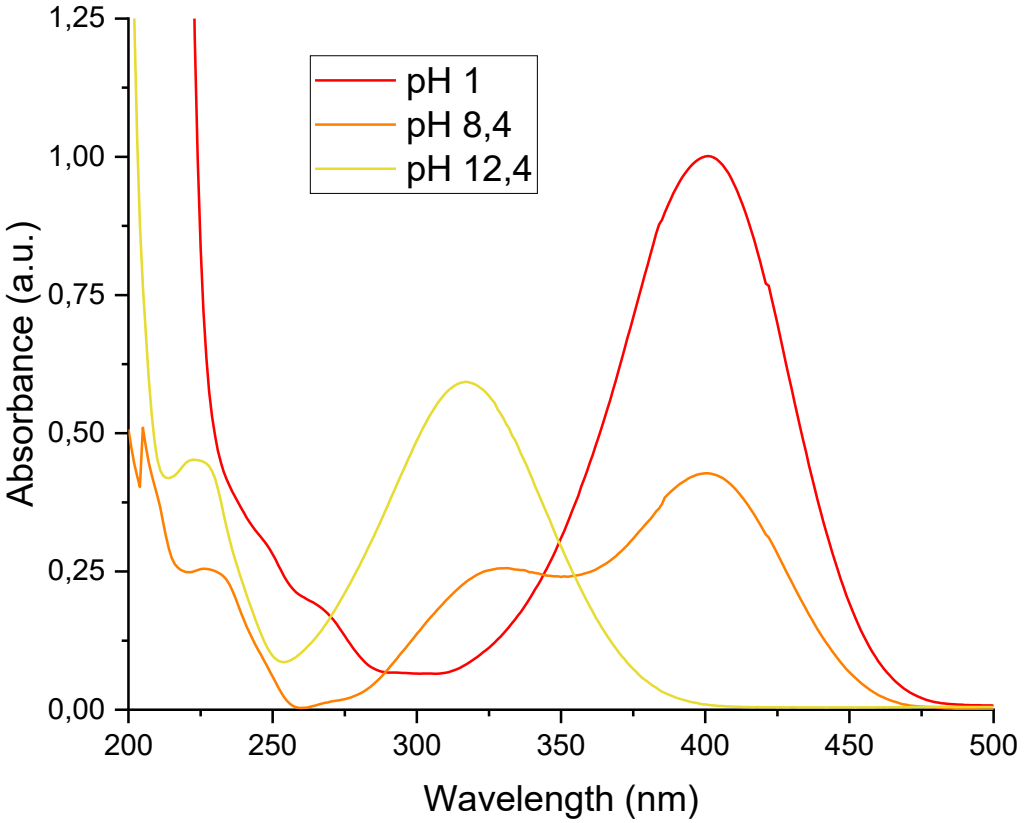


Fig.7.5 – Evolution of the spectra of 4Nph with the pH variation.

To evaluate the adsorption performances of Cls- and Chn-based materials, the experiments were conducted with stock solutions of $1.0 \times 10^{-5}$ M concentration for each molecule. Before starting the adsorption tests, it was recorded the UV-Vis spectrum for each molecule (named Time 0), the absorbance of which is proportional to the initial dye concentration as dictated by the Lambert-Beer law.

The experiments were carried out by using 10 ml of the solution and 100 mg of adsorbent material. The batch was left under magnetic stirring for 15 minutes, centrifuged for 3 minutes at 4000 rpm, and analysed with the UV-Vis spectrophotometer. After the measurement, the experiment starts again. To observe the kinetics behaviour the measurements were taken at the beginning in small time intervals and going ahead with the experiment the

time intervals were larger. For each experiment were taken 9 measures: Time 0, 15 minutes, 30 minutes, 1 hour, 2 hours, 3 hours, 5 hours, 7 hours and 24 hours.

Considering the Lambert-Beer's Law (eq. 7.4), the absorbance only depends on the solution concentration, assuming constant both the cell thickness (1 cm) and the molar absorption coefficient (ε) of the chemical species during the adsorption experiments.

Thanks to these experiments, it was possible to calculate and evaluate the adsorption kinetics, through the calculation of the percentage of the organic dyes adsorbed by the materials tested and their adsorption capacity.

The percentage of the organic dyes adsorbed was calculated with the following formula:

$$\%\text{adsorbed} = \frac{(A_{T0} - A_{Ti})}{A_{T0}} * 100 \qquad (7.17)$$

where $A_{T0}$ was the absorbance extrapolated by the graph at the maximum wavelength and $A_{Ti}$ was the absorbance extrapolated by the graph at the same wavelength for each measurement done.

After that was calculated the resulting concentration of the dye still in solution thanks to the formula:

$$C_i = \frac{C_0(100 - \%ads_{Ti})}{100} \qquad (7.18)$$

where $C_i$ was the concentration relative to the measures done at different times, $C_0$ was the concentration relative to the measurement at Time 0, which matches the concentrations of the stock solutions, and $\%ads_{Ti}$ was the percentage adsorbed at all the measurements done.

Obtained all the concentration relatives of all the measures done, knowing the volume of the solution and the weight of the Cls-based material used for

the experiments was possible to calculate the adsorption capacity for all the measures done with the following formula:

$$\text{Adsorption capacity} = \frac{(C_0 - C_i) * V * M_w}{m_c} \qquad (7.19)$$

where $C_0$ (mg/L) was the concentration relative to the measure at time 0, which matches the concentrations of the stock solutions, $C_i$ (mg/L) was the concentration relative to the measures done at different times, V (L) is the volume of the solutions using during the experiments, $M_w$ (g/mol) is the molar weight of the organic dyes and $m_c$ (g) was the weight of the Cls-based material.

In a preliminary stage, the adsorption tests involved a comparison between all the Cls-based materials obtained with the Fr method (washed in the Sxl with Et or unwashed) and with the Sxl using two different solvents (Ac or Et). In this way, it was possible to identify the best adsorbent material by evaluating the adsorption capacity for each experiment (tab.7.1).

The Cls-based material obtained after the Soxhlet washing with Ac didn't work with 4Nph and the same behaviour was observed with the freeze-dried sample.

Only the sample obtained by Fr and washed with the Sxl and the sample obtained by the Sxl using Et as the solvent had good results with all three organic dyes. Comparing these two materials, it was noticed that the best results were obtained using the Cls-based adsorbent material obtained with Fr process and washed with Sxl using Et as the solvent, but there weren't substantial differences in the adsorption capacity and considering the reduced time and consumption in the use only of the Sxl it was decided to choose it as synthesis protocol.

In the specific case of 4Nph, analysing the UV-Vis spectra of the Cls-based material obtained with Sxl using Ac as the solvent reported in Fig. 7.6, it can be observed a relative increase of the band intensity associated with anionic

form of the organic compound. This increase accompanied the gradual quenching of the absorption band ascribable to the neutral form of 4Nph referred to the Time 0 spectrum.

The stock solution is prepared with deionized water at pH = ~ 6.0; the addition of the adsorbent material into the solution changes the pH, thus influencing the absorption spectrum of 4Nph. After 3 hours, it wasn't possible to measure the spectrum because the signal was out of recording scale due to high concentration of the analyte (> 0.01 M). The possible explanation of this phenomenon is that the 4Nph dye is not adsorbed on the surface of the Cls-based material after the pH changing of the solution. The variation of the pH from acid to basic regime can be rationalized in the light of the presence of the amine groups deriving from bPEI branching agent.

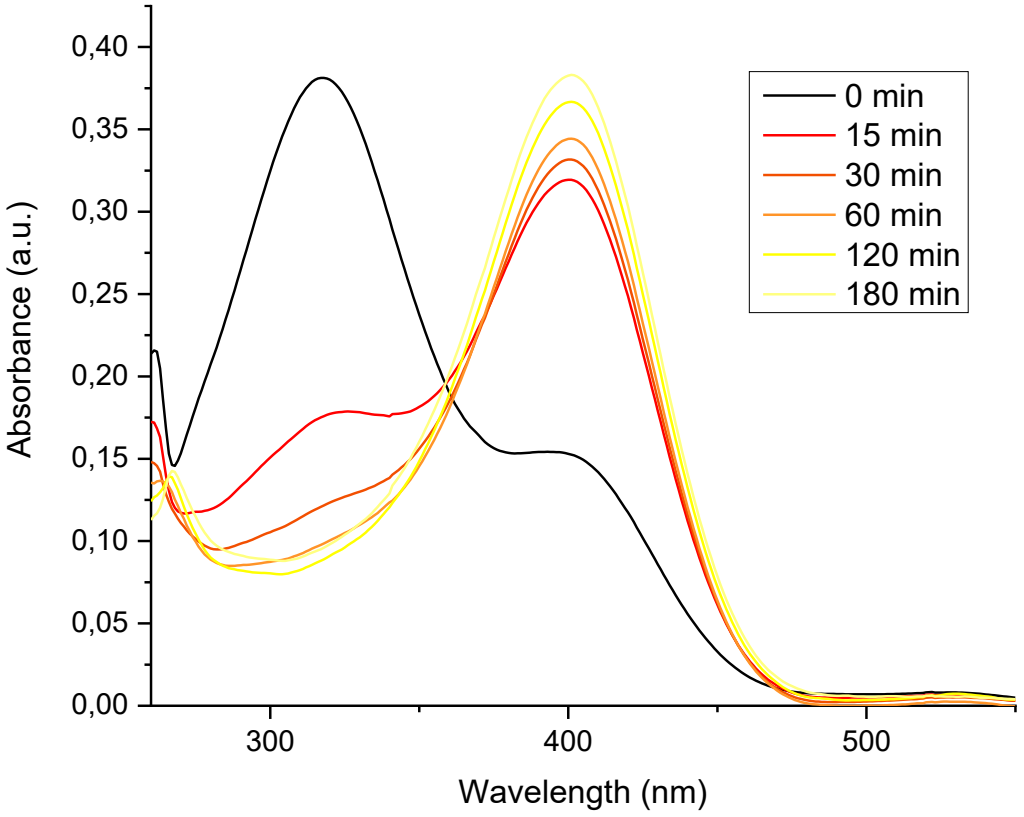


Fig. 7.6 – Evolution of the absorption spectra during the adsorption tests with Cls-based material obtained with Sxl using Ac as the solvent and 4Nph as the dye.

A completely different behaviour was observed in the experiment with Cls-based material obtained using the Sxl with Ac as the solvent and 4NBAld as the dye. As shown in Fig. 7.7, the peak at 268 nm completely disappears after 15 minutes with the emergence of a new absorption band at 240 nm. Therefore, considering the absorption band at 268 nm to calculate the 4NBAld elimination, after 15 minutes there was the total adsorption of the molecule. However, it is more correct to state that in the first 60 minutes, there is a conversion of 4NBAld into a species that absorbs at 240 nm (probably the hydrate form of the aromatic aldehyde) catalysed

by the Cls-based material surface. After this reaction, it was observed a gradual absorption of the new derivative.

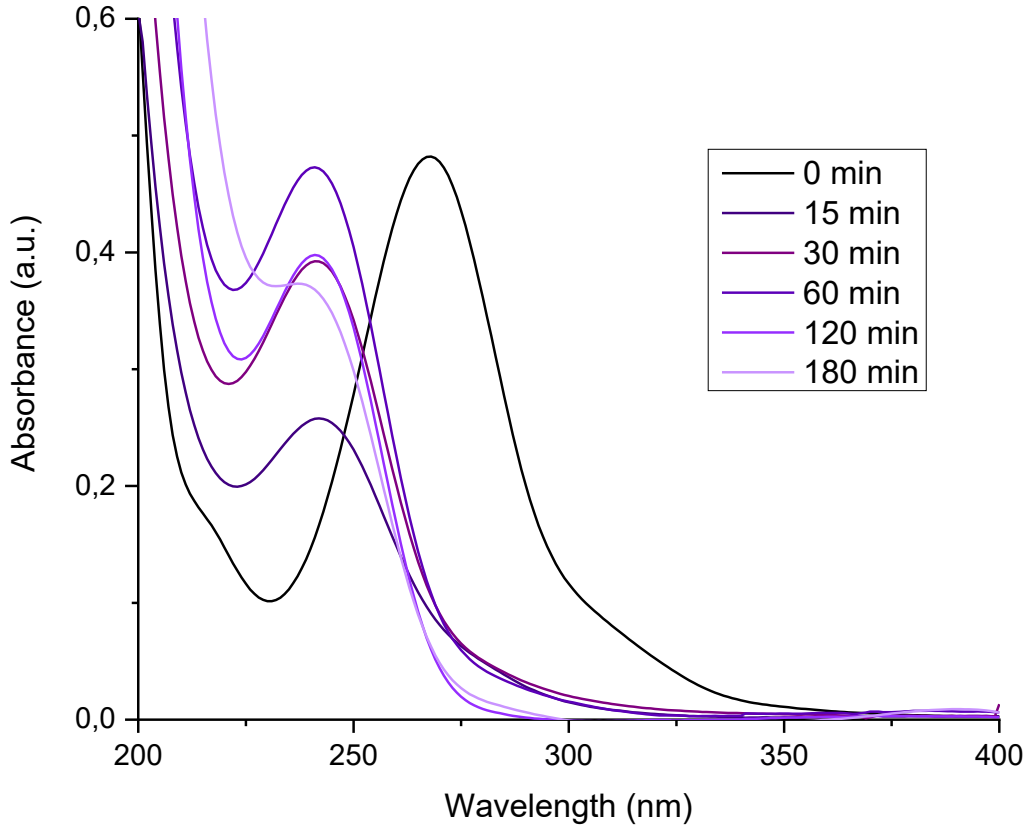


Fig. 7.7 – Evolution of the absorption spectra during the adsorption tests with Cls-based material obtained with Sxl using Ac as the solvent and 4NBAld as the dye.

In the case of the adsorption tests with MB (Fig. 7.8), it can be observed the gradual absorbance decreasing as a function of time. Being preserved the absorption profile of the dye, it is possible to assert that the MB is adsorbed at the surface of the Cls-based material.

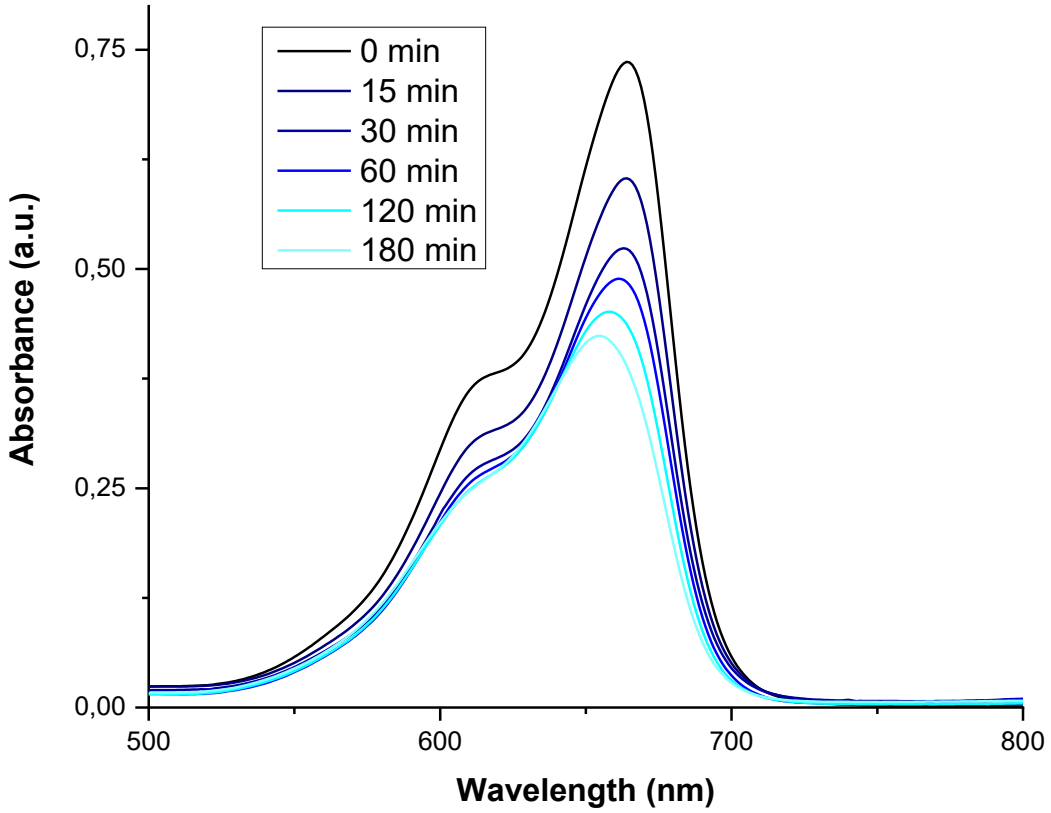


Fig. 7.8 – Evolution of the absorption spectra during the adsorption tests with Cls-based material obtained with Sxl using Ac as the solvent and MB as the dye.

Implementing in a graph the adsorbed dye percentage as a function of time (Fig. 7.9), it can be deduced that 4NBAld is the preferentially adsorbed molecule of the series by the Cls-based material obtained with Sxl using Ac as the solvent. The observed kinetics is in a very short period of time, therefore it allows to affirm that being the percentage adsorbed in this period of time is low, the kinetics of the adsorption is slow. It would be necessary to carry out further tests in a longer period of time in order to be able to state with certainty if the kinetics is slow, therefore it takes more time to arrive at a 100% adsorption.

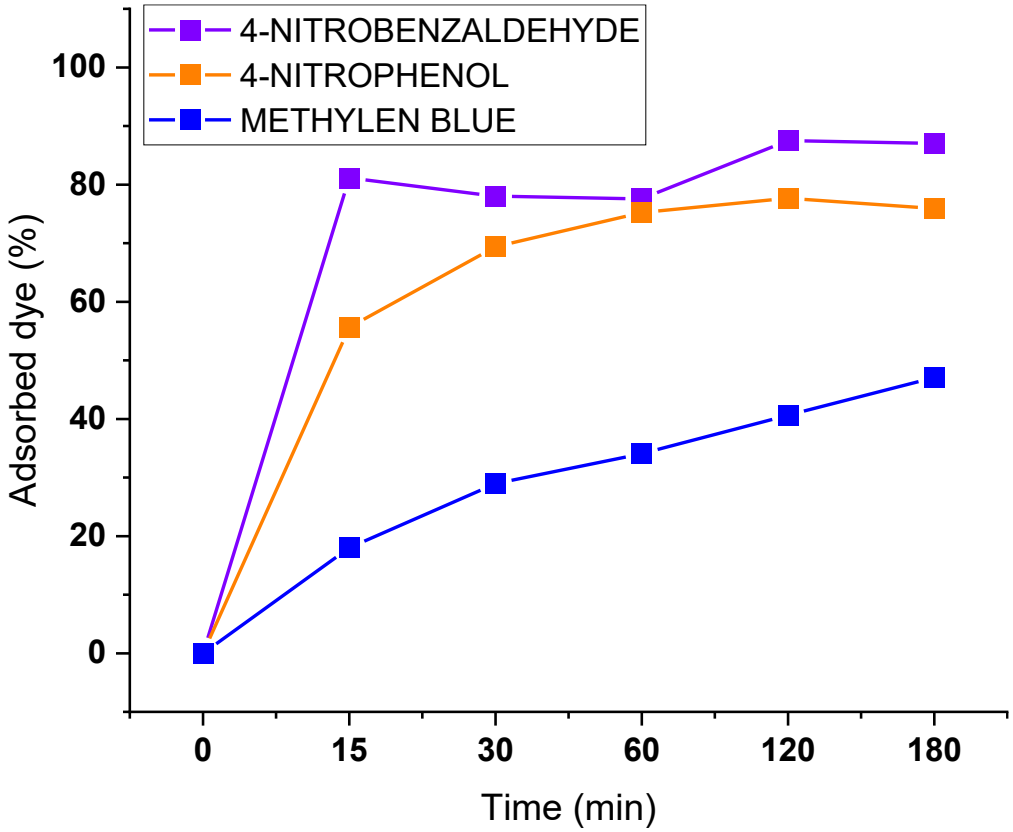


Fig 7.9 – Percentage of contaminant adsorbed by the Cls-based material obtained with Sxl using Ac as solvent.

The second material tested in adsorption experiments was the Cls-based material obtained from a Fr process. In the case of 4Nph, it was observed a red shift of the absorption maximum of the species upon the introduction of the adsorbent into the dye solution. This result suggests the evolution of the anionic species of 4Nph, that, as evident from Fig. 7.10, was not adsorbed by the material.

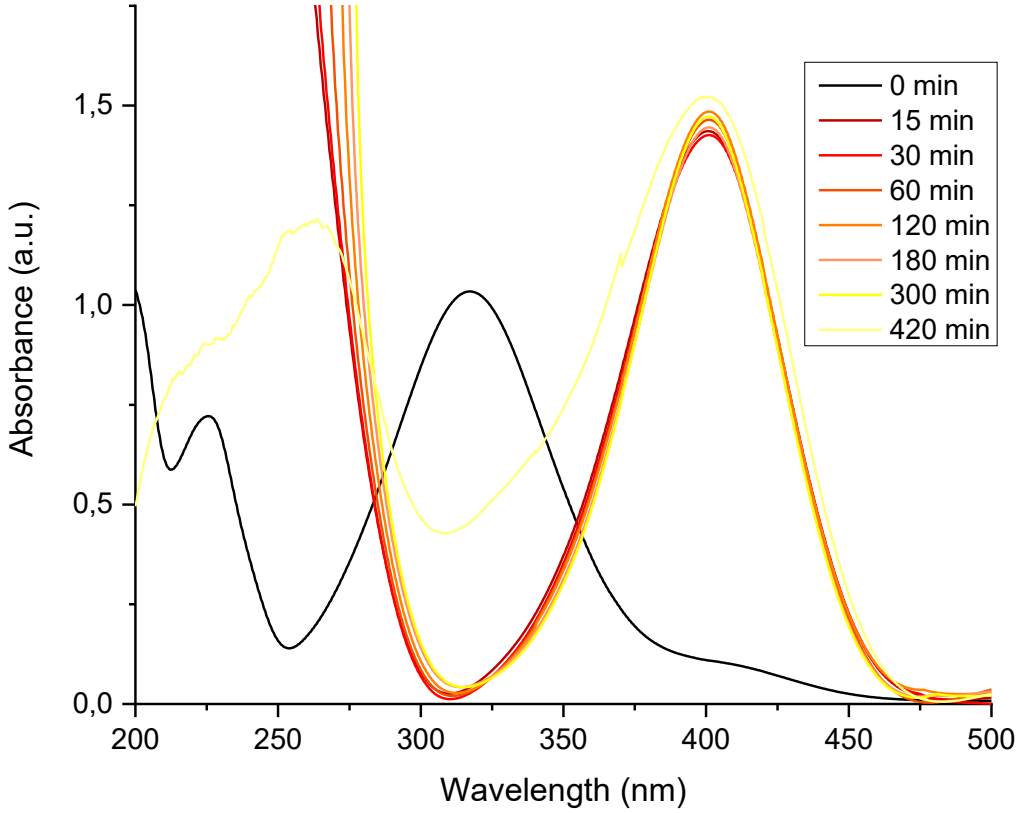


Fig. 7.10 – Evolution of the absorption spectra during the adsorption tests with Cls-based material obtained with Fr and 4Nph as the dye.

The Cls-based material was also tested with MB (Fig7.11) and it was possible to observe that the peak was decreasing. This means that MB was adsorbed on the Cls-based material surface.

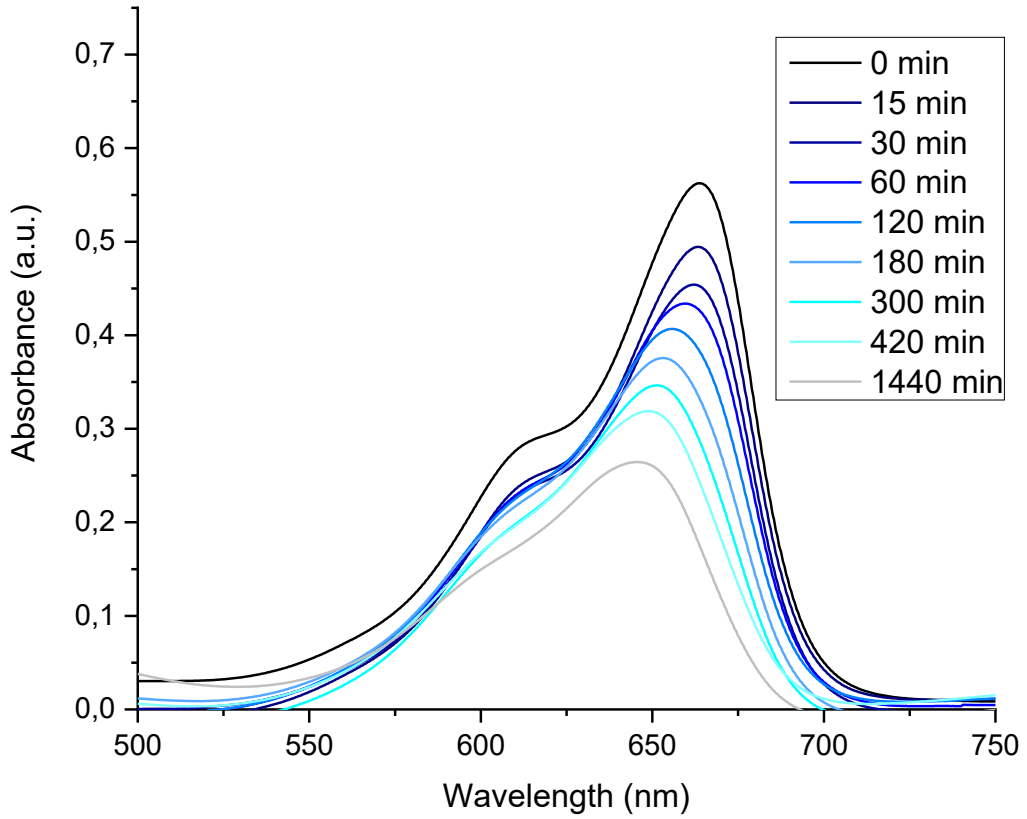


Fig. 7.11 – Evolution of the absorption spectra during the adsorption tests with Cls-based material obtained with Fr with MB as the dye.

The evaluation of the 4NBAld adsorption was not possible with these dye concentrations, because after 30 minutes the signal was out of recording scale.

Only the kinetics of MB and 4Nph were evaluated and reported in the graph (fig. 7.12). Also in this case the MB kinetics is very slow. After 24 hours (1440 minutes) only the 70% was adsorbed by the Cls-based material. The 4Nph was adsorbed for the 95% in only 15 minutes, but after 7 hours (420 minutes) was released and the percentage adsorbed decreased at 50%.

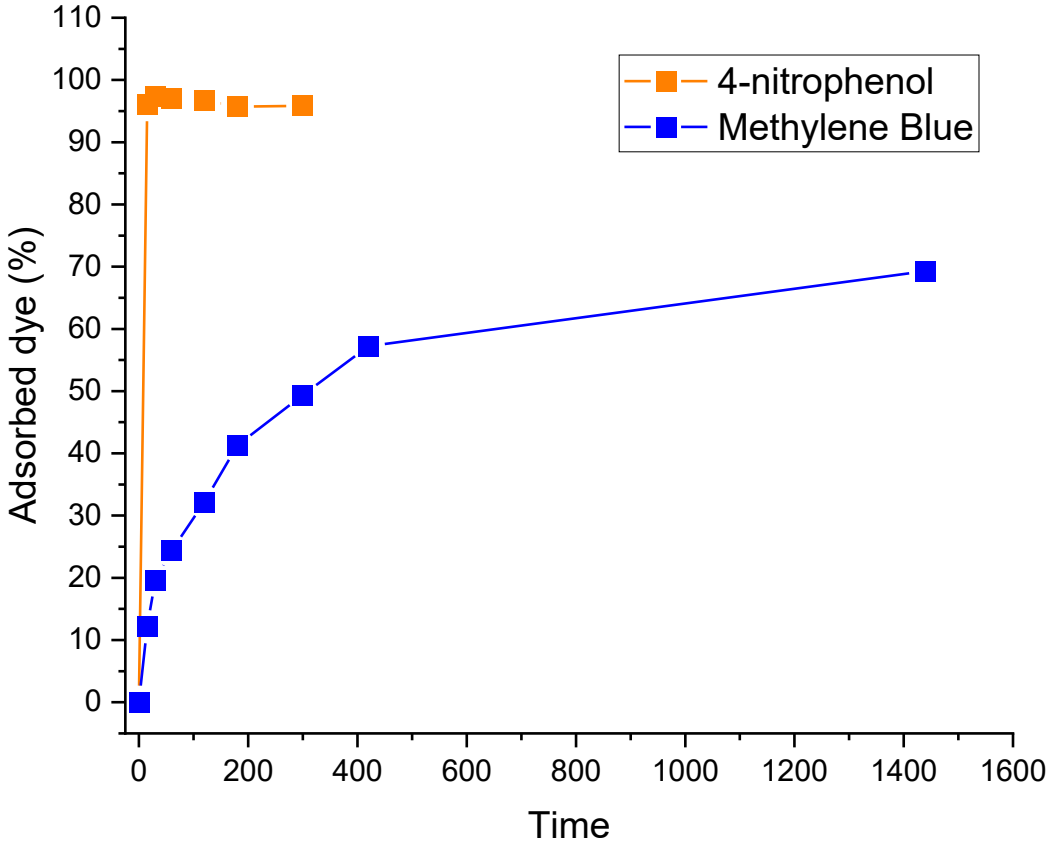


Fig 7.12 – Percentage of contaminant adsorbed by the Cls-based material obtained with Fr.

The third material tested was the Cls-based material obtained with Fr and washed in the Sxl with Et.

The behaviour of the 4Nph was the same as in the other tests. The peak at 268 nm is red shifted at 400 nm and its intensity increased instead of decreased (Fig7.13). In the kinetics was considered the peak at 268 nm and resulted a percentage of absorption equal to 95%.

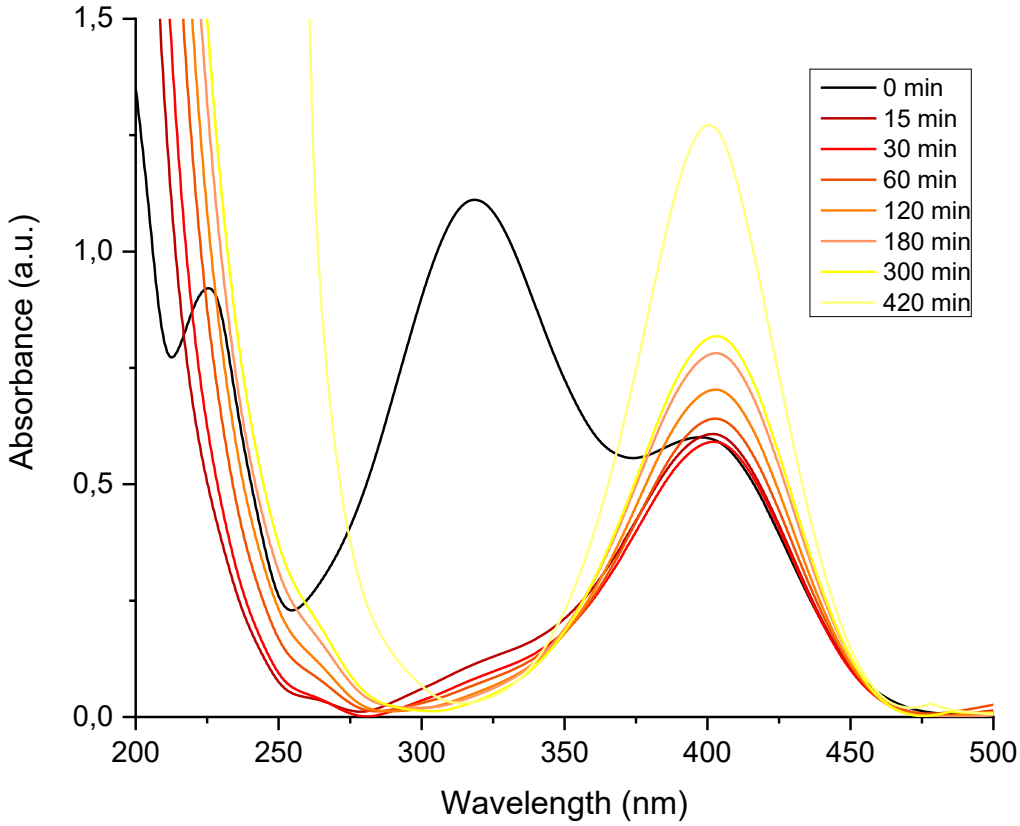


Fig. 7.13 – Evolution of the absorption spectra during the adsorption tests with Cls-based material obtained with Fr and washed in Sxl using Et as solvent and 4Nph as the dye.

The Cls-based material obtained with freeze drying and washed with Et was tested with 4NBAld (Fig. 7.14). Also in this case there was an unexpected behaviour. In 15 minutes the adsorption is very high, so the peak decrease, but in 30 minutes the 4NBAld was released again in solution and after 60 minutes the signal went out of scale so the experiment was stopped.

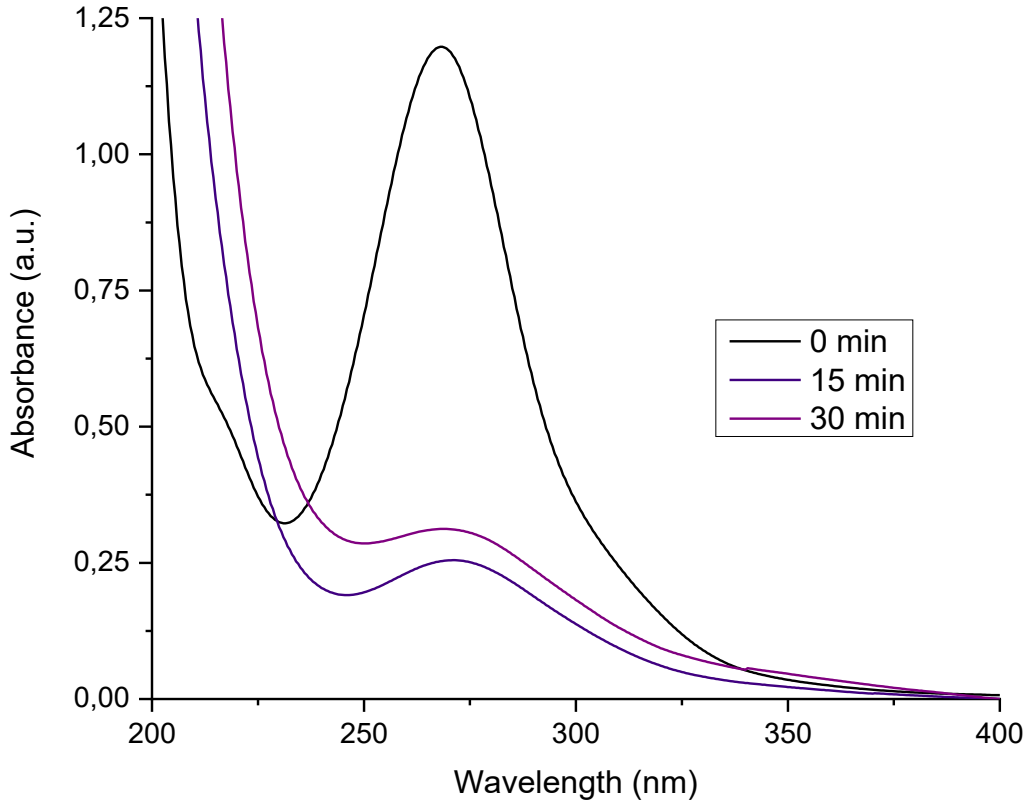


Fig. 7.14 – Evolution of the absorption spectra during the adsorption tests with Cls-based material obtained with Fr and washed in Sxl using Et as solvent and 4NBAld as the dye.

The last experiment with Cls-based material obtained by Fr and washed in Sxl with Et was with the MB solution (Fig.7.15). In this case was possible to observe a small decreasing of the signal after 15 minutes.

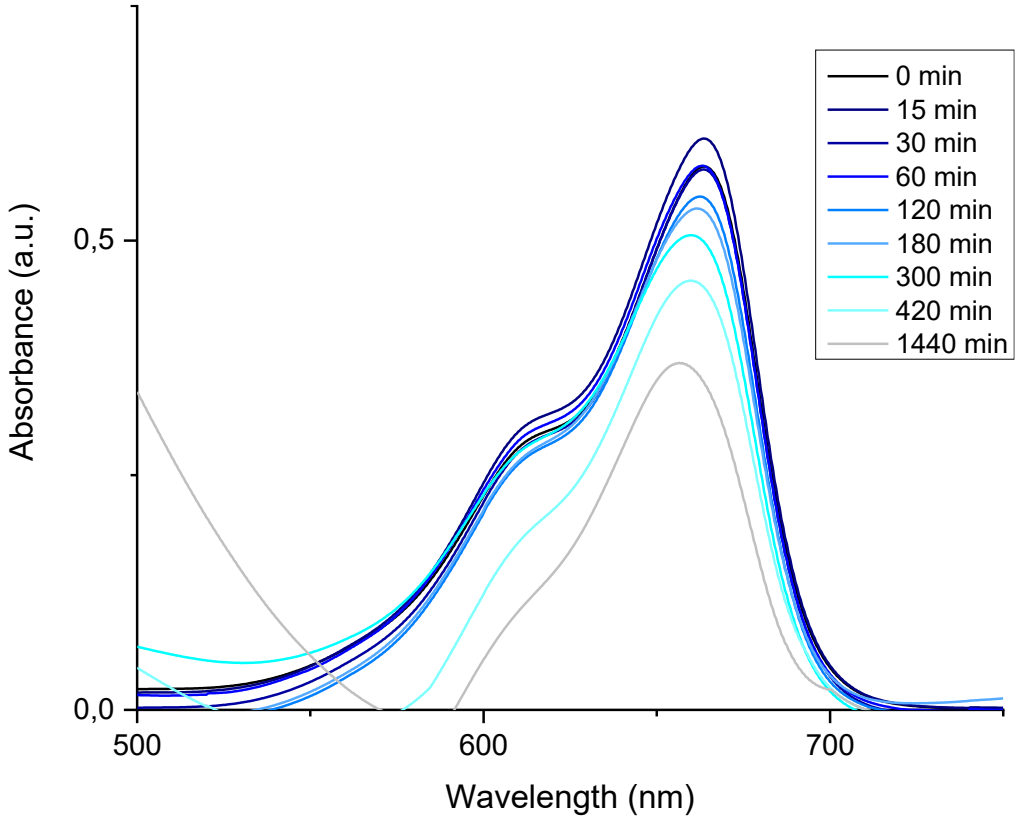


Fig. 7.15 – Evolution of the absorption spectra during the adsorption tests with Cls-based material obtained with Fr and washed in Sxl using Et as solvent and MB as the dye.

Comparing the dye adsorption percentage it is possible to affirm that the MB removal is very slow (>50% after 24 hours). Even if the 4Nph had an adsorption over the 90% the problem is the red shift and the possible conversion from 4Nph to another molecule that absorb the light at 400 nm.

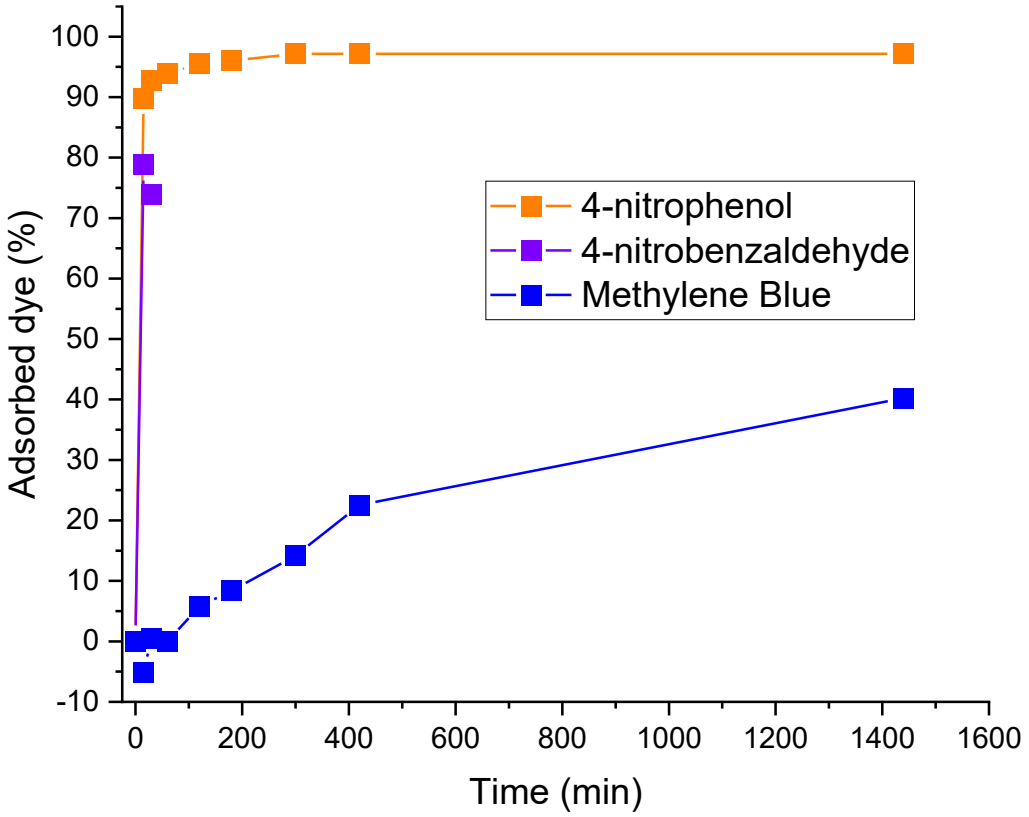


Fig 7.16 – Percentage of contaminant adsorbed by the Cls-based material obtained with Fr and washed in Sxl using Et as solvent.

The last Cls-based material tested was obtained with the Sxl using Et as solvent. The first test was with 4Nph solution, and also in this case there was the red shift of the peak from 268 nm to 400 nm (Fig. 7.17). The signal at 400nm decreased for the first 3 hours (180 minutes), but after 5 hours (300 minutes) it was increased and after that it went out of scale and the experiment was stopped.

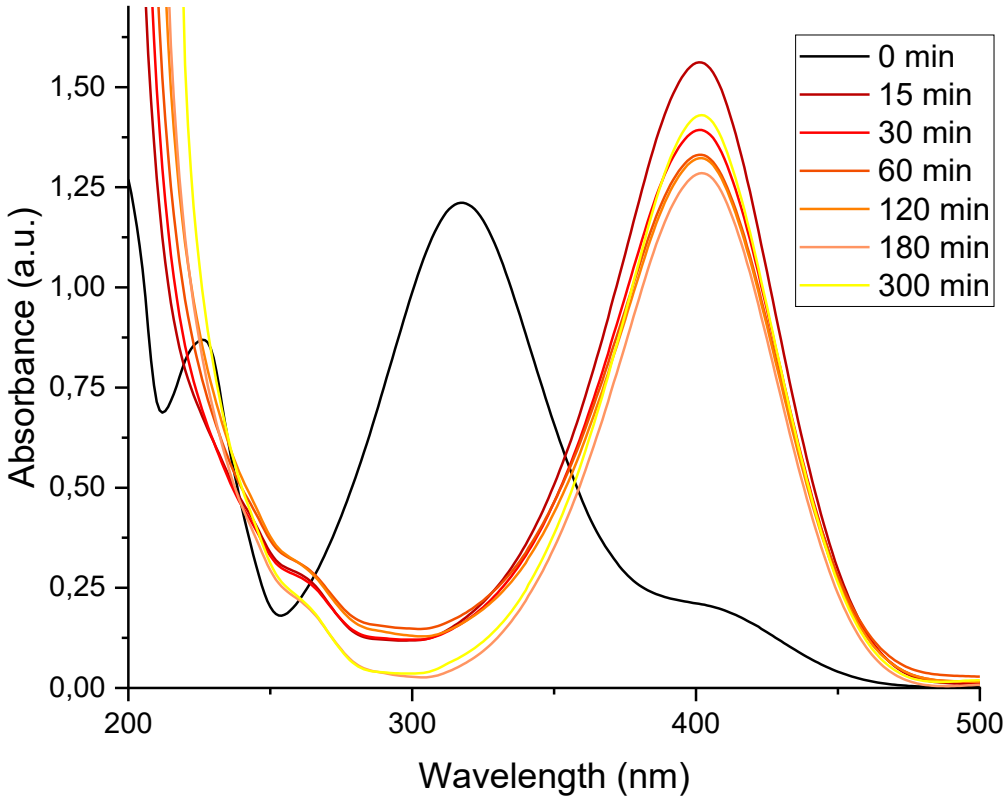


Fig. 7.17 – Evolution of the absorption spectra during the adsorption tests with Cls-based material obtained with Sxl using Et as solvent and 4Nph as the dye.

The 4NBAld solution tested with Cls-based material obtained with Sxl using Et as solvent gave good results after 15 minutes (Fig. 7.18). After 24 hours (1440 minutes) there was only adsorption and nothing was released in solution.

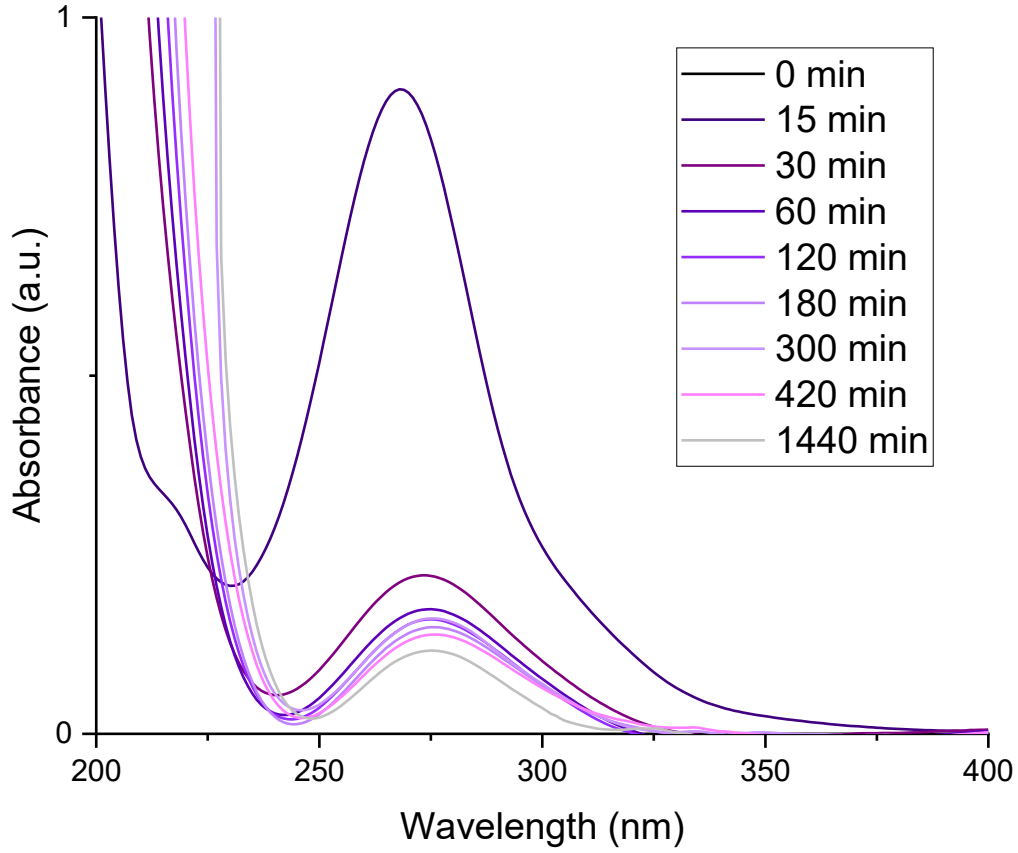


Fig. 7.18 – Evolution of the absorption spectra during the adsorption tests with Cls-based material obtained with Sxl using Et as solvent and 4NBAld as the dye.

Also MB was adsorbed by Cls-based material obtained with the Sxl using Et as solvent, but after 24 hours (1440 minutes) the peak was not too much smaller than the peak registered at time 0 (Fig. 7.19).

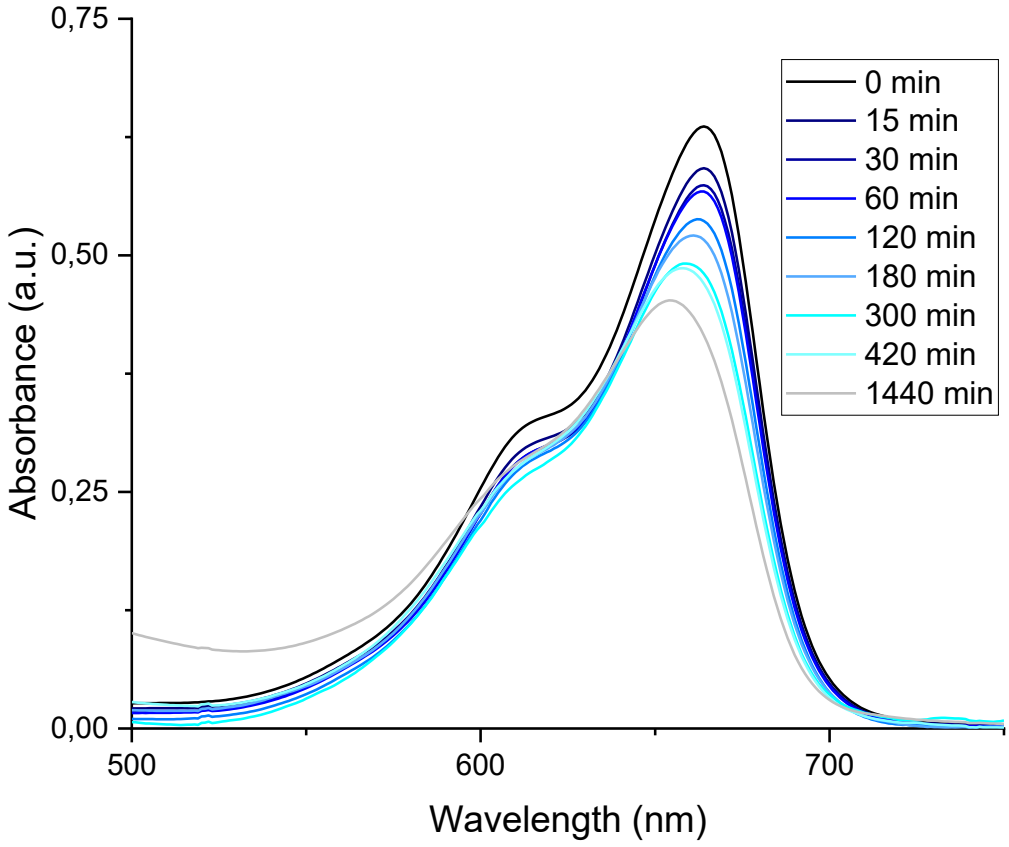


Fig. 7.19 – Evolution of the absorption spectra during the adsorption tests with Cls-based material obtained with Sxl using Et as solvent and MB as the dye.

Evaluating the kinetics of the three solutions (Fig.7.20) only the 4Nph didn't give good results because after 5 hours (300 minutes) the experiment was stopped and the contaminant was released again in the solution so the signal went out of scale during the measure.

The 4NBAld was adsorbed after 15 minutes for 80% and this percentage remained stable for 24 hours.

The trend of the MB was better than the trend that it had with the previous Cls-based materials, but it stopped at 40% also in this case.

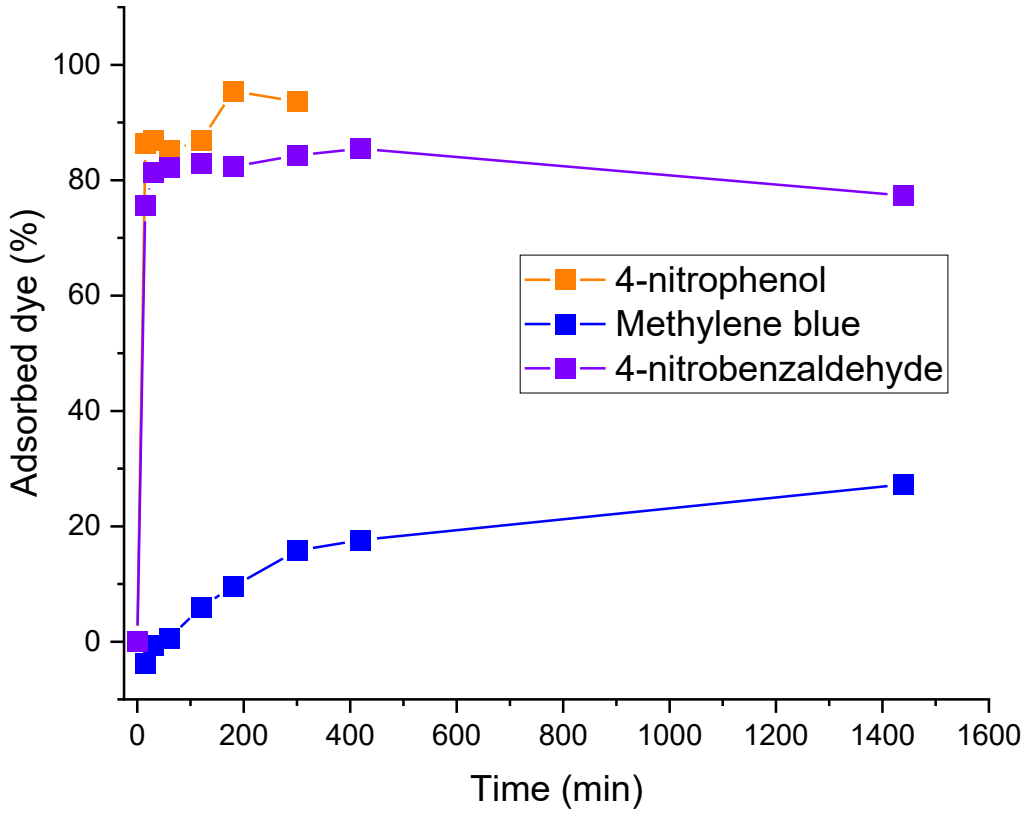


Fig. 7.20 - Percentage of contaminant adsorbed by the Cls-based material obtained with Sxl using Et as solvent.

Comparing all the Cls-based materials it is possible to affirm that the best results were obtained with the material obtained with the Fr and washed in the Sxl with Et as solvent and the material obtained with the Sxl using Et as solvent. The results of these two materials are very closed in terms of absorption capacity, but it was observed better properties and more resistance during the experiments in the second one because the Cls-based material obtained with the Sxl using Et as solvent didn't crumble during the 24 hours of the experiments. The worst material, that crumbled after a few minutes, was the Cls-based material obtained by Fr process.

After all these preliminary tests it is possible to assert that considering the adsorption tests results and the time and the energy necessary to produce the material the best compromise is obtained with the Cls-based material obtained with Sxl using Et as solvent.

Table 7.1. Adsorption capacity obtained from the adsorption tests.

| **Sample** | **Dye** | **Adsorption capacity (mg/g)** | **Initial dye concentration (mol/L)** | **Final dye concentration (mol/L)** | **Cellulose (g)** |
|---|---|---|---|---|---|
| Sxl 5h with Ac | 4-nitrophenol | X | $1.2*10^{-4}$ | X | 0.1 |
| | 4-nitrobenzaldehyde | 1.4 | $10^{-4}$ | $7*10^{-6}$ (5h) | 0.1 |
| | Methylene Blue | 16 | $10^{-3}$ | $4.5*10^{-4}$ (4h) | 0.1 |
| Freeze-dryed | 4-nitrophenol | 0.9 | $1.2*10^{-4}$ | $5.3*10^{-5}$ (3h) | 0.1 |
| | 4-nitrobenzaldehyde | X | $10^{-4}$ | X | 0.1 |
| | Methylene Blue | 22 | $10^{-3}$ | $3*10^{-4}$ | 0.1 |
| Freeze-dryed + Sxl 24 h | 4-nitrophenol | 1.6 | $1.2*10^{-4}$ | $3.4*10^{6}$ | 0.1 |
| | 4-nitrobenzaldehyde | 1.1 | $10^{-4}$ | $2.6*10^{-5}$ (30min) | 0.1 |
| | Methylene Blue | 12 | $10^{-3}$ | $6*10^{-4}$ | 0.1 |
| Sxl 24 h with Et | 4-nitrophenol | 1.5 | $1.2*10^{-4}$ | $6.5*10^{-6}$ (7 h) | 0.1 |
| | 4-nitrobenzaldehyde | 0.9 | $10^{-4}$ | $4.6*10^{-5}$ | 0.1 |
| | Methylene Blue | 8.4 | $10^{-3}$ | $7.3*10^{-4}$ | 0.1 |

After these experiments was possible established that the better way to produce the Cls-based material was the Sxl and the best solvent Et.

This synthesis protocol is optimized also for the Chn-based material.

The Chn-based material was also tested with the same three organic dye, in the same conditions of Cls-based materials.

These two materials were compared in adsorption tests preparing three replicates for each experiment.

All these three organic dyes were tested with both Cls-based and Chn-based materials obtained with the Soxhlet extraction using Et as the solvent. For each adsorbent material tested with a dye, summarizing data were based on the average of three replicates.

Table 7.2 reports all the results for each experiment, while the graphs reported the adsorbed dye (%) in function of the time are the media of the three replicates with the associated error.

The first material tested was Cls-based with the 4Nph solution. Because of the previous results with this dye, in this second phase, more extensive tests were carried out and the behaviour of this dye at different pH values was investigated.

The first test was done with a pH equal to 12.4. It is possible to observe that there is only a signal at 400 nm (Fig.7.21). The decrease in the peak is not significant this may be due to poor adsorption on the surface of the material.

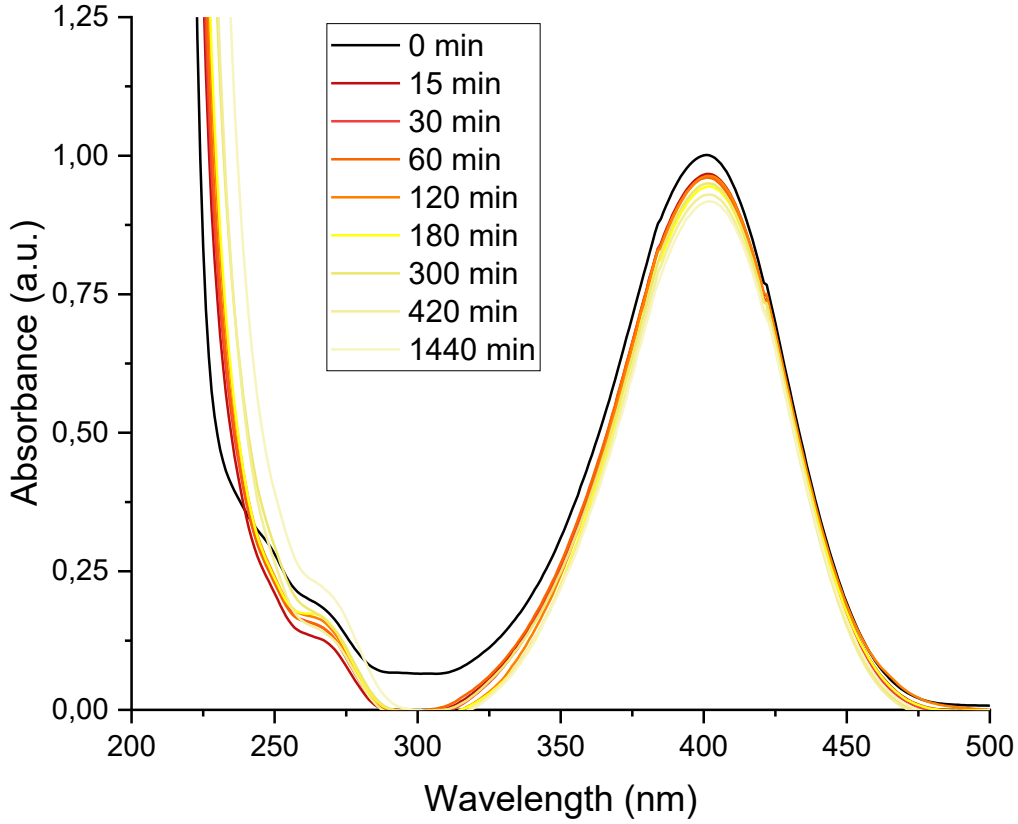


Fig. 7.21 – Evolution of the absorption spectra during the adsorption tests with Cls-based material obtained with Sxl using Et as solvent and 4Nph as the dye with pH~12.4.

The second test was done with a pH equal to 8.4 (Fig. 7.22). It is possible to observe that the principle signal was at 400 nm and there was a secondary signal at 323 nm. The higher signal at 400 nm means that in the solution there was its basic form, phenate, in greater quantity than the phenol form.
As in the previous experiments, it was possible to observe that the signal at 323 nm was completely knocked down in 15 minutes, while the phenate peak increased and then decreased.

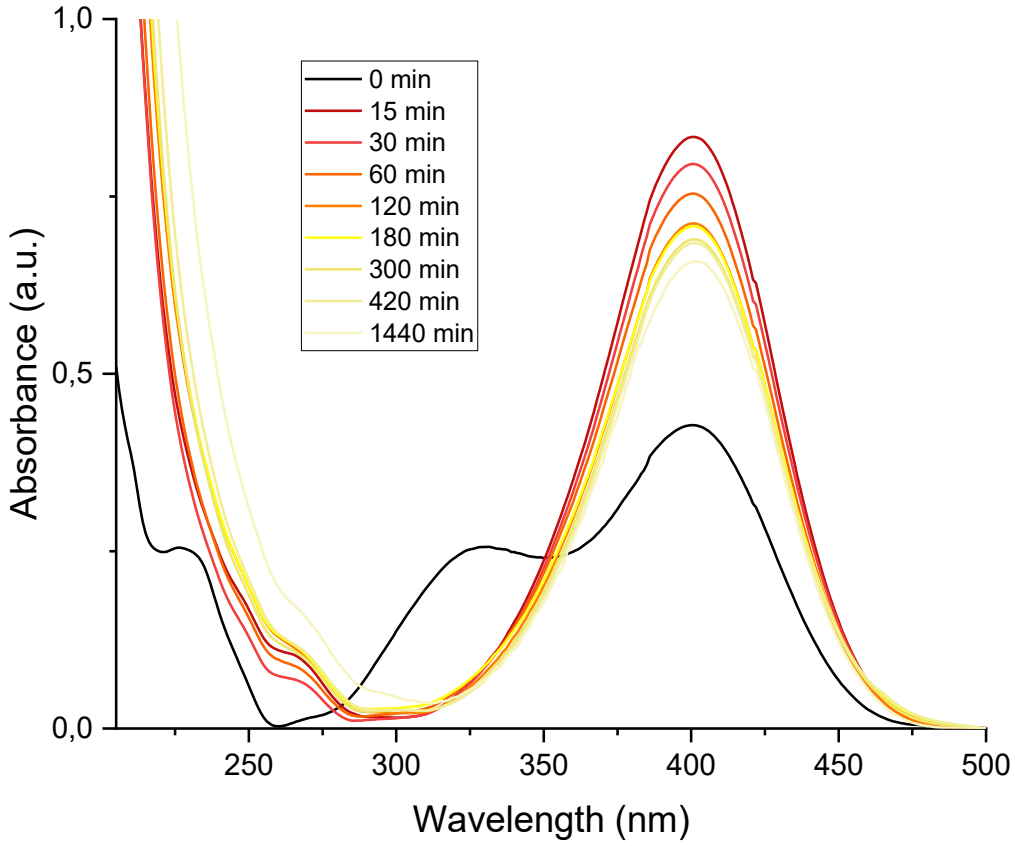


Fig. 7.22 – Evolution of the absorption spectra during the adsorption tests with Cls-based material obtained with Sxl using Et as solvent and 4Nph as the dye with pH ~ 8.4.

After that, another 4Nph solution was prepared with a pH equal to 1 (fig.7.23). In the graph, the only signal visible is at 317 nm, which is the typical signal of the 4Nph. The absorption process is very slow and only after 24 hours (1440 minutes) it was possible to observe a small decrease in the signal.

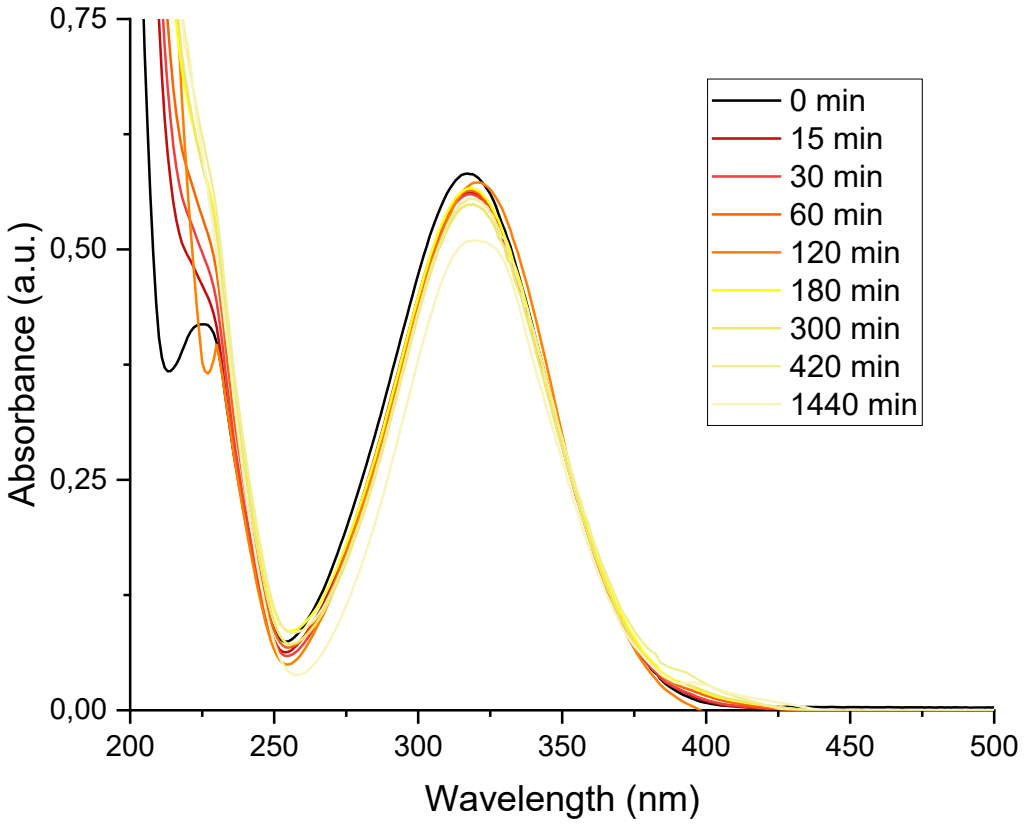


Fig. 7.23 – Evolution of the absorption spectra during the adsorption tests with Cls-based material obtained with Sxl using Et as solvent and 4Nph as the dye with pH ~ 1.

The second dye tested was 4NBAld (Fig. 7.24); by the graphs is possible to note that after 15 minutes the most of the dye was adsorbed by the Cls-based material and the concentration in the solution decreased with time.

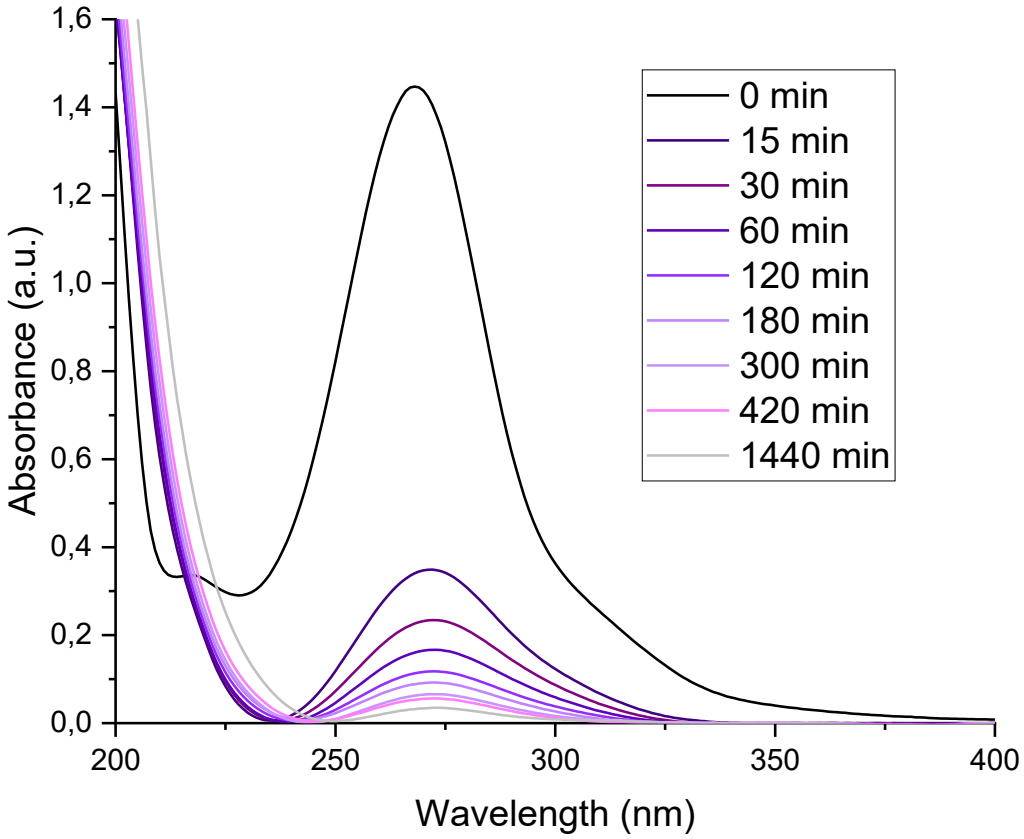


Fig. 7.24 – Evolution of the absorption spectra during the adsorption tests with Cls-based material obtained with Sxl using Et as solvent and 4NBAld as the dye.

In the case of MB, it can be observed that, even if there was a gradual lowering of the dye absorption (Fig. 7.25), the adsorption entity on this Cls-based material cannot be considered satisfactory.

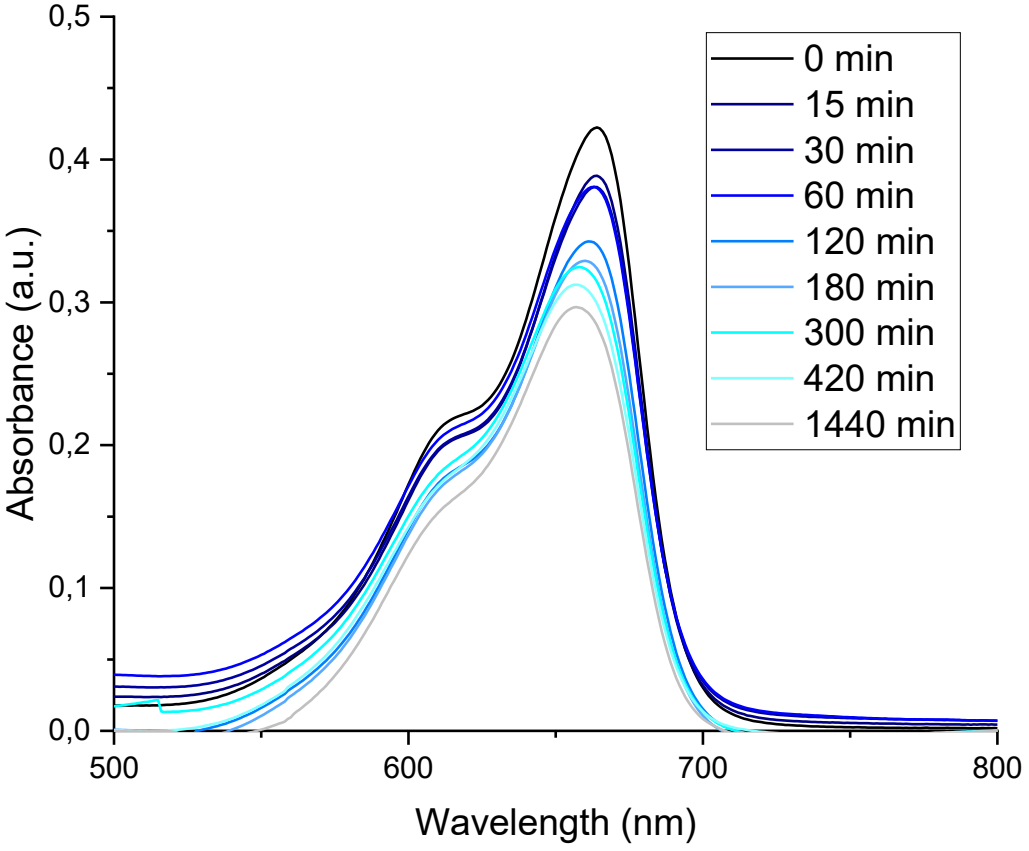


Fig. 7.25 - Evolution of the absorption spectra during the adsorption tests with Cls-based material obtained with Sxl using Et as solvent and MB as the dye.

Comparing the dyes adsorption percentages reported in Fig. 7.26, it is possible to assert that the Cls-based material suppressed ~80% of 4NBAld in only 15 minutes reaching 97% upon 24 h. Conversely, the MB adsorption increased slowly up to ~30% in 24 h. Interestingly, the adsorption behaviour of 4Nph solutions at pH equal to 12.4, 8.4 and 1.

The solution at pH 12.4 gave the worst result because the adsorption was nearby the 15%. For the solution at pH equal to 8.4, there are two lines: the first with squared is relative to the signal at 323 nm and it's possible to observe that the adsorption was equal to 75 %, instead the line relative to the peak at 400 nm (with the sphere) had the negative sign because there

was an increase after 15 minutes due the transformation from the phenol form to the phenate form. After 24 hours (1440 minutes) there was -60% absorption on Cls-based material. So the percentage of adsorption was equal to 40%.

For the 4Nph solution with a pH equal to 1 the percentage of the adsorption is very small, about 10%.

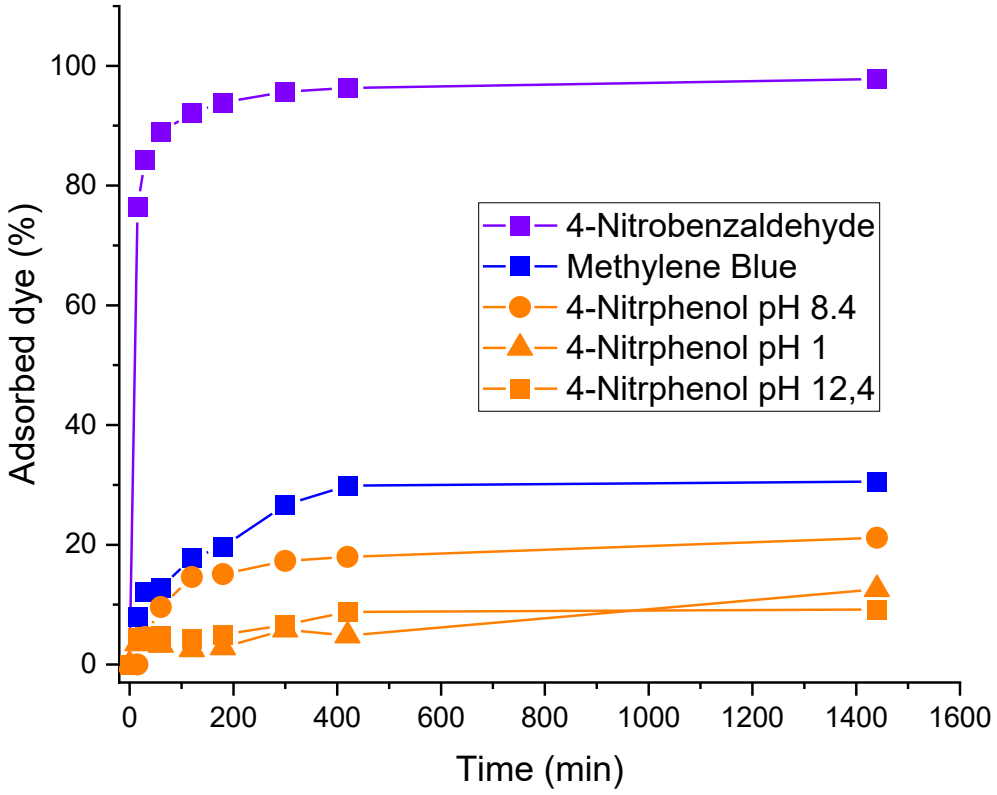


Fig. 7.26 - Average (based on three replicates) of the contaminants adsorption percentages performed by the Cls-based material.

The tests were also conducted in the same conditions with the Chn-based material. The first dye tested was the 4Nph both at pH equal to 12.4, 8.4 and 1.

The basic solution showed the adsorption peak at 400 nm (Fig. 7.27). it is possible to observe that in the first minutes, there was no significative adsorption.

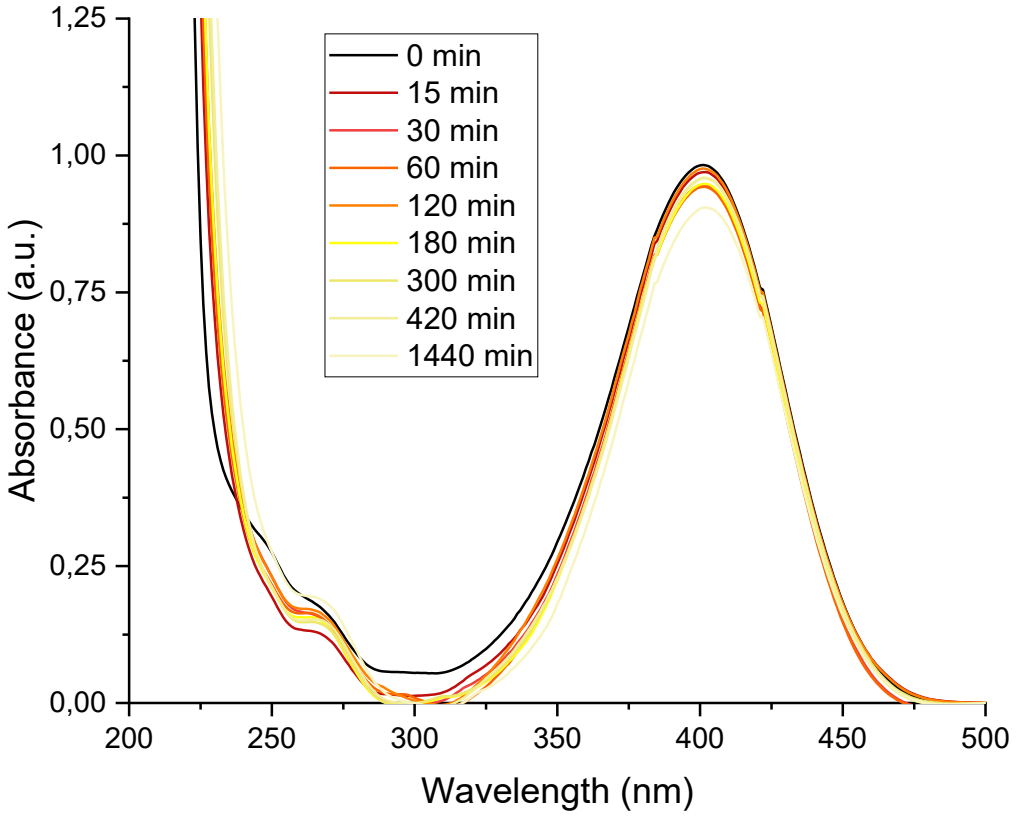


Fig. 7.27 – Evolution of the absorption spectra during the adsorption tests with Chn-based material obtained with Sxl using Et as solvent and 4Nph as the dye with pH ~ 12.4.

The solution at pH 8.4 showed two absorption bands at 400 nm (anionic form) and 323 nm (neutral form) ascribable to the dye. After 15 minutes the signal at 323 nm went down and there was the formation of the phenate and the increase of the relative signal at 400 nm. After 30 minutes from the beginning of the experiments, the phenate form was adsorbed on the Chn-based material, and after 3 hours (180 minutes) the adsorption seemed to be stopped and the signal didn't go down.

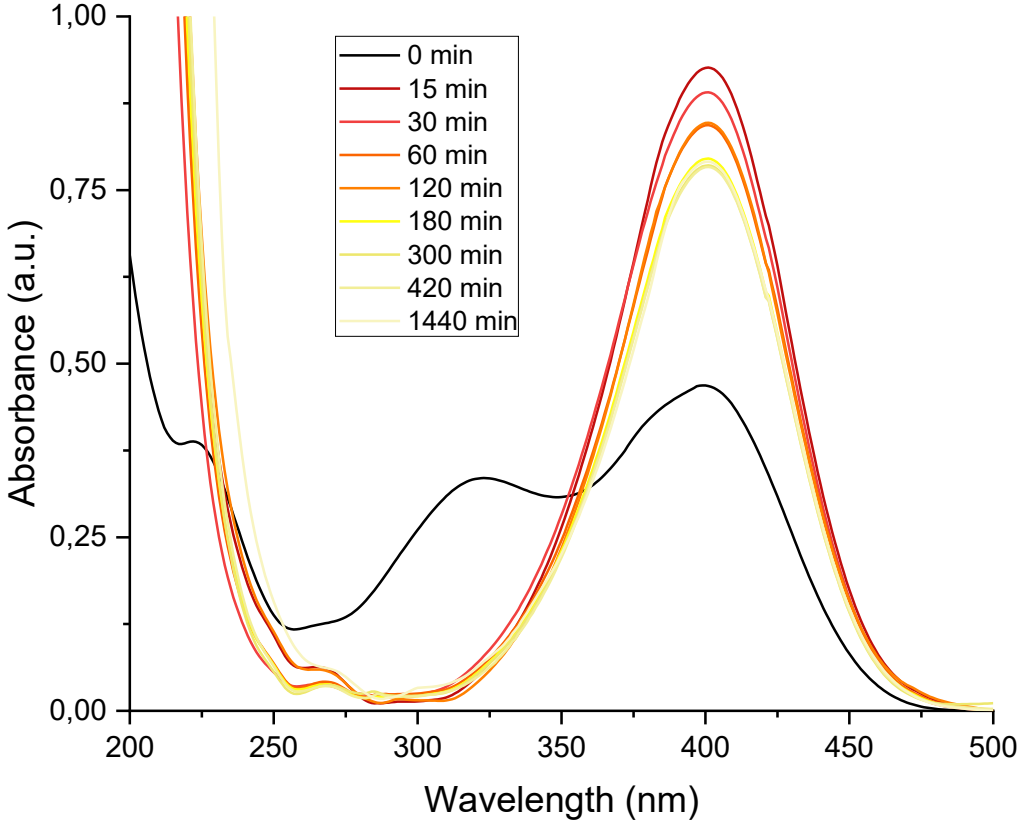


Fig. 7.28 – Evolution of the absorption spectra during the adsorption tests with Chn-based material obtained with Sxl using Et as solvent and 4Nph as the dye with pH ~ 8.4.

The test with the solution with a pH equal to 1 gave only one peak at 317 nm and unlike Cls-based material after 15 minutes there was a first drop in signal that remained constant for the majority of the time and decreased after 24 hours (1440 minutes).

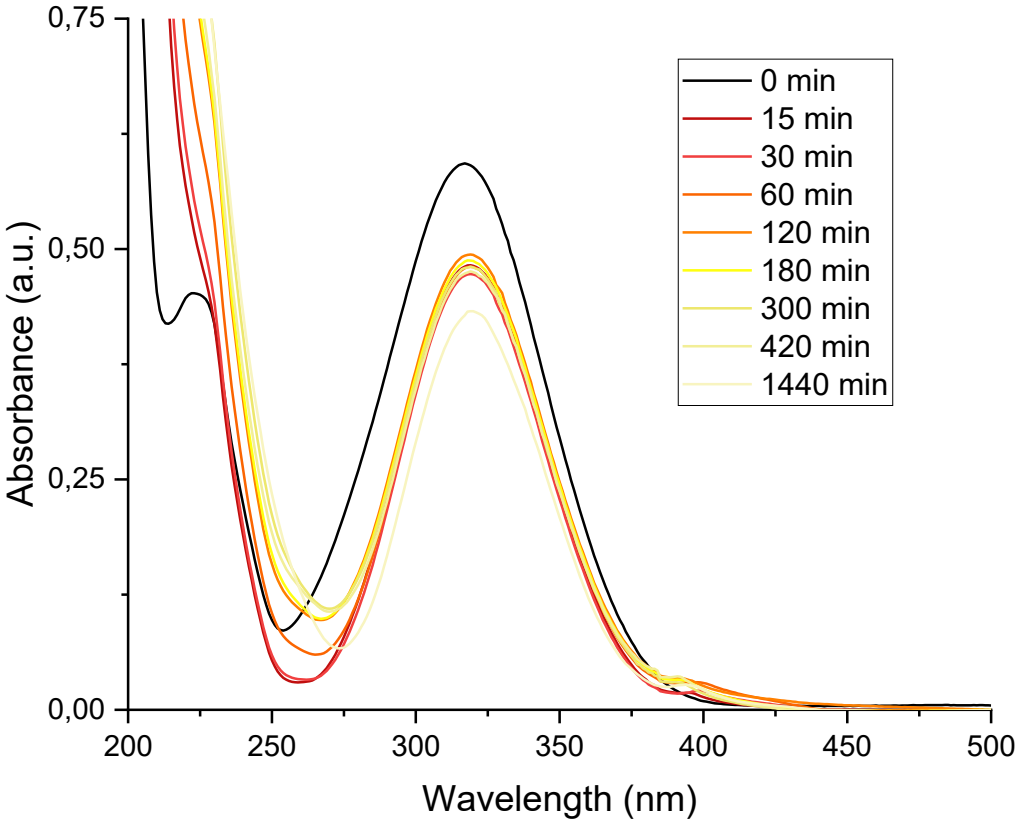


Fig. 7.29 – Evolution of the absorption spectra during the adsorption tests with Chn-based material obtained with Sxl using Et as solvent and 4Nph as the dye with pH ~ 1.

The second dye tested was the 4NBAld which demonstrated that was adsorbed very fast because the peak decreased a lot in the first 15 minutes and continued for the rest of the time.

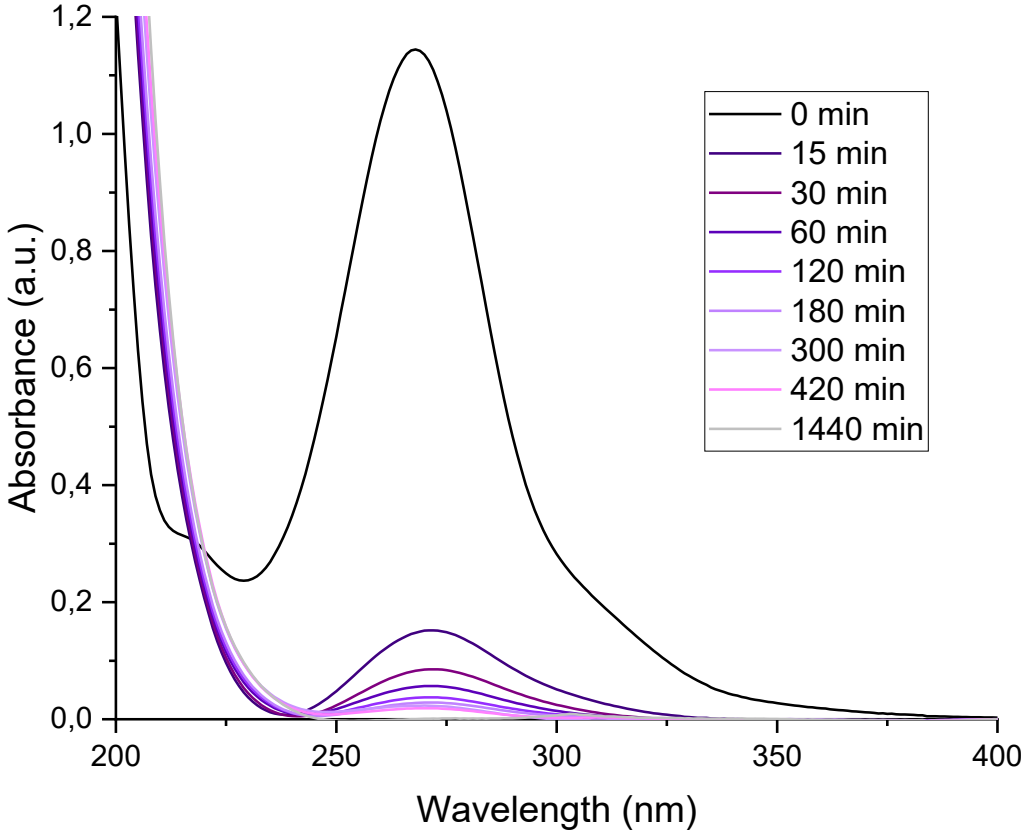


Fig. 7.30 – Evolution of the absorption spectra during the adsorption tests with Chn-based material obtained with Sxl using Et as solvent and 4NBAld as the dye.

The Chn-based material was tested with MB and it is possible to observe a decrease in the signal after 15 minutes and a small decrease with time.

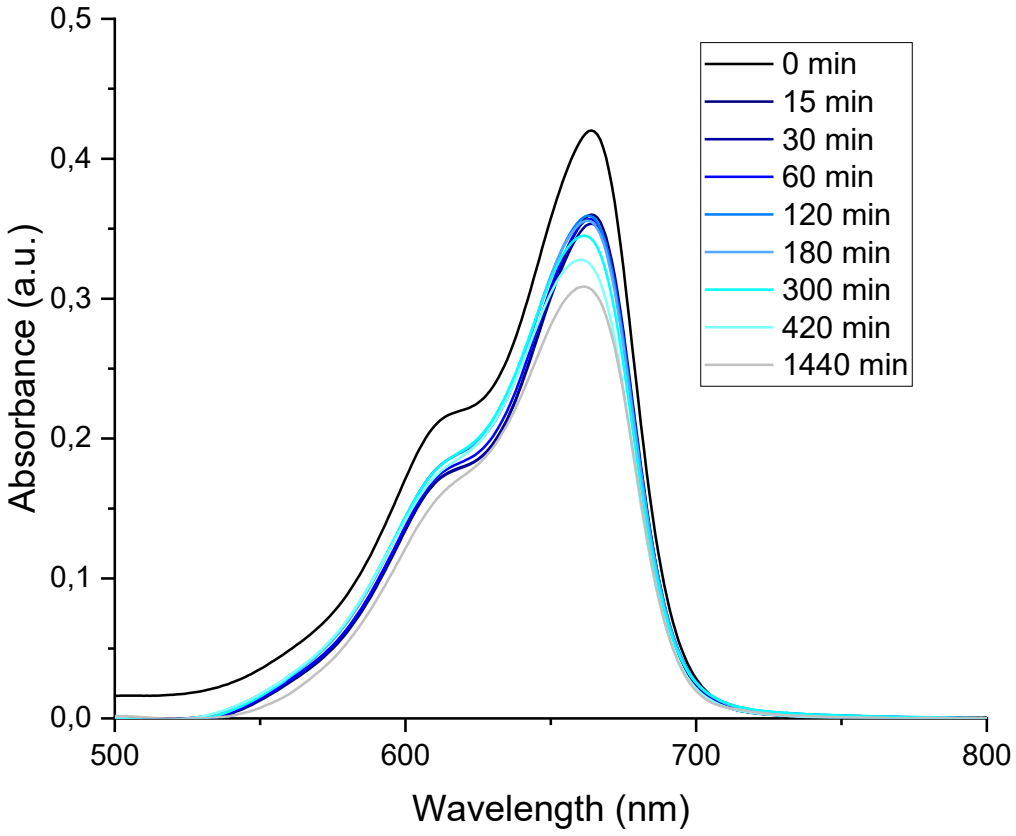


Fig. 7.31 - Evolution of the absorption spectra during the adsorption tests with CHn-based material obtained with Sxl using Et as solvent and MB as the dye.

Reporting the dyes adsorption percentage for all the experiments as a function of time, it is possible to scrutinize the more efficient removal (up to 99.99% in 24 h) of 4NBAld with respect to the other organic pollutants. Concerning 4Nph in an acid medium (pH = 1), considering the signal at 317 nm the dye adsorption percentage stands over the 20%, which is twice the value recorded for the Cls-based material.

The solution at pH 8.4, considering the signal at 400 nm exhibits a percentage nearby the 20%. The solution at basic pH had an adsorption under 10% and it was the worst result.

The MB solution didn't have a better performance, only the 20%.

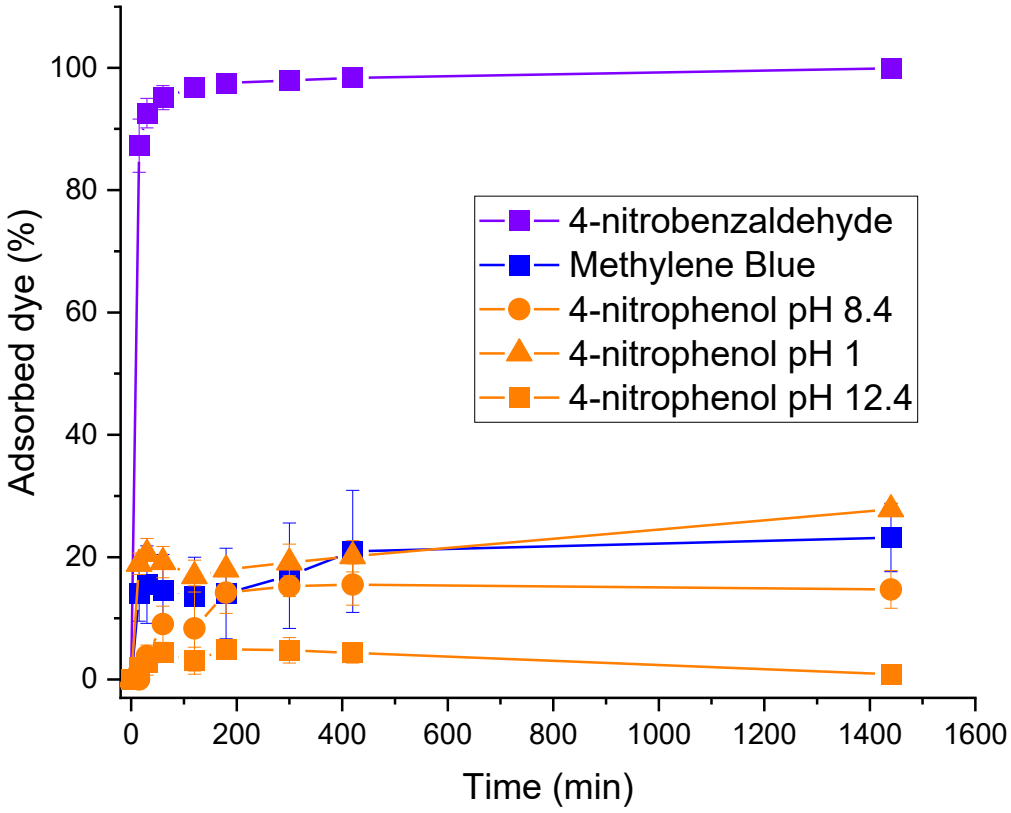


Fig. 7.32 - Average (based on three replicates) of the contaminants adsorption percentages performed by the Chn-based material.

Comparing the two materials the behaviour with all the dyes is similar. The only exception is the 4Nph at pH equal to 1, that is more adsorbed on Chn-based material.

Table 7.2. Adsorption capacity obtained from the adsorption tests.

| **Sample** | **Dye** | **Adsorption capacity (mg/g)** | **Initial dye concentration (mol/L)** | **Final dye concentration (mol/L)** | **Adsorbent material (g)** |
|---|---|---|---|---|---|
| Cellulose-based | 4-nitrophenol (pH=12.4) | 0.16 | $0.6*10^{-4}$ | $5.5*10^{-5}$ | 0.1 |
| | | 0.19 | | $5.4*10^{-5}$ | |
| | | 0.17 | | $5.4*10^{-5}$ | |
| | 4-nitrophenol (pH=8.4) | 1.4 | $0.6*10^{-4}$ | $1.8*10^{-5}$ | 0.1 |
| | | 1.5 | | $1.5*10^{-5}$ | |
| | | 1.4 | | $1.7*10^{-5}$ | |
| | 4-nitrophenol (pH=1) | 0.2 | $0.6*10^{-4}$ | $5.2*10^{-5}$ | 0.1 |
| | | 0.2 | | $5.3*10^{-5}$ | |
| | | 0.2 | | $5.2*10^{-5}$ | |
| | 4-nitrobenzaldehyde | 3.1 | $10^{-4}$ | $3*10^{-6}$ | 0.1 |
| | | 3.1 | | $1.0*10^{-6}$ | |
| | | 3.1 | | $2*10^{-6}$ | |
| | Methylene Blue | 1.4 | $10^{-4}$ | $5.6*10^{-5}$ | 0.1 |
| | | 0.8 | | $7.5*10^{-5}$ | |
| | | 0.7 | | $7.7*10^{-5}$ | |

| Sample | Dye | Adsorption capacity (mg/g) | Initial dye concentration (mol/L) | Final dye concentration (mol/L) | Adsorbent material (g) |
|---|---|---|---|---|---|
| Chitin-based | 4-nitrophenol (pH=12.4) | 0.15 | $0.6*10^{-4}$ | $5.5*10^{-5}$ | 0.1 |
| | | 0.2 | | $5.3*10^{-5}$ | |
| | | 0.2 | | $5.3*10^{-5}$ | |
| | 4-nitrophenol (pH=8.4) | 1.5 | $0.6*10^{-4}$ | $1.2*10^{-5}$ | 0.1 |
| | | 1.7 | | $6*10^{-6}$ | |
| | | 1.3 | | $2*10^{-5}$ | |
| | 4-nitrophenol (pH=1) | 0.5 | $0.6*10^{-4}$ | $4.9*10^{-5}$ | 0.1 |
| | | 0.5 | | $4.4*10^{-5}$ | |
| | | 0.5 | | $4.2*10^{-5}$ | |
| | 4-nitrobenzaldehyde | 3.2 | $10^{-4}$ | $2.4*10^{-7}$ | 0.1 |
| | | 3.2 | | $3*10^{-7}$ | |
| | | 3.2 | | $1.0*10^{-8}$ | |
| | Methylene Blue | 0.8 | $10^{-4}$ | $8*10^{-5}$ | 0.1 |
| | | 0.9 | | $7*10^{-5}$ | |
| | | 0.6 | | $8.3*10^{-5}$ | |

*7.1.3 Adsorption tests in marine water*

The three organic dyes were added in marine water and Cls- and Chn-based materials were tested.

Marine water was filtered and characterized measuring pH and salinity. The pH is equal to 9 (+/- 0.1) and the salinity measured was 40 ‰ and it measured the ratio between the salt (NaCl) dispersed in water (mg/L).

Also in this case, 10 mL of mono-contaminated solution and 100 mg of adsorbent material were used. The batch was left under magnetic stirring for 15 minutes, centrifuged for 3 minutes at 4000 rpm, and analysed with the UV-Vis spectrophotometer. After the measurement, the experiment starts again. To observe the kinetics behaviour the measurements were taken at the beginning in small time intervals and going ahead with the experiment the time intervals were bigger. For each experiment were taken 9 measures: time 0, 15 minutes, 30 minutes, 1 hour, 2 hours, 3 hours, 5 hours, 7 hours and 24 hours.

Also the percentage of adsorbed dye and the final concentration is calculated as in the previous experiments.

The first test was done with MB and Cls-based material. As it is possible to observe from the uv-vis spectra (fig.7.33) there is not a high variation of the maximum absorbance of the spectra with time. It is possible also to observe that after 30 minutes the equilibrium adsorption is achieved.

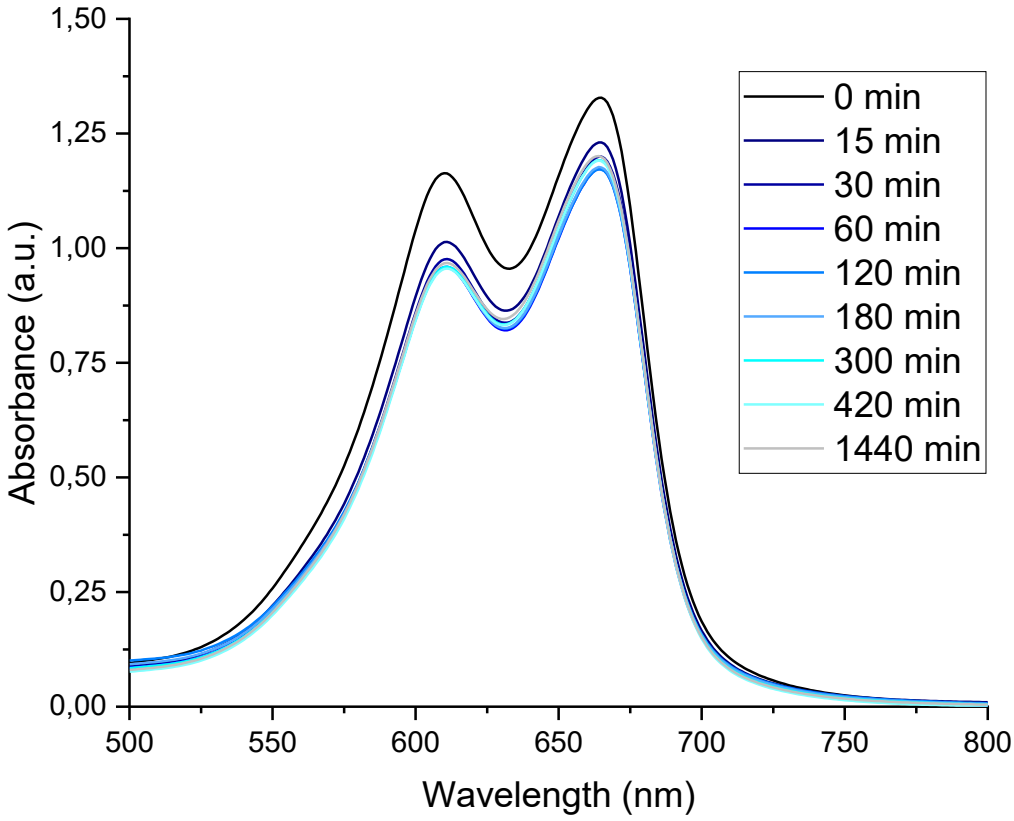


Fig. 7.33 - Evolution of the absorption spectra during the adsorption tests with Cls-based material obtained with Sxl using Et as solvent and MB as the dye in marine water.

The second dye tested was the 4NBAld and from the spectra (fig. 7.34) is possible to assert that after 15 minutes the majority of the dye was adsorbed.

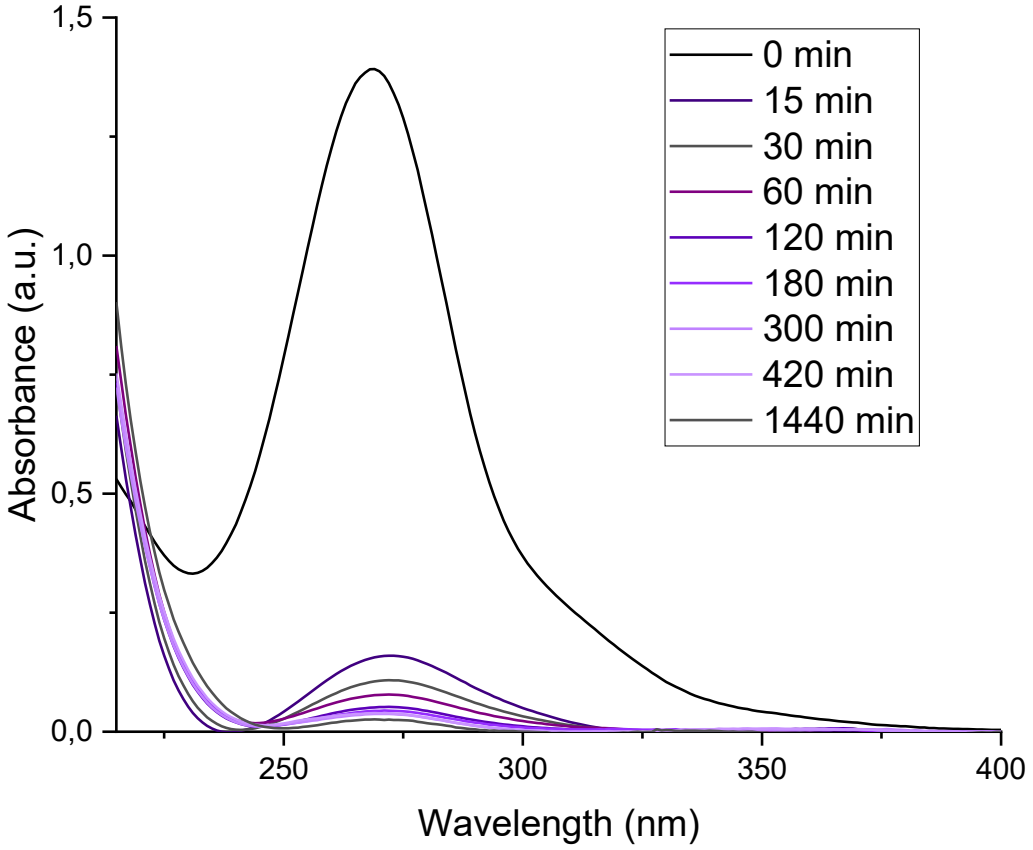


Fig. 7.34 – Evolution of the absorption spectra during the adsorption tests with Cls-based material obtained with Sxl using Et as solvent and 4NBAld as the dye in marine water.

The last dye tested was the 4Nph which in this case appears in its basic form with a peak at 400 nm (fig.7.35). After 15 minutes the adsorption equilibrium was obtained, but there was not a big difference in absorbance from the measure at time 0.

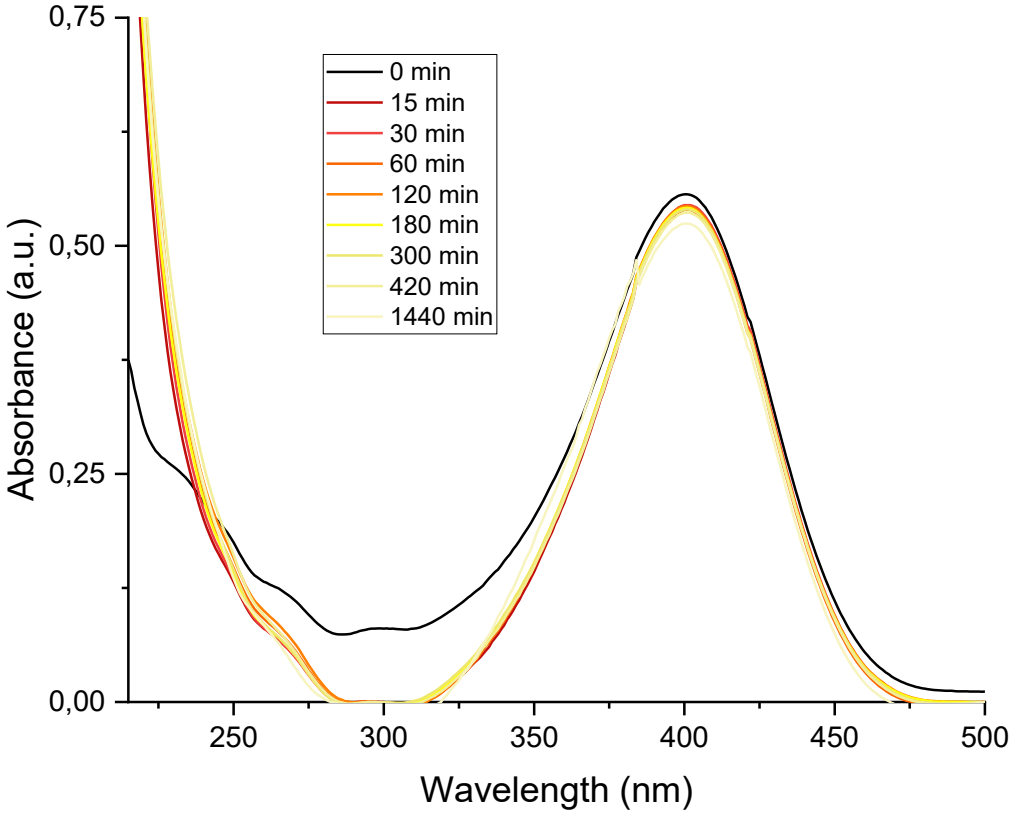


Fig. 7.35 – Evolution of the absorption spectra during the adsorption tests with Cls-based material obtained with Sxl using Et as solvent and 4Nph as the dye in marine water.

Comparing the percentage of the adsorption with time (fig. 7.36) of the 3 dyes is possible to assert that the 4-nitro benzaldehyde had the higher percentage of adsorption and the 4Nph and the MB had after 24 hours (1440 min) almost the same adsorbed quantity. The only difference is that the MB seemed to have a more rapid kinetic adsorption than the 4Nph.

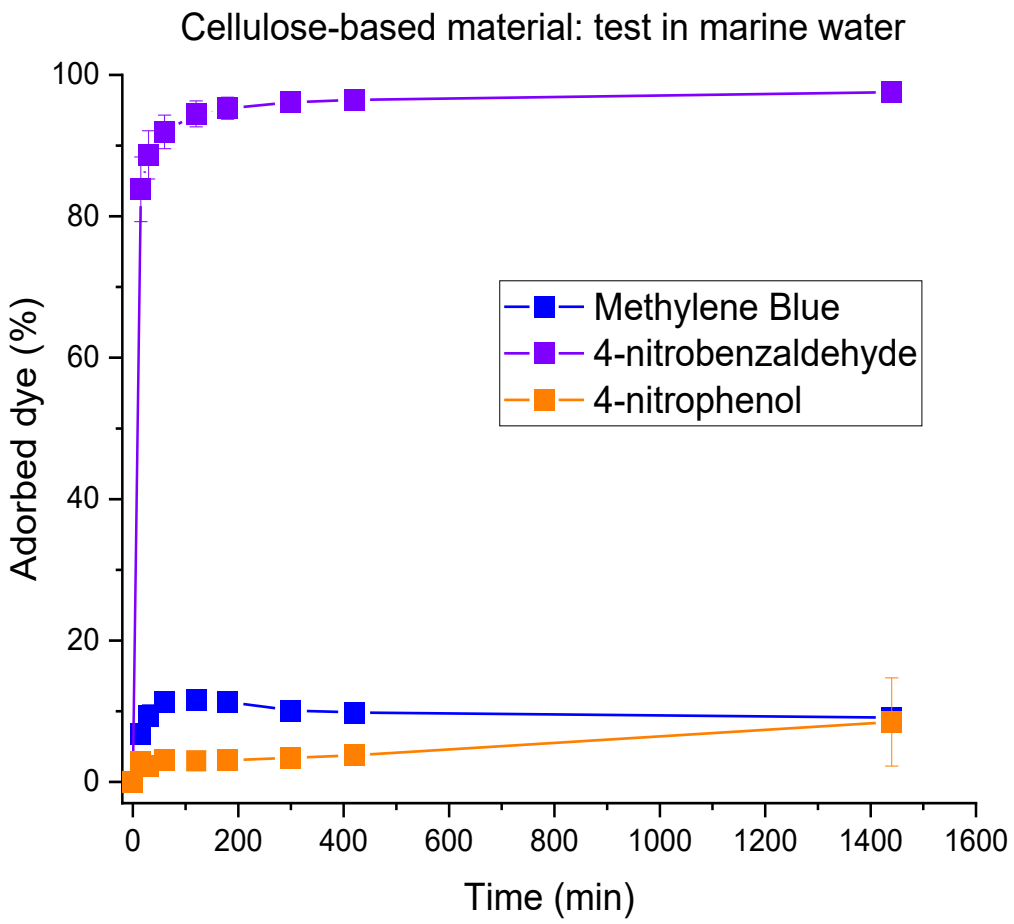


Fig. 7.36 - Average (based on three replicates) of the contaminants adsorption percentages performed by the Cls-based material.

The same tests were done with Chn-based material.

The first dye tested was MB (fig.7.37) and it is possible to observe that after 15 minutes there was a higher quantity adsorbed, but after 30 minutes something was released again in the solution and about 2 hours (120 min) the equilibrium was obtained.

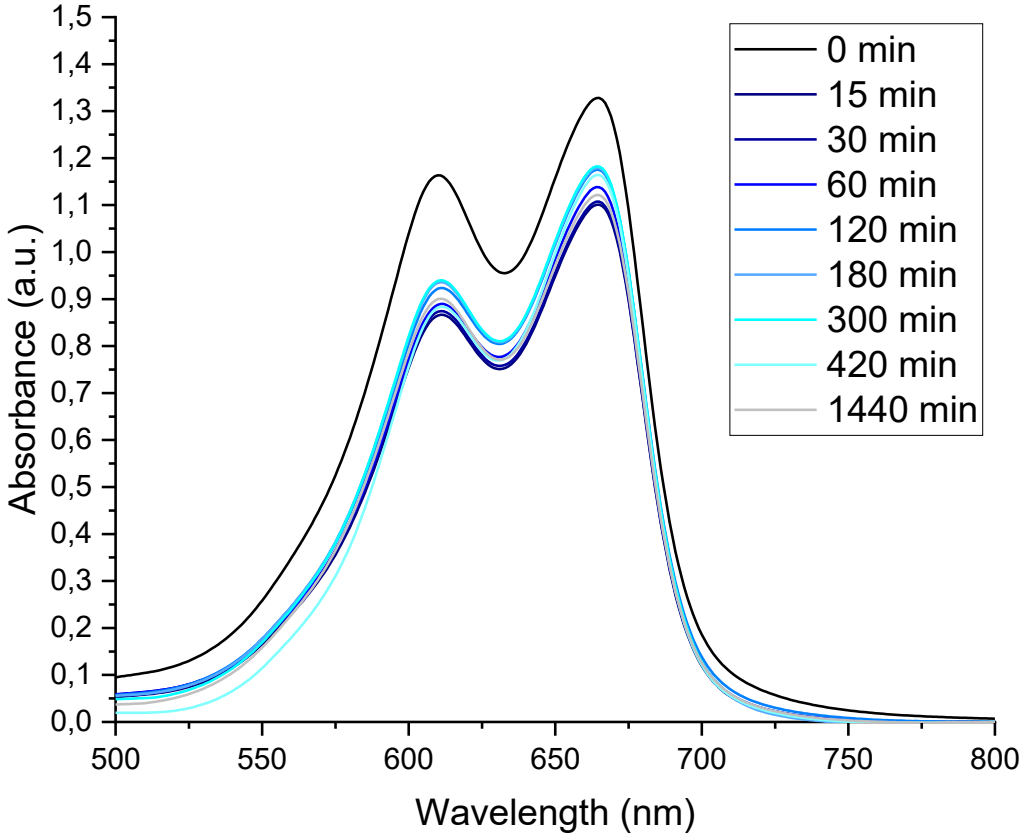


Fig. 7.37 - Evolution of the absorption spectra during the adsorption tests with Chn-based material obtained with Sxl using Et as solvent and MB as the dye in marine water.

The second dye tested was the 4NBAld (fig.7.38) which after 15 minutes had a low absorbance signal and it was decrease in time.

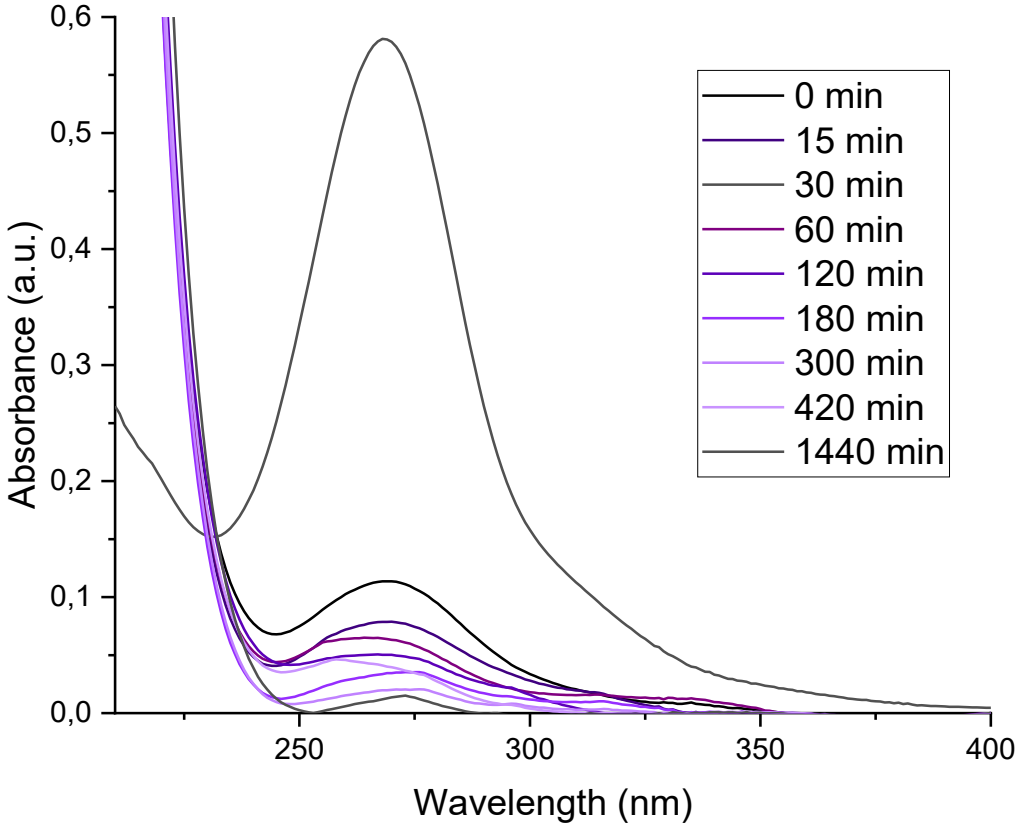


Fig. 7.38 – Evolution of the absorption spectra during the adsorption tests with Chn-based material obtained with Sxl using Et as solvent and 4NBAld as the dye in marine water.

The third dye was the 4Nph (fig 7.39) and to observe a decrease in the signal it was necessary to wait 3 hours (180 min) and after 24 hours (1440 min) there was an appreciable decrease.

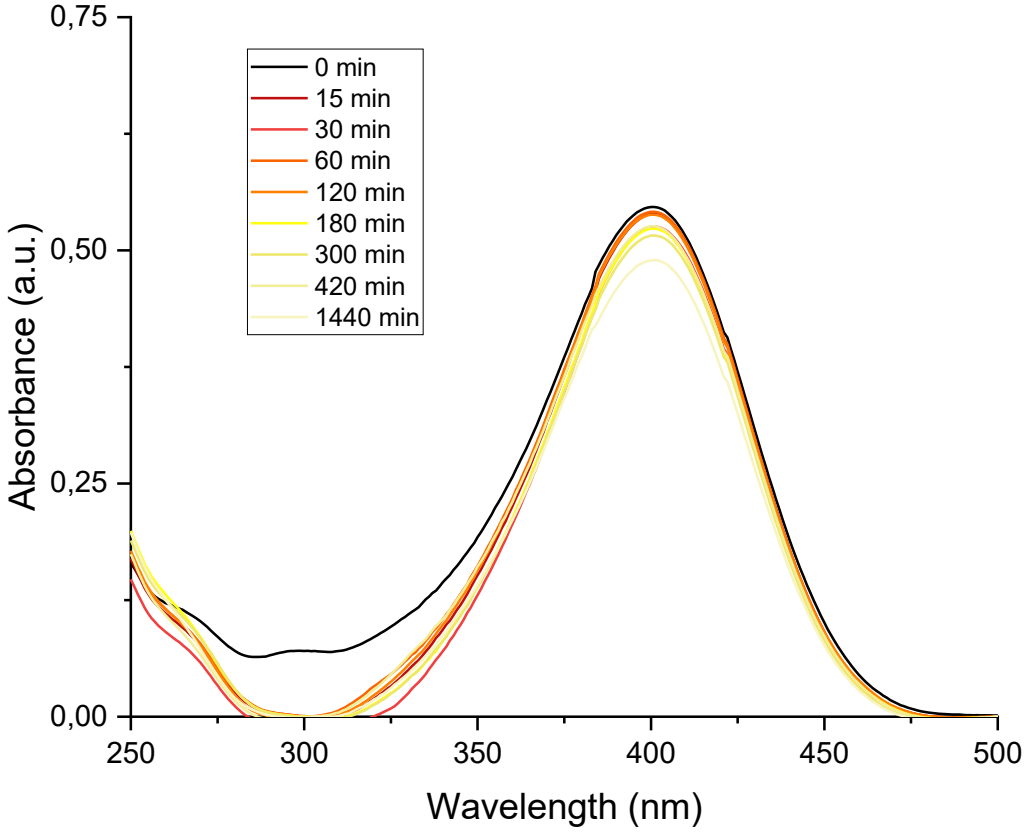


Fig. 7.39 – Evolution of the absorption spectra during the adsorption tests with Chn-based material obtained with Sxl using Et as solvent and 4Nph as the dye in marine water.

Comparing the percentage of dye adsorbed in time it is possible to assert that the 4NBAld reached a percentage equal to 99%, as in the test with deionized water. 4Nph and MB had a percentage of adsorption of about 15 %.

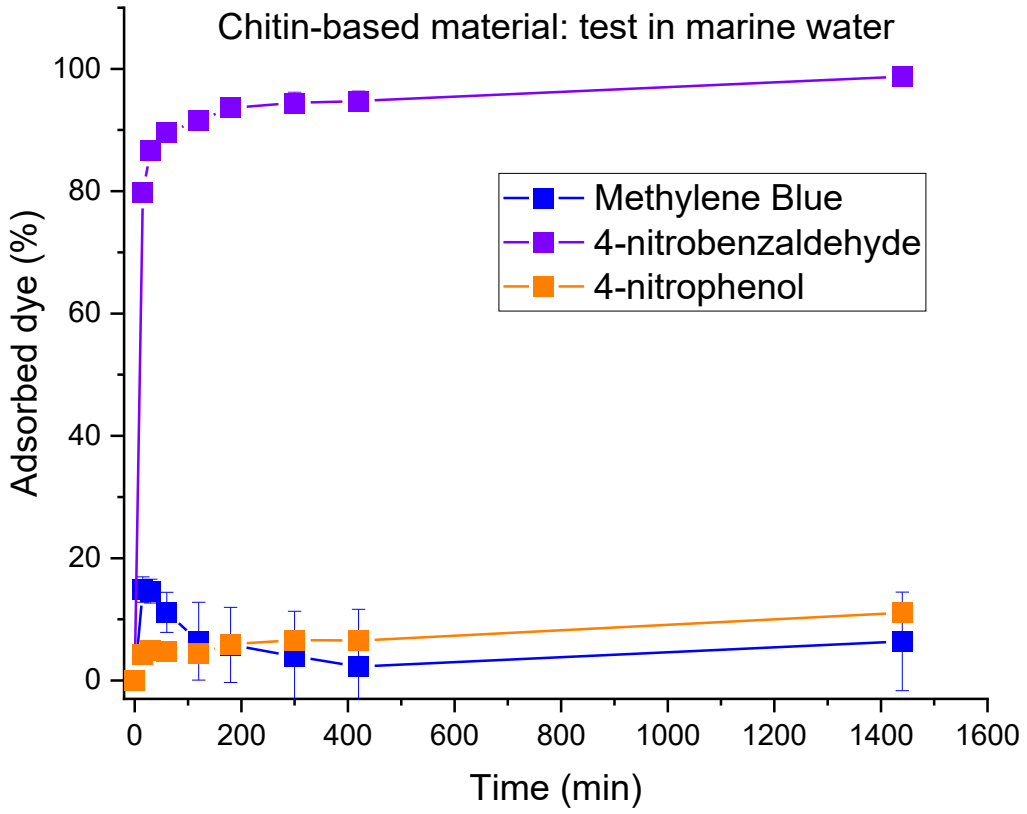


Fig. 7.40 - Average (based on three replicates) of the contaminants adsorption percentages performed by the Chn-based material.

Considering the values reported in Tab 7.3, the adsorption capacity of the 4NBAld is very similar for the Cls- and Chn-based materials. It is also comparable with the adsorption capacity obtained from the tests done in deionized water.

On the other hand, the adsorption of MB is decreased, but not in a significant way for the Cls-based material. For Chn-based material the results of the tests in marine water gave a worst result.

Table 7.3. Adsorption capacity obtained from the adsorption tests in marine water.

| Sample | Dye | Adsorption capacity (mg/g) | Initial dye concentration (mol/L) | Final dye concentration (mol/L) | Adsorbent material (g) |
|---|---|---|---|---|---|
| Cls-based material | 4-nitrophenol | 0.37 | $0.6*10^{-4}$ | $4.8*10^{-5}$ | 0.1 |
| | | 0.69 | | $3.8*10^{-5}$ | |
| | | 0.44 | | $4.6*10^{-5}$ | |
| | 4-nitrobenzaldehyde | 3.1 | $10^{-4}$ | $3.0*10^{-6}$ | 0.1 |
| | | 3.14 | | $2.0*10^{-6}$ | |
| | | 3.12 | | $3.0*10^{-6}$ | |
| | Methylene Blue | 0.28 | $10^{-4}$ | $9.1*10^{-5}$ | 0.1 |
| | | 0.28 | | $9.1*10^{-5}$ | |
| | | 0.28 | | $9.1*10^{-5}$ | |
| Chn-based material | 4-nitrophenol | 0.43 | $0.6*10^{-4}$ | $4.7*10^{-5}$ | 0.1 |
| | | 0.79 | | $3.5*10^{-5}$ | |
| | | 0.69 | | $3.8*10^{-5}$ | |
| | 4-nitrobenzaldehyde | 3.17 | $10^{-4}$ | $1.0*10^{-6}$ | 0.1 |
| | | 3.13 | | $2*10^{-6}$ | |
| | | 3.17 | | $1.0*10^{-6}$ | |
| | Methylene Blue | 0.009 | $10^{-4}$ | $1.0*10^{-4}$ | 0.1 |
| | | 0.49 | | $8.4*10^{-5}$ | |
| | | 0.10 | | $9.7*10^{-5}$ | |

## *7.2 Heavy metals*

### *7.2.1 ICP-OE Spectroscopy*

Inductively Coupled Plasma Optical Emission Spectroscopy, a method employed to analyse metals quantitatively and qualitatively, operates by measuring the emitted light intensity from each metal within a sample using a specialized optical setup comprising mirrors, lenses, and gratings. Liquid samples are required for analysis in ICP-OES, while solid samples necessitate a prior mineralization step, which involves converting the solid matrix into a liquid solution through a disintegration technique.

ICP-OES enables the analysis of metals across a wide range of concentrations and various sample types, making it the most adaptable method for assessing metals in water, soils, sediments, as well as food and petroleum products. To prepare the sample, the solvent is evaporated, and the remaining components are vaporized, breaking molecules into atoms. This process generates an ICP-OES plasma—a highly ionized gas—within an oscillating radio frequency (RF) field. The RF field causes the ions within the gas to oscillate, generating intense heat. Temperatures within the plasma can reach as high as 10,000°C.

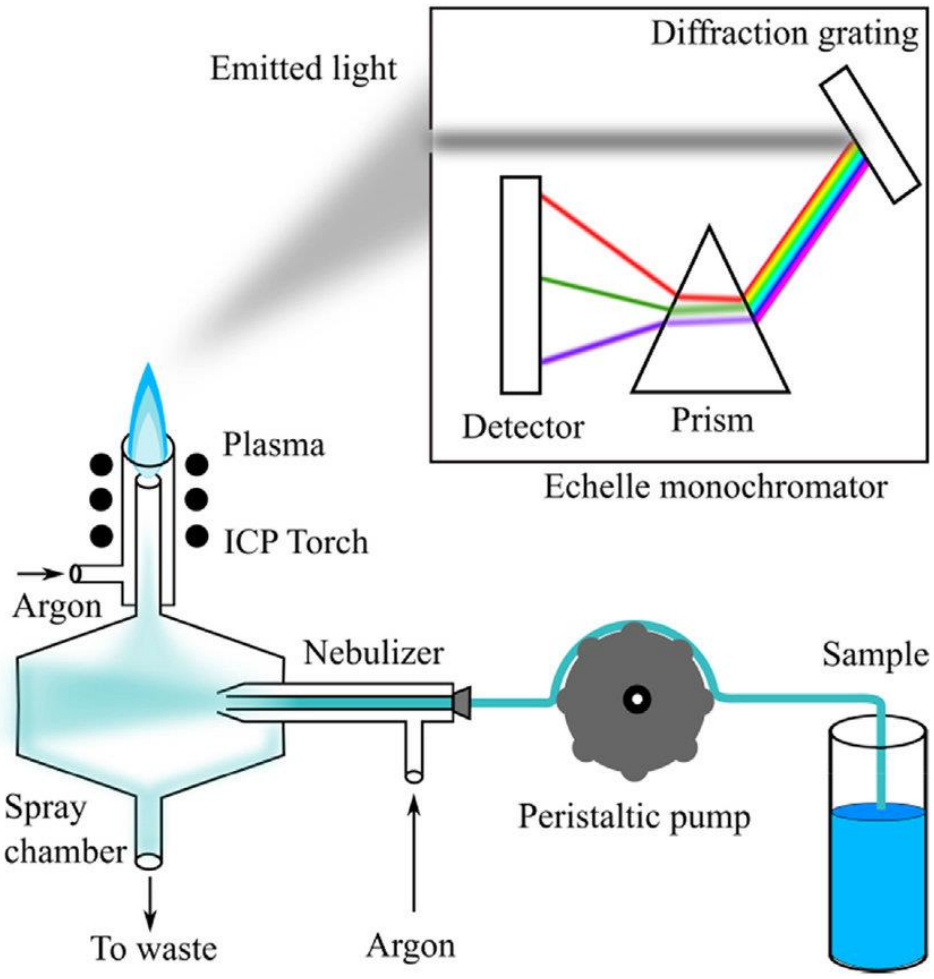


Fig. 7.41 - Scheme of ICP-OES

The plasma is generated in the plasma "torch" that consists of three quartz tubes: the outer torch tube, the auxiliary tube, and the injector tube (Figure 7.41). Between the outer tube and the auxiliary tube, a tangential flow of cool gas is introduced to envelop the plasma, preventing it from reaching the outer torch tube and avoiding its meltdown. This auxiliary gas flow also serves to lift the bottom of the plasma away from the injector tube. The sample aerosol is injected into the plasma via a thin injector tube

typically featuring a 1–2 mm aperture, through which a fine jet of sample aerosol is emitted, creating an aperture in the center of the plasma.

A robust and efficient radio frequency (RF) generator plays a crucial role in initiating and sustaining the plasma, capable of thoroughly dissociating nearly any sample matrix, thus minimizing oxide formation and other chemical interferences.

The development of an RF generator poses various challenges including size, durability, efficiency, reliability, and ease of maintenance. The stability of an RF generator heavily relies on its ability to adapt to changing plasma conditions resulting from different samples or sample matrices. This adaptation is achieved by adjusting power conditions to accommodate variations, a process known as 'matching'.

Two primary approaches have been employed for controlling and matching RF generators: crystal-controlled and free-running. Crystal-controlled generators synchronize the frequency of the RF generator with the oscillation of a reference crystal. On the other hand, free-running generators adjust the generated power to meet the plasma's requirements, allowing slight frequency variations. In ICP-OES, the plasma can usually be observed in two ways:

- Radially, which means observation of a plasma cross-section from the side
- Axially, which means observation of the plasma from the end and along the entire length of the plasma

The radial plasma view, while less sensitive than the axial view, is preferable for analyzing challenging samples like organics or those with high amounts of dissolved solids. On the other hand, the axial view provides greater sensitivity, but it increases susceptibility to spectral interferences due to observing the plasma along its entire length.

ICP-OES systems typically offer two torch configurations: a dedicated radial view instrument and a dual view instrument with both axial and radial observation options. In dual-view systems, the torch is positioned

horizontally to extract heat and fumes from the plasma, keeping the mirrors in the fore-optics clean. This configuration suits relatively clean aqueous samples. Conversely, a dedicated radial view instrument features a vertical torch and is favored for complex matrices and organic samples due to its robust torch configuration.

For UV wavelength analysis in ICP-OES, optical pathways leading into the spectrometer must be purged to ensure accuracy. This involves purging the cones used for light collection with gas flow from the spectrometer.

Echelle-based optical designs are commonly used in ICP-OES for producing emission spectra. These designs consist of an echelle grating, a prism, and multiple focusing mirrors. Unlike monochromators, polychromators allow simultaneous detection of multiple elements in a sample, enhancing stability, reducing sample consumption, and shortening analysis time considerably.

The light from the plasma is selectively focused through an entrance slit and then onto a prism, which separates the light by wavelength at low resolution. An echelle grating orders the separated light, creating a high-resolution, two-dimensional spectrum known as an echellogram. Finally, a mirror collects and focuses the dispersed spectrum onto the detector.

Solid-state charge transfer devices (CTDs), such as charge injection devices (CIDs) and charge-coupled devices (CCDs), have largely replaced photomultiplier tubes for light intensity measurement in ICP-OES. CIDs allow for individual, pixel-by-pixel integration, offering excellent anti-blooming capability and optimum signal-to-noise ratio. These devices feature a light-sensitive surface subdivided into thousands of pixels, enabling thorough collection and readout of signals.

CIDs typically cover a wavelength range of 160 nm to 900 nm. Fullframe imaging captures all data from the CID, regardless of specified elements, facilitating retrospective analysis, batch analysis, or contamination identification. Analysts can subtract Fullframes from each other for tasks

like matrix stripping and contamination identification, yielding more accurate results.

Figure 7.42 - ICP-OES iCAP 7000 Series

### *7.2.3 Results*

The adsorption tests with heavy metal was made of preliminary tests with seven different concentrations (from 0.5 to 150 ppm) to set ad initial concentration over the concentration of the Italian law.

The operative system used for measuring the samples was based on a calibration line. The first step was preparing five solutions of known concentration, between 0.1 and 200 ppb of heavy metals using a multielement standard solution.

The experiments were conducted by preparing 7 monocontaminated solutions at different concentrations. All the experiments were conducted on three replicates. 15 ml of solution were put in contact with 12 mg of adsorbent materials and shaken for 24 hours. After 24 hours, the filtrated solution was diluted under 200 ppb and was analyzed with the ICP-OES.

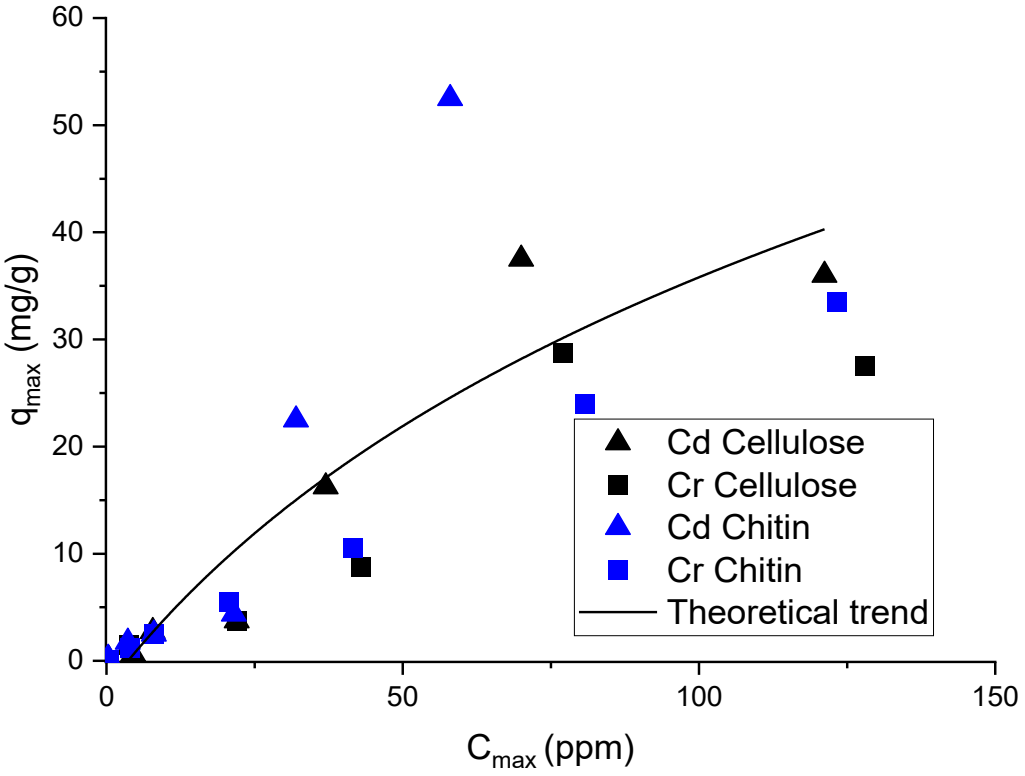


Figure 7.43 - The x-axis shows the concentration after 24 hours ($C_{max}$) expressed in ppm, while the y-axis shows the maximum capacity adsorbed in 24 hours ($q_{max}$) expressed in mg/g.

Thanks to these preliminary tests with HM, is possible to assert that Cls- and Chn-based materials worked also with inorganic compounds. Specifically, the Cd was adsorbed from Chn-based material that showed an adsorption capacity of 52.5 mg/g with a starting concentration of 100 ppm, on the other hand, Cls-based material showed a higher adsorption capacity with Cr (28.75 mg/g) with the starting concentration equal to 100 ppm.

It is also interesting to observe that the starting concentration equal to 150 ppm the Chn-based material was again better performing than Cls-based material.

Table 7.4 - Concentrations of stock solutions and after 24 hours of Cadmium and Chromium monocontaminated solutions.

| Concentrations (ppm) | Cd | | | | Cr | | | |
|---|---|---|---|---|---|---|---|---|
| | Cellulose | | Chitin | | Cellulose | | Chitin | |
| | Concentrations (24h, ppm) | Adsorption capacity (mg/g) | Concentrations (24h, ppm) | Adsorption capacity (mg/g) | Concentrations (24h, ppm) | Adsorption capacity (mg/g) | Concentrations (24h, ppm) | Adsorption capacity (mg/g) |
| 0.5 | 0,38 | 0,15 | 0.3 | 0.25 | 0,48 | 0,025 | 0,43 | 0,0875 |
| 5 | 4,5 | 0.625 | 3.6 | 1.75 | 3.8 | 1.5 | 4 | 1.25 |
| 10 | 7,8 | 2.75 | 8 | 2.5 | 8 | 2.5 | 8 | 2.5 |
| 25 | 22 | 3.75 | 21.5 | 4.38 | 22 | 3.75 | 20.6 | 5.5 |
| 50 | 37 | 16.25 | 32 | 22.5 | 43 | 8.75 | 41.6 | 10.5 |
| 100 | 70 | 37.5 | 58 | 52.5 | 77 | 28.75 | 80.8 | 24 |
| 150 | 121,2 | 36 | 134.6 | 19.25 | 128 | 27.5 | 123.2 | 33.5 |

# 8. ENVIRONMENTAL SUSTAINABILITY: LIFE CYCLE ASSESSMENT

The ongoing development of Life Cycle Assessment (LCA) methodology aims to enhance comprehension and facilitate actions towards mitigating potential environmental impacts linked to products, processes and services. LCA methodology entails the systematic evaluation of the environmental facets and consequences of product systems, aligned with defined objectives and boundaries. LCA is a comparative methodology grounded in a functional unit, where the delineation of system boundaries aligns with the objectives and scope definition, encompassing decisions about the selected unit processes and the extent of specificity regarding inputs and outputs. (ISO 14040, 2006; ISO 14044, 2006).

LCA analysis is a very important tool for assessing the impact and the carbon footprint that the synthesis procedure and the application of new materials and technologies have. In last ten years, LCA was applied to marine sediments remediation as a valuable tool for assessing the environmental foot print of sediment remediation projects and for sustainable sediment management. (Sparrevik et al., 2011)

The two principal techniques adopted for the marine sediments remediation are ex-situ Solidification/Stabilization and in-situ reactive capping. Both are good at neutralize and degrading contaminants in marine sediments, but the ex-situ Solidification/Stabilization technique even if diminish greatly the potential risks associated to metals leaching, this technique induce additional impacts in various other categories that are associated to the use of stabilizers and solidification agents. (Barjoveanu et al., 2018)

Reactive Capping placement allows to respect environmental standards of the pollutants concentration in the sea water. Using active materials such as Activated Carbon, Zero Valent Iron or Organoclay is possible to obtain both chemical isolation and degradation with an efficiency varying between 40% to 95%. Thanks to the LCA analysis is possible to state that in-situ reactive capping is an effective remediation strategy with small impacts and low costs. (Todaro et al., 2021)

Another important aspect to assess is the environmental impact that the materials chosen for the active capping may have on the environment. Some materials, such as Nano Zero Valent Iron, can be produced in many different ways and LCA analysis could help to know which one is the more sustainable. (Visentin et al., 2021) In other case the scientists found that the major production hotspots stay in the consumption of electricity, in the use and in the acquisition of all input chemicals to the process. The LCA approach may serve as base for identification of new chemical formulations for improvement of the environmental sustainability associated with the process. (Ingrao et al., 2021). Although the use of LCA analysis can be complicated in laboratory-scale synthesis protocols, it remains a useful tool not only for identifying critical steps that need to be improved, but above all a key tool in the development of a production scale-up. It was found that certain materials produced in small quantities at laboratory scale had a significantly higher environmental impact than large-scale production of the same. (Bartolozzi et al., 2020; Gavankar et al., 2015)

With a view to the circular economy and sustainability is important to improve an LCA analysis alongside the lab-scale experiments. Marine sediments remediation is a big challenge and is very important to find new good technology, but likewise important to find sustainable technologies. Materials that have as precursors biomaterials derived from waste could be not enough. The aim of this

study is to use the LCA to verify if the material production processes are sustainable and if there are better strategies in order to implement the sustainability in the production stage. It will be investigating also a small scale up in order to know how much the production procedure could be optimized to reduce environmental impact.

### *8.1 LCA planning: system limits, functional unit*

The system boundaries were established from cradle-to-gate, namely from the acquisition of raw materials to the production of the bio-based material. The functional unit considered was 1 g of bio-based material produced.

The impact assessment method applied was ReCiPe 2016 Midpoint (H). The following 18 impact categories were considered: Global warming, Stratospheric ozone depletion, Ionizing radiation, Ozone formation, Human health, Fine particulate matter formation, Ozone formation, Terrestrial ecosystems, Terrestrial acidification, Freshwater eutrophication, Marine eutrophication, Terrestrial ecotoxicity, Freshwater ecotoxicity, Marine ecotoxicity, Human carcinogenic toxicity, Human non-carcinogenic toxicity, Land use, Mineral resource scarcity, Fossil resource scarcity and Water consumption.

The study covered one production process, but five different ways to obtain the final structured bio-based material and also the impact that mg of contaminant adsorbed per grams of adsorbent material has.

The first step was to study the synthesis protocol in order to know which of the chemicals have the high environmental impact. After this step we studied and compared the five different ways adopted to obtain the final bio-based material: using Fr, Fr with washing in Sxl, Sxl using Ac as solvent, Sxl using Me as solvent and Sxl using Et as solvent. Thanks to LCA analysis we are able to state which is the best procedure to adopt in terms of reduced environmental impacts.

Finally LCA analysis conducted were on the maximum adsorption capacity on the investigation of mg of contaminants adsorbed on each g of adsorbent material.

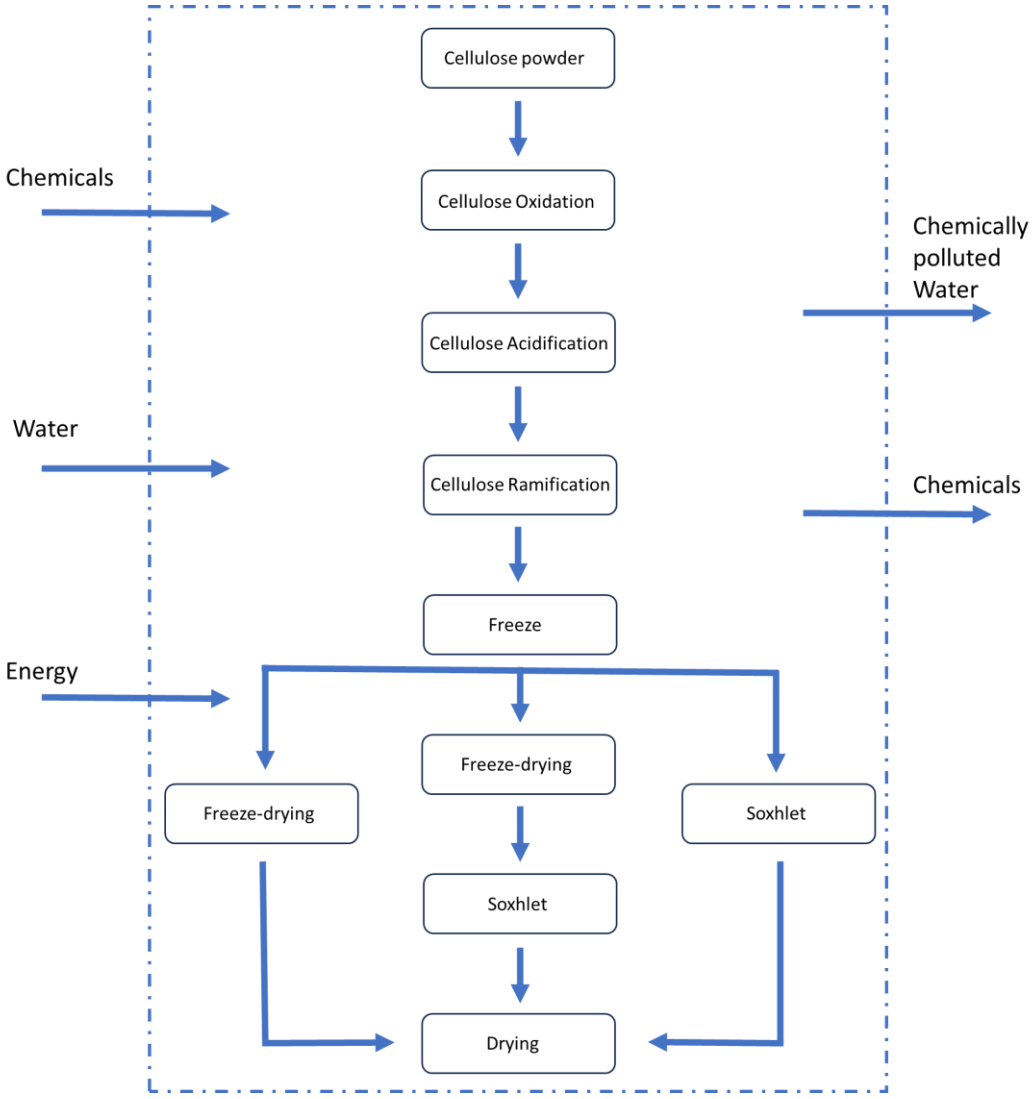


Figure 8.1. System boundaries.

### *8.2 Life cycle inventory*

In the processing of the inventory, the following assumptions and limitations were employed. Cellulose microcrystalline powder and Chitin from shrimp shell powder inputs are based on two inventory created with literature data. The big difference between this two source materials is that chitin is always from waste materials.

For LCA study was used SimaPro LCA software (version 9.2.0.2) and all data were from Ecoinvent database version 3. Most of the data from Ecoinvent database were chosen using the methodological approach of attributional modelling in which burdens are attributed proportionally to the specific processes (APOS, allocations at the point of substitution).

The data collected were then modelled using the ReCiPe Midpoint (H) (v1.02) method. The challenge with LCA study based on lab scale data is the uncertainties and it is very important to be precise with input data quantity (e.g. amounts of chemicals and energy consumption).

Table 8.1. Inventory for Cls- and Chn-based material.

| **Inventory entry** | **Eco-invent process** | **unit** | **Quantity for Cls-based material** | **Quantity for Chn-based material** |
|---|---|---|---|---|
| ***Input*** | | | | |
| *Cellulose microcrystalline powder* | Cellulose powder | g | 1.33 | ✕ |
| *Chitin from shrimp shell powder* | Chitin powder | g | ✕ | 2.7 |
| *KBr* | Bromine {GLO}\| market for \| APOS, U | g | 0.20 | 0.40 |
| *2,2,6,6-tetramethylpiperidinyloxyl (TEMPO)* | Dimethylamine (Production from Alcohols), at producer, 100% active substance/EU-27 | g | 0.03 | 0.052 |
| *Deionised water* | water, deionised {Europe without Switzerland}\| market for water, deionised \| APOS, U | g | 368.85 | 523.33 |
| *NaClO 10%* | Sodium hypochlorite/RER | g | 15 | 30.5 |
| *NaOH 0.5 M* | Neutralising agent, sodium hydroxide-equivalent {GLO}\| market for \| APOS, U | g | 1.94 | 3.95 |
| *HCl 37% v/v* | Hydrochloric acid, without water, in 30% solution state {RER}\| market for \| APOS, U | g | 0.59 | 0.59 |
| *bPEI Mw=25000* | Ethylamine {RER}\| production \| APOS, U | g | 1.36 | 3.3 |

| | | | | |
|---|---|---|---|---|
| *Ethanol* | Ethanol, without water, in 99.7% solution state, from ethylene {RER}\| market for ethanol, without water, in 99.7% solution state, from ethylene \| APOS, U | g | 394.5 | 394.5 |
| *Magnetic stirring* | Electricity, low voltage {IT}\| electricity voltage transformation from medium to low voltage \| APOS, U | KWh | 0.02 | 0.02 |
| *Centrifugation* | Electricity, low voltage {IT}\| electricity voltage transformation from medium to low voltage \| APOS, U | KWh | 0.425 | 0.175 |
| *Sonication* | Electricity, low voltage {IT}\| electricity voltage transformation from medium to low voltage \| APOS, U | KWh | 0.48 | 0.16 |
| *Freeze* | Electricity, low voltage {IT}\| electricity voltage transformation from medium to low voltage \| APOS, U | KWh | 0.17 | 0.17 |
| *Soxhlet* | Electricity, low voltage {IT}\| electricity voltage transformation from | KWh | 0.47 | 0.47 |

| | | | | |
|---|---|---|---|---|
| | medium to low voltage \| APOS, U | | | |
| *Drying process* | Electricity, low voltage {IT}\| electricity voltage transformation from medium to low voltage \| APOS, U | KWh | 0.21 | 0.09 |
| ***Outputs*** | | | | |
| *Ethanol* | Ethanol | g | 80 | 80 |
| *Chemically polluted water* | Chemically polluted water | g | 352.46 | 352.46 |
| *alcohols* | Alcohols, unspecified | g | 315 | 315 |
| *Amine* | Amine, tertiary | g | 0.33 | 0.33 |

### *8.3 Environmental profiles*

The most used protocol to produce Cls-based adsorbent material is with Fr process in order to have an aerogel-like material with a high surface area to volume ratio. The question is if it is the fastest and the cheapest method and also the method with the lowest environmental impact. For these reason, it was decided to try to obtain an aerogel-like material with the Sxl.

Three different processes and for the Sxl procedure also three different solvents are compared.

For all the processes analyzed the high impact is from electricity used, especially for Fr and Sxl. The categories with the big impact are: Global Warming, Terrestrial ecotoxicity, Human non-carcinogenic toxicity, Land use and Fossil resource scarcity. The impact on fossil resource scarcity is due to the electricity consumption, so using the Sxl gave small impact. Using chitin as precursors instead of cellulose is important so as to reduce the impact by up to a quarter for land use. For all the other categories using the Sxl showed more or less the same value in terms of impact.

Comparing the charts of the three Cls-based material obtained with Sxl, it's clear that the choice of the solvent has its relevance. As expected by the literature the solvent with the highest impact is the Ac, followed by Me and the best is Et. The solvent impacts in all the 18 categories with a varying percentage from 5% to over 50%.

The first decision done in the laboratory to use Et as solvent both because it was considered that this solvent gave the best qualities of the material and because it was considered the least impactful in the literature (Capello et al., 2007).

Table 8.2: Impacts for all the materials.

| **Impact category** | **Abbreviation** | **Unit** | **Cls freeze-dried** | **Cls freeze-dried + Sxl** | **Cls Sxl Ac** | **Cls Sxl Me** | **Cls Sxl Et** | **Chn Sxl Et** |
|---|---|---|---|---|---|---|---|---|
| **Global warming** | CC | kg $CO_2$ eq | 6,08759 | 6,38586 | 1,88905 | 1,20475 | 1,34666 | 1,35489 |
| **Stratospheric ozone depletion** | OD | kg CFC11 eq | 0,00000 | 0,00000 | 0,00000 | 0,00000 | 0,00000 | 0,00000 |
| **Ionizing radiation** | IR | kBq Co-60 eq | 0,66864 | 0,69408 | 0,11782 | 0,10500 | 0,10057 | 0,10154 |
| **Ozone formation, Human health** | OF-HH | kg $NO_x$ eq | 0,01072 | 0,02112 | 0,00562 | 0,00596 | 0,01244 | 0,01289 |
| **Fine particulate matter formation** | PM | kg PM2.5 eq | 0,00632 | 0,00661 | 0,00202 | 0,00122 | 0,00129 | 0,00150 |
| **Ozone formation, Terrestrial ecosystems** | OF-ECO | kg $NO_x$ eq | 0,01091 | 0,02742 | 0,00700 | 0,00834 | 0,01872 | 0,01936 |
| **Terrestrial acidification** | TA | kg SO2 eq | 0,01878 | 0,01964 | 0,00606 | 0,00357 | 0,00380 | 0,00391 |
| **Freshwater eutrophication** | FE | kg P eq | 0,00173 | 0,00183 | 0,00041 | 0,00031 | 0,00045 | 0,00047 |
| **Marine eutrophication** | ME | kg N eq | 0,00042 | 0,00043 | 0,00029 | 0,00029 | 0,00029 | 0,00004 |
| **Ecotoxicity** | TOX | kg 1,4-DCB | 4,08166 | 4,29543 | 1,22807 | 0,84910 | 1,14949 | 1,24744 |
| **Human** | HC-TOX | kg 1,4- | 0,16116 | 0,16932 | 0,03505 | 0,02847 | 0,03683 | 0,04202 |

| | | | | | | | | |
|---|---|---|---|---|---|---|---|---|
| **carcinogenic toxicity** | | DCB | | | | | | |
| **Human non-carcinogenic toxicity** | HNonC-TOX | kg 1,4-DCB | 0,21006 | 0,22068 | 0,04518 | 0,03742 | 0,04792 | 0,05458 |
| **Land use** | LAND | m2a crop eq | 0,23344 | 0,24610 | 0,05899 | 0,04567 | 0,05491 | 0,06320 |
| **Mineral resource scarcity** | MIN | kg Cu eq | 3,35788 | 3,51538 | 0,70959 | 0,60095 | 0,69291 | 0,80597 |
| **Fossil resource scarcity** | FOS | kg oil eq | 3,03970 | 3,09322 | 1,91710 | 1,90871 | 1,91798 | 0,18688 |
| **Water consumption** | WAT | $m^3$ | 0,00551 | 0,00588 | 0,00146 | 0,00122 | 0,00187 | 0,00231 |

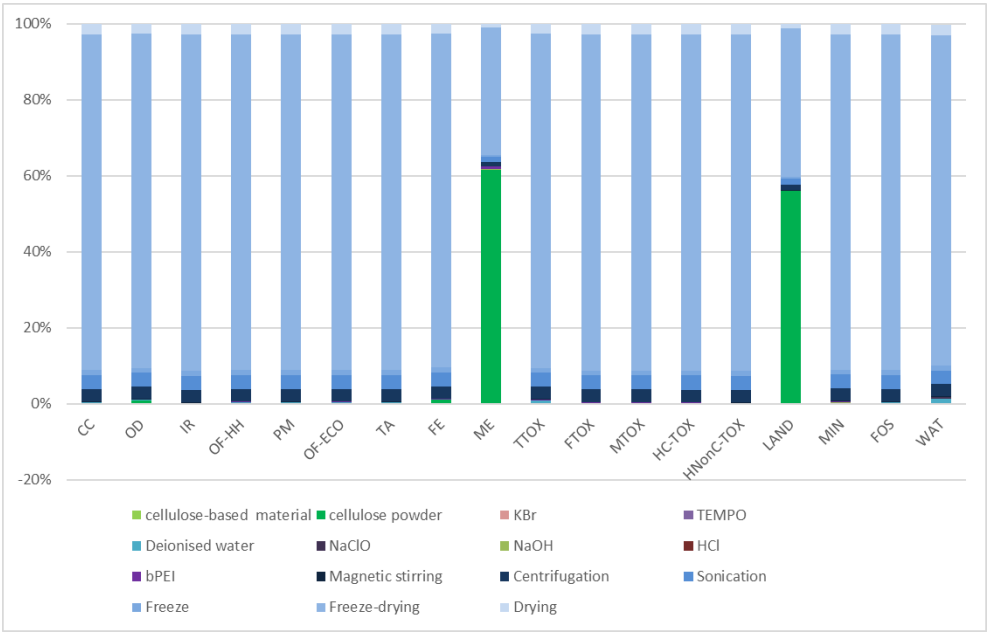


Fig. 8.2 - Cls-based material obtained by Fr process.

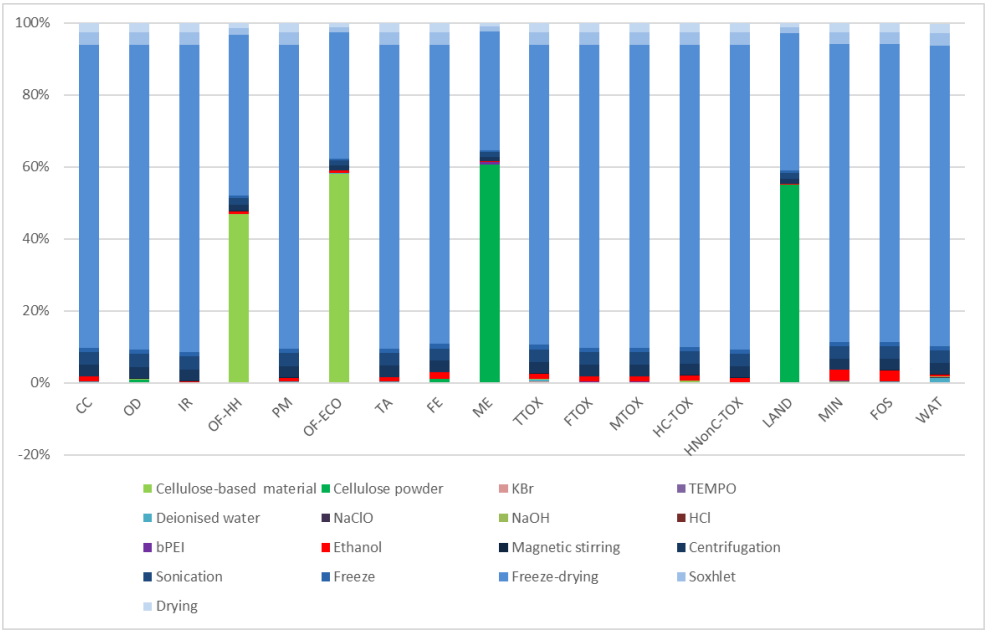


Fig. 8.3 - Cls-based material obtained by Fr process and washed in the Sxl using Et as solvent.

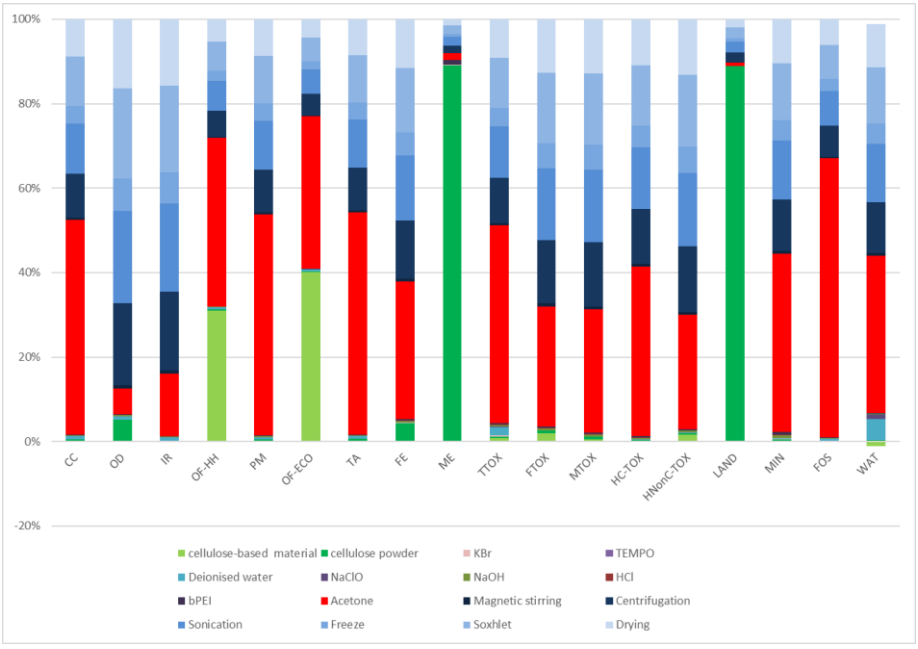


Figure 8.4. Cls-based material obtained by Sxl using Ac as solvent.

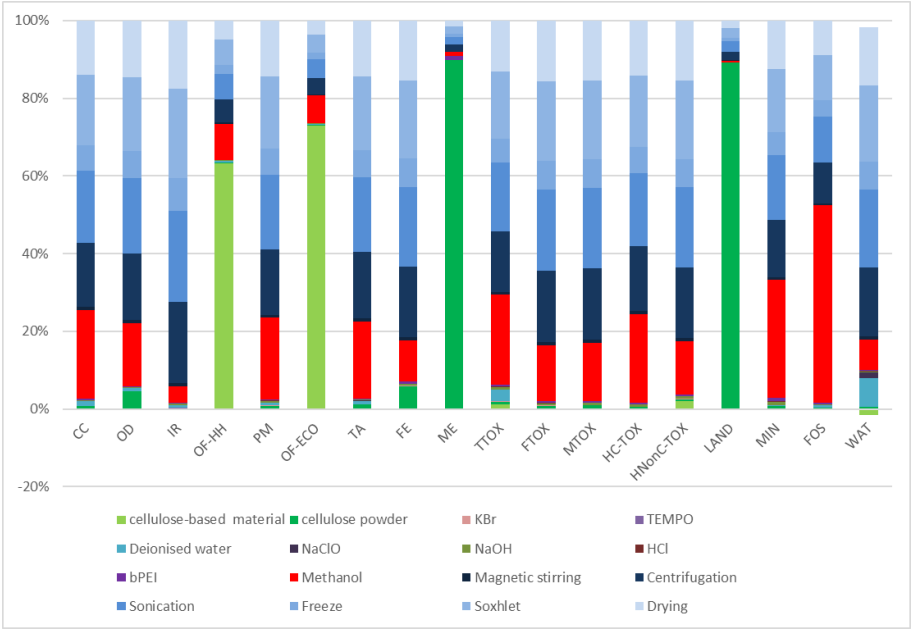


Fig. 8.5 - Cls-based material obtained by Sxl using Me as solvent.

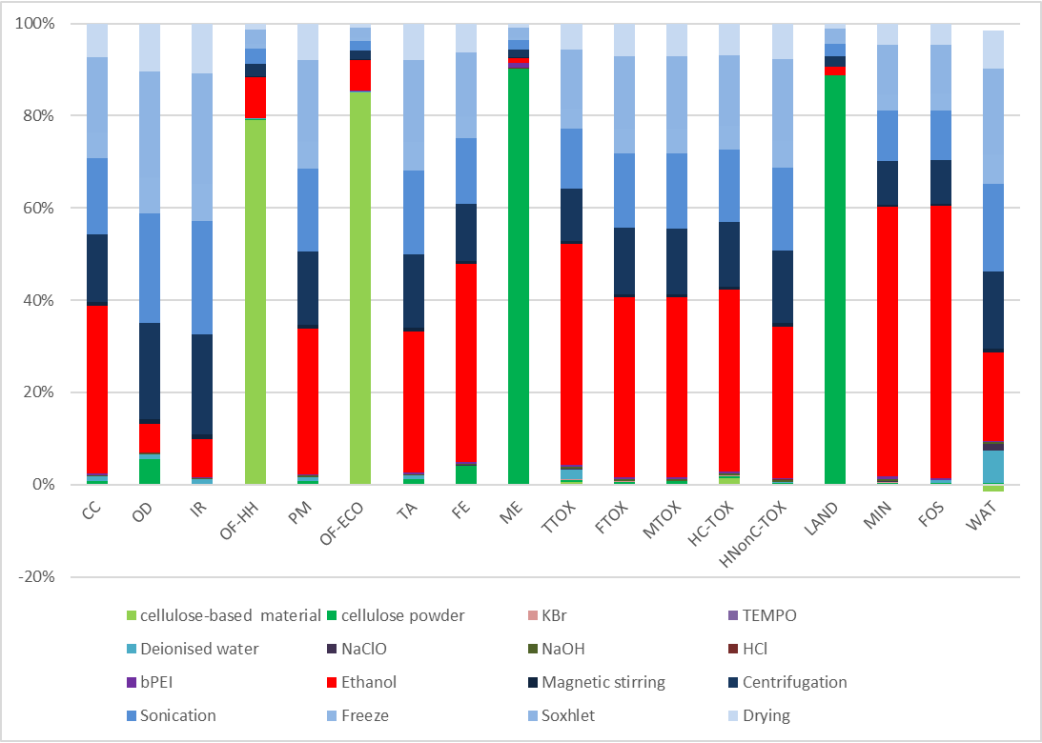


Figure 8.6. Cls-based material obtained by Sxl using Et as solvent.

As a consequence the best protocol to obtained bio-adsorbent material was considered the one with the Sxl using Et as solvent and it was decided to use it also for the Chn-based material.

The protocol is also adapted for the chitin used as precursor, so in this way it was possible to reduce a little bit the global impact from the electricity amount.

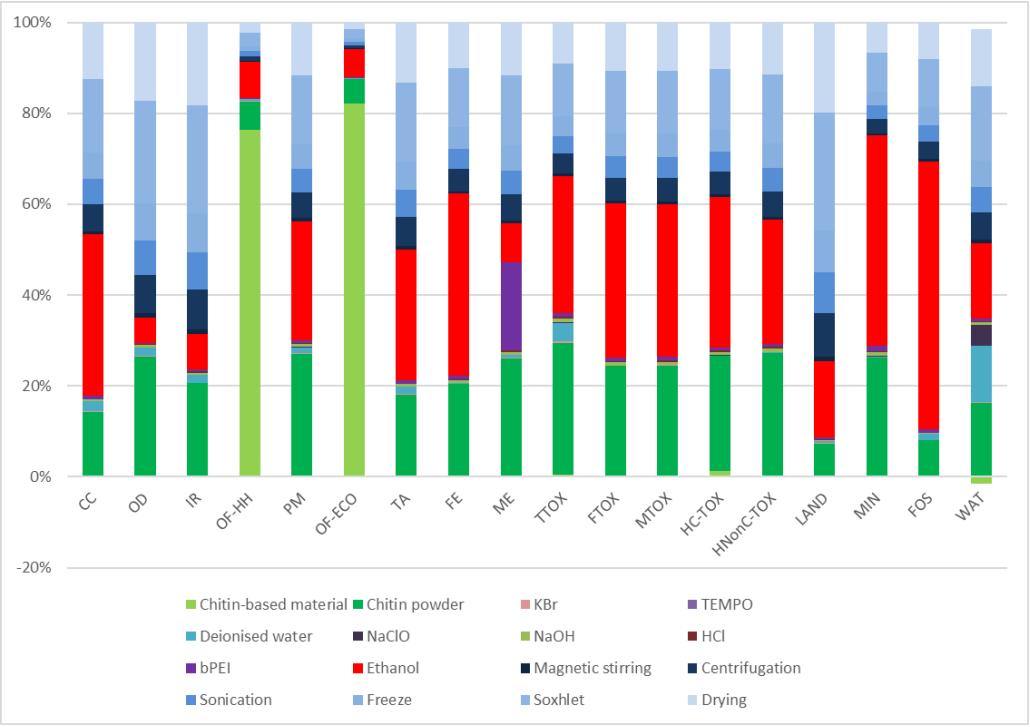


Fig. 8.7 - Chn-based material obtained by Sxl using Et as solvent.

All the materials were tested for adsorption of 3 organic dye (4NBAld, 4Nph and MB) and only Cls-based obtained with Sxl using Et as solvent and Chn-based materials were tested for adsorption of 2 heavy metals (Cd and Cr).

The Cls-based material obtained with Sxl using Me as solvent was not tested because it looks harder and more rigid than the other material and without the typical inner structure of the other materials.

The adsorption tests were implemented in a first phase with the study of the kinetics of three organic dyes. The first results appreciable were the different resistance during the 24 hours of the tests and this behavior has repercussions on the adsorption capacity of the adsorbent material. The worse material is Cls-based freeze-dried, follow by the Cls-based freeze-dried washed with Sxl. The Cls-based material obtained with Sxl using Ac as

solvent was not bad, but not better than the first two materials. Between all the Cls-based materials the best results were for the one obtained with Sxl using Et as solvent and these results are also better than the results of Chn-based material.

A second phase of adsorption tests was implemented on the heavy metals (Cd(II) and Cr(VI)) only for the two best materials Cls-based obtained with Sxl using Et as solvent and Chn-based material. The Cls-based material has the best result with chromium instead of the Chn-based material has the best result with cadmium and in this second case the difference of adsorption capacity is very high.

From an environmental impact point of view were implemented the analysis using as a functional unit the mg of contaminant adsorbed per gram of adsorbent material. First, Cls-based material obtained in all the 4 different ways was tested with organic dyes. It is clear that the highest impact is from Cls-based freeze-dried washed in the Sxl tested with the 4NBAld and afterwards the impact from the Cls-based material freeze-dried tested for the 4Nph was calculated. The MB is the only one which has the lowest impact for all the materials tested.

After that, only the Cls-based material obtained with Sxl using Et as solvent was tested with two heavy metals Cadmium and Chromium and its environmental impact were compared with the environmental impact of the adsorption tests of Chn-based material. It is possible to observe that the highest impact is from the test of Chn-based material with 4NBAld and 4Nph. Also for the Cls-based material, these are the two dyes with the higher impact. The difference is for the MB because for the Cls-based material, the impact is lower than the Chn-based material. The environmental impact for the heavy metals is for both the material very small and their impacts are very similar for both materials.

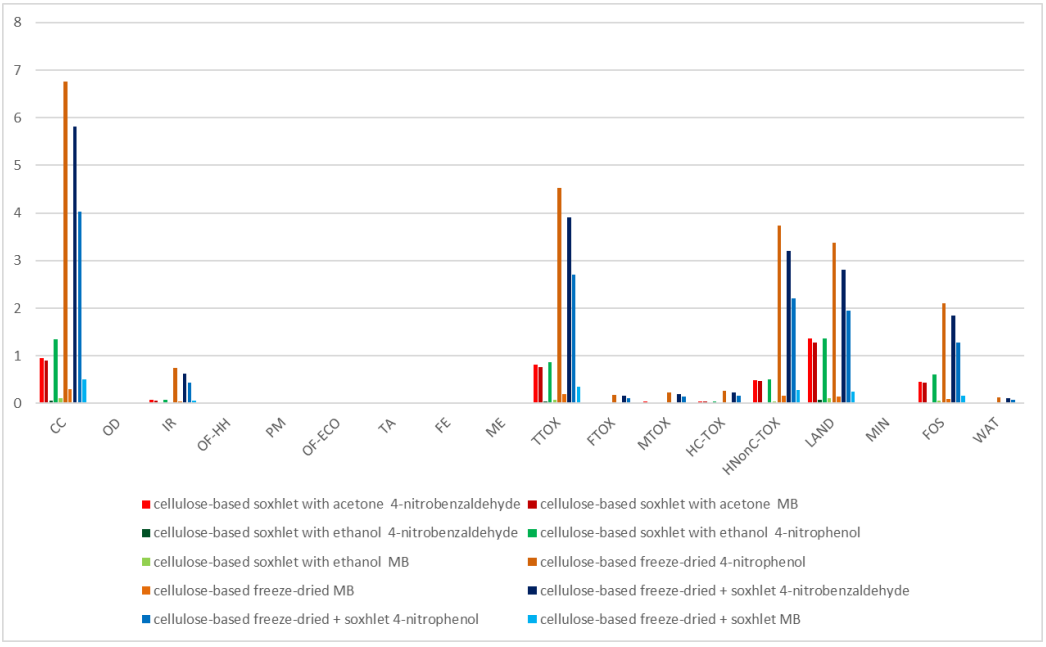


Fig. 8.8 - LCA comparison of adsorption capacity for organic dye of Cls-based material obtained with Sxl using Ac or Et as solvent and Cls-based material obtained with Fr without and with the final washing with Sxl.

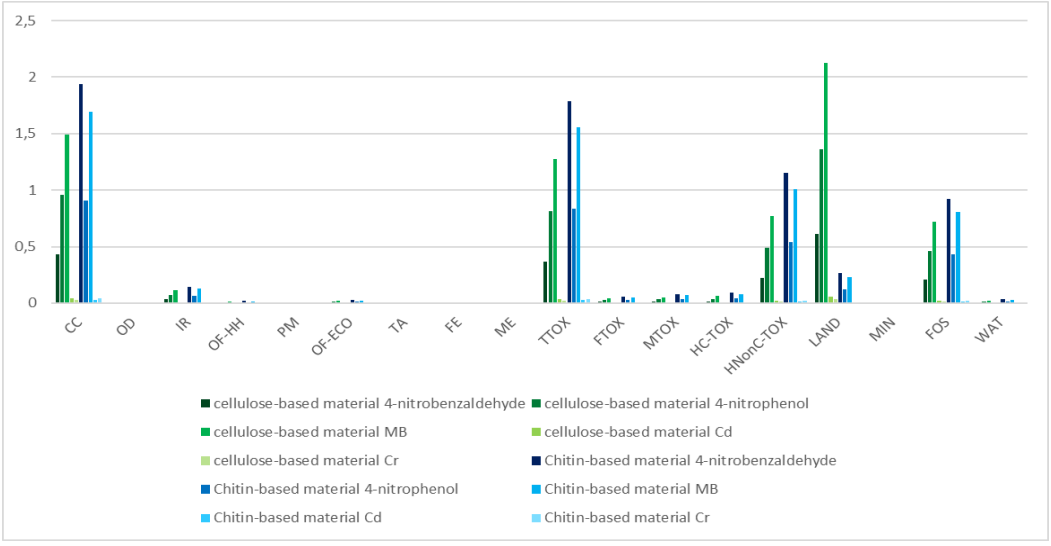


Fig. 8.9 - LCA comparison of adsorption capacity for organic dye and heavy metals of Cls-based material obtained with Sxl using Et as solvent and Chn-based material.

### *8.4. Scale-up scenarios*

To produce these materials on an industrial scale for use in the environmental field as contaminant-reactive materials, the synthesis procedure for the Cls-based material obtained with the Sxl using Et as solvent and for Chn-based material was tested for a small scale-up. Only the reagents amount is doubled and all the other parameters were left unchanged. A new inventory is implemented on Simapro to know how this small scale-up could affect the environmental impacts.

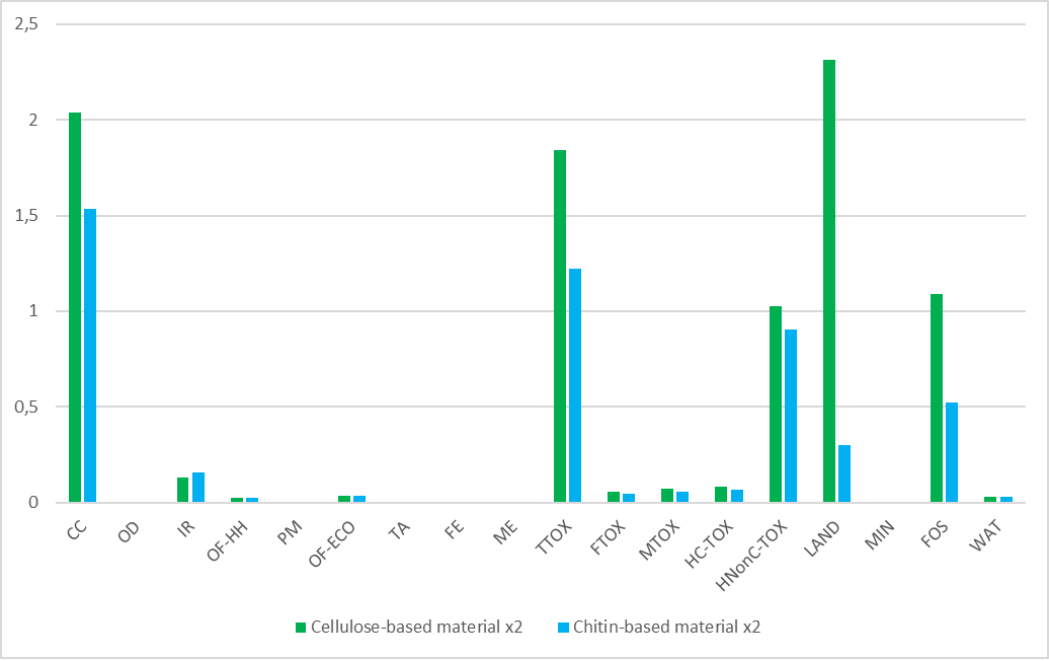


Fig. 8.10 - LCA comparison between the small scale-up for the Cls-based material and the small scale-up for the Chn-based material.

By comparing the Cls-based material with the Chn-based material scaled-up it is possible to see that the impact of the Chn-based material is lower, especially for land use. This is due to the substitution of cellulose with chitin because to produce chitin it is not necessary land for cultivation. Also,

Global warming, terrestrial ecotoxicity, Human non-cancerogenic toxicity and Fossil resource scarcity are lower for Chn-based material than Cls-based material because producing Chn-based material requires less electricity which is the voice with a higher impact.

The comparison of the environmental impact of scale-up materials with the impact of standard quantities showed that the impacts increase by increasing energy consumption. A possible explanation for this is the capacity of the laboratory equipment. In fact in this case the higher consumption of electricity is due to the Sxl. For the standard quantity, the Sxl is used for 24 hours, when the quantities produced are doubled the quantity the Sxl is used two times more.

Another important aspect that emerged from scale-up is that Chn-based material production is optimized, passing from an initial yield of 38% to 60% and it has consequences also on the environmental impact. It is possible to notice that Global warming is more or less the same for Cls-based material and Chn-based material in the starter synthesis protocol, but when the quantities are doubled the environmental impact of the Cls-based material increased over 2 kg $CO_2$ eq, instead of the Chn-based material that increased from 1.4 kg $CO_2$ eq to 1.5 kg $CO_2$ eq.

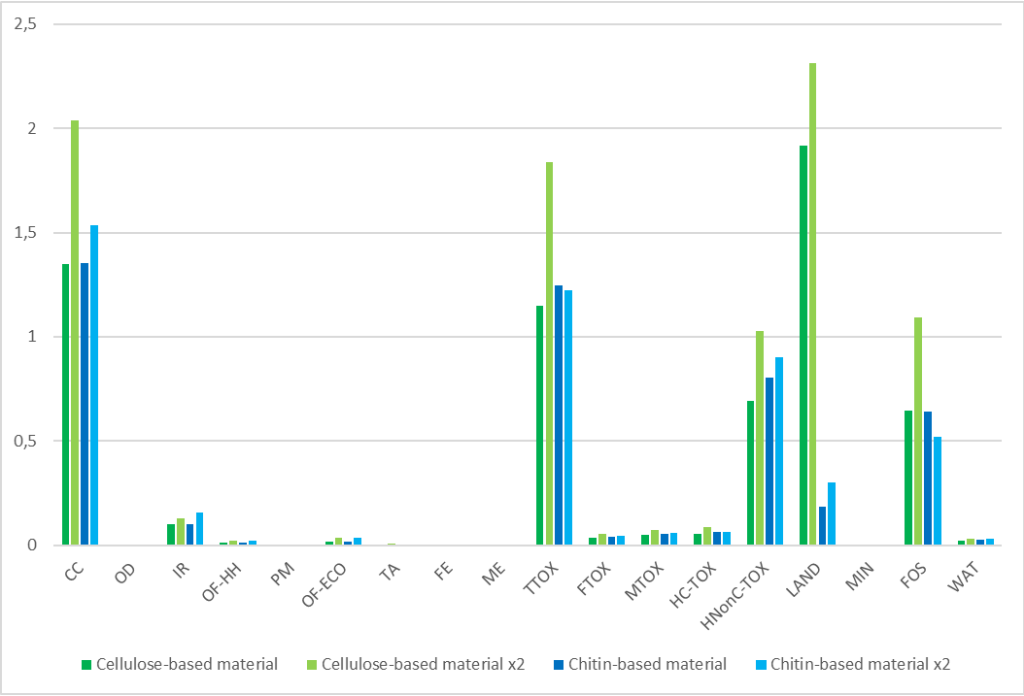


Fig. 8.11 - LCA comparison between cellulose and chitin processes with their scale-up.

### *8.5 Sensitivity Analysis*

A sensitivity analysis was performed to understand and evaluate the stochastic uncertainties related to how the inventory data affects the LCIA results by means of Monte Carlo simulations (in 10 000 points).

The sensitivity analysis was focused on the energy used for freeze drying process and Sxl processes which were found to be the most important impact contributors in the Global Warming category.

It is possible to state that if Cls-based material obtained by Fr is compared with Cls-based material obtained by Fr washed with Sxl using Et as solvent the electricity amount due to the Sxl decisive impact on global warming.

For Monte Carlo analysis of Cls-based material obtained by Fr compared with Cls-based material obtained by Sxl using Et as solvent it was possible to confirm what was hypothesized in the previous paragraphs, namely that the

use of the Sxl alone reduces energy consumption and therefore also the impact on global warming.

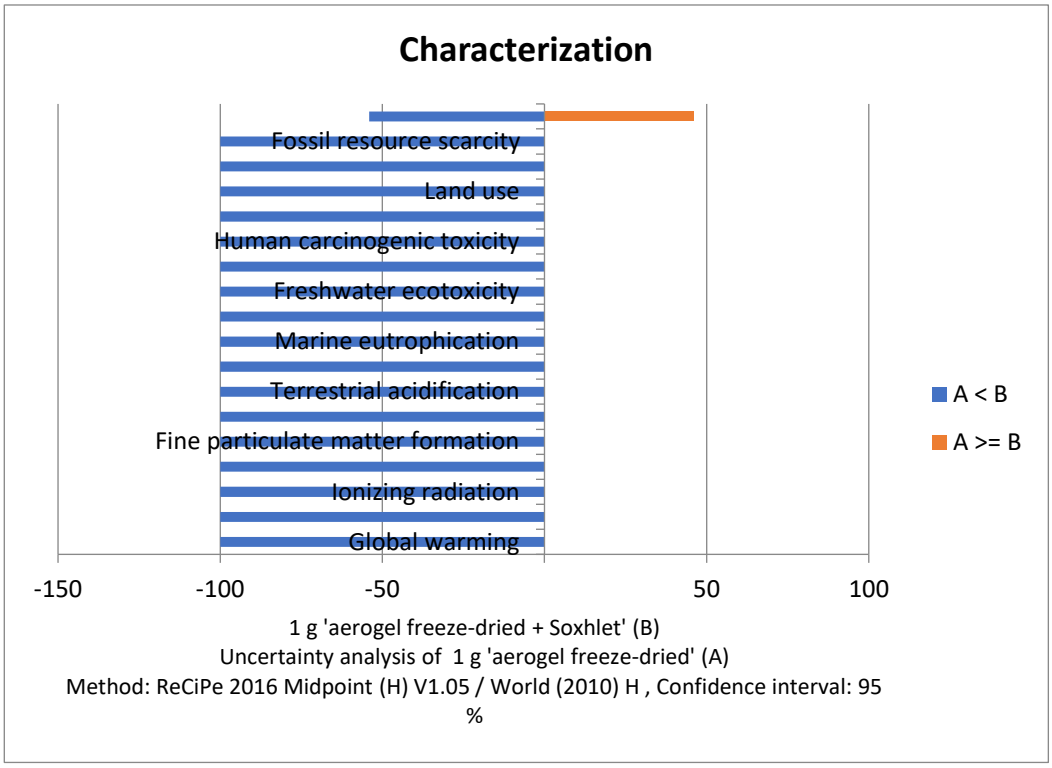


Fig. 8.12 - Monte Carlo analysis of Cls-based material obtained by Fr vs Cls-based material obtained by Fr washed with Sxl using Et as solvent.

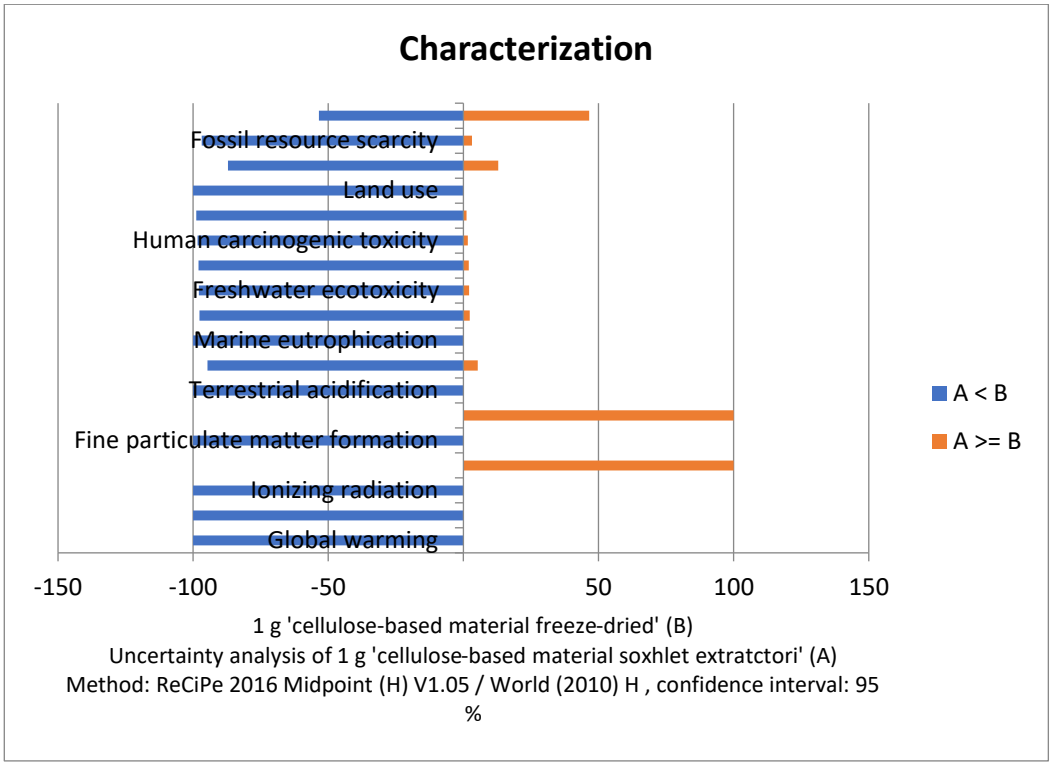


Fig. 8.13 - Monte Carlo analysis of Cls-based material obtained by Fr vs Cls-based material obtained by Sxl using Et as solvent.

This LCA study aims to study the environmental impact of different ways of new material production at a lab scale to choose the least impactful to the scale-up of the production. It can be stated that the process that has the highest impact is the electricity amount from the Fr process and Sxl. The Sxl process is less impactful than the Fr from an energy point of view and it is possible to further reduce the impact by choosing an appropriate solvent.
Another important fact to consider is that changing the cellulose with the chitin an impacts of Land use is lower, this is because the chitin powder used as a precursor is extracted from the shells of shrimps that would otherwise be wasted, while the microcrystalline cellulose used as a precursor is extracted from cotton linters.

This study confirms that the right direction for the production of new high-performance and sustainable adsorbent materials is not only to choose waste as the starting material but also to optimise the consumption of electricity used for the processes.

# CONCLUSIONS

The PhD thesis was elaborated thanks to a National Operative Program of Research and Innovation -innovative industrial research PhD- for the years from 2014 to 2020. The goal of this project is to connect academic research with the real needs of the industry.

The present thesis is the result of a multidisciplinary work that combines chemistry, material science and environmental technologies, aiming at remediating to the global problem of heavy contamination of sediments and seas. The research has been finalized to design new performing and sustainable materials for pollution remediation, particularly for the in-situ remediation technology as the reactive core mat. Among all the materials already studied in literature, the attention was focused on the bio-based materials potentially recovered from waste, namely Cls-based and Chn-based materials.

The experimental activities carried out in the chemistry and environmental technologies laboratories of the Polytechnic University of Bari were focused on the development of a reproducible and scalable synthesis protocol for both Cls- and Chn-based materials and the development of appropriate adsorption tests on these materials for organic and inorganic species individuated as potential pollutants. At the end of the experimental phase in the laboratories, a Life Cycle Assessment was carried out to estimate the environmental impacts both of the production phase and the application of these materials.

Although the synthesis protocol of Cls-based materials was adapted from literature, the method was developed with the intention of optimizing energy and time. The first part of the protocol was the same for all the Cls-based materials. The synthetic sequence can be divided into three fundamental steps, all carried out at room pressure and temperature:

- The oxidation of the microcrystalline cellulose in water with KBr and NaClO and catalysed by TEMPO with a basic pH.
- The pH adjustment to make the oxidized cellulose insoluble in water.
- The addition of the brancher (bPEI) to obtain a cross-linked structure. The porous structure is obtained by freeze overnight the solution obtained thanks to the formation of the ice-crystal.

After having identified in detail the necessary times and techniques (magnetic stirring, sonication and centrifugation) to complete these first three steps, two methods of purification to obtain the final material were compared: Fr and Sxl. The Fr process required a lot of time (48 hours) and electric energy for a small account of the final material obtained. It is also necessary to wash the final material for 24 hours with Et in a Sxl and dry it under vacuum for some hours. The Sxl was also used with three different solvents Acetone (Ac), methanol (Me) and Ethanol (Et). All the materials obtained have been compared with each other morphologically and chemically and no chemical, structural and morphological differences have emerged from FTIR and SEM analyses. Comparing also the density of these materials, it is within a range between 0.20 and 0.30 g/cm$^3$, being equal to 0.23 g/cm$^3$ for the Cls-based material obtained by lyophilisation and washed in the Sxl, 0.26 g/cm$^3$ for the cellulosic-based material obtained by freezing drying 0.31 g/cm$^3$ for the Cls-based material obtained by Sxl using Et as the solvent.

Therefore, no data allowed to discriminate which was the best protocol to obtain the Cls-based material, and the second stage of the experimental work was based on the adsorption tests of these materials with both organic contaminants (4Nph, 4NBAld and MB). The adsorption tests with organic dyes indicated that the Cls-based material obtained with Sxl using Et as solvent afforded the best performances exhibiting the highest adsorption percentages (4NPh: 90%, 4NBAld: 80% and MB: 30%) and capacities (4NPh: 1.5 mg/g, 4NBAld: 0.9 mg/g and MB: 8.4 mg/g) of the

series. Only the adsorption percentages (4NPh: 95%, 4NBAld: 80% and MB: 40%) and capacities (4NPh: 1.6 mg/g, 4NBAld: 1.1 mg/g and MB: 12 mg/g) of the Cls-based material obtained with Fr and washed in the Sxl using Et as solvent were very closed or even better than the Cls-based material obtained with Sxl using Et as solvent. The latter material was also more resistant than the others because the other materials crumbled with the magnetic stirring during the 24 hours of the experiments. However, through these preliminary tests was possible to assert that the best synthesis protocol in terms of time, energy, and adsorption attitude was the Cls-based material obtained with Sxl using Et as solvent.

This protocol was applied to obtain Chn-based material, an innovative microporous material. The microcrystalline cellulose amount in the synthesis protocol was replaced with an equal weight with chitin powder from shrimp shells. Keeping constant the weight instead of the molar ratio, an excess of the oxidant with respect to chitin was used allowing to obtain some innovations:

- Analysed with FTIR, the chitin oxidation was clearly visible in the signal at 1731 $cm^{-1}$ obtained thanks to the pH equal to 1;
- The addition of the bPEI to the oxidated chitin allowed to obtain a new material with a density equal to 0.15 $g/cm^3$.

This material was tested with organic dyes (4Nph, 4NBAld and MB) and compared with the Cls-based material obtained with the same protocol.

In this stage, it was also studied the influence of the pH of the 4Nph solution on the adsorption behaviour. While no substantial differences were observed for the Cls-based material, in the case of the Chn-based material it was possible to observe that only the test with a pH equal to 12.4 afforded negative results (< 10% of adsorbed dye). The other two tests (pH = 8.4 and 1.0) showed satisfactory results with adsorption capacities up to 20%.

In the case of the MB adsorption, the better result was obtained for the Cls-based material (adsorbed dye percentage = 30%), while the Chn-based material exhibited lower values (adsorbed dye percentage = 20%).

The best results for the two materials obtained with the 4NBAld solution was about 99.8% for Cls-based material and 99.99% for the Chn-based material.

These two materials were also tested with the same three organic dyes in marine water. The results were very close for both the materials, the 4Nph (in its basic form) and MB were both adsorbed with a low percentages (~10%). Also in this case the 4NBAld was adsorbed for the 97% on Cls-based material and for the 99% on Chn-based material.

On these two materials were also conducted preliminary tests with two heavy metals (Cd and Cr). It was possible to assert that starting from a concentration of 100 ppm the adsorption capacity of the Chn-based material (52.5 mg/g) is higher than the Cls-based material (37.5 mg/g) for the Cd; testing the Cr the trend is opposite, in fact, the Cls-based material gave a higher adsorption capacity (28.75 mg/g) than the Chn-based material (24 mg/g) with a starting concentration of 100 ppm. The trend is inverted with a starting concentration of 150 ppm: the adsorption capacity of the Cls-based material is equal to 27.5 mg/g and it was lower than Chn-based material (33.5 mg/g).

So with these results obtaining from the adsorption tests with organic and inorganic compounds it is possible to assert that both materials Cls- and Chn-based had good attitude and they are great candidates as new materials for environmental remediation.

Another aspect that is necessary to consider is the possibility of the scale-up of their production. Aiming at up-grading the production from the laboratory to the industrial scale, a scale-up for the synthesis of these materials was studied by adopting 2-fold and 4-fold quantities of all the reagents, while their molar ratios were kept constant. The calculated yield for the Chn-based material was about 38% and increased to 95%, for the Cls-based material the trend was the opposite and it started at 75% and decreased to 63% when the quantities were doubled, but when quantities were four times higher the synthesis didn't work. So it is possible to assert

that the Chn-based material is ready to implement an industrial scale-up, but the Cls-based material needs more study before implementing the production on an industrial scale.

The last phase of this project was the evaluation of the environmental impact of all the remediation processes, so a LCA analysis was implemented. From this analysis, it is possible to assert that the major problem derived from the synthesis protocol was the electricity consumption. The higher impact was from the Cls-based material obtained with Fr and washed in Sxl using Et as solvent. The comparison of the different solvents used in Sxl showed that Et is the less impactful.

The comparison between Cls-based and Chn-based materials showed very similar results for electricity consumption, but the chitin powder is always produced from the wastes of the seafood industry, while the cellulose powder is produced from cotton linters showing a high impact for land use.

In conclusion, the comparative analysis of the two materials presented similar results in adsorption tests; however, chitin emerges as the preferable choice because of its scale-up possibilities for industrial applications. Notwithstanding the chitin raw material derives from waste, its utilization requires significant efforts to reduce the environmental impact of electricity consumption.

# ACKNOWLEDGEMENTS

I would like to thank my supervisor prof. Notarnicola Michele to have bet on a stranger and to give me the possibility to grow as a student, as a researcher and as a person. It was a huge act of confidence to have the opportunity to set the trial in full freedom, still under his guidance.

I wish to thank also Prof. Todaro Francesco for being a mentor, an anchor and a friend.

I want to thank Prof. Andrea Petrella for always having an answer to all my questions with a smile even when I came to him with bad news, he showed me the positive side.

I am grateful to all the Environmental Technologies group, every one of you gave me support in the bad periods and funny in the better ones.

I would like to thank Prof. Teodosiu Carmen and George Barjoveanu for their hospitality at the Technical University of Iasi and for allowing me to have an educational experience both professionally and personally. Thanks also to the whole research group and especially to Dana-mica for being my anchor during all the time I spent in Iasi, and also thanks to Andreea, Luana and Ramona for the laughter and food.

My heartfelt thanks go to Prof Suranna Gian Paolo because, since the master thesis, he has been a mentor and an anchor, always ready to give support, to drive me to do better and to confirm when I was doing something good.

I would like to thank Prof. Grisorio Roberto for being, since the master thesis, an ever-ready source of advice and always ready to listen to ideas and conjectures, encouraging me to give my best as a student and researcher and always ready to recognize when I was doing well. He showed me the researcher type that I would like to be.

A special thank goes to Sergio always present on this path a tireless and fundamental support; it's not easy to live with a PhD student.

A very special thank goes to my mother, I could not have achieved any goal without her constant support.

# BIBLIOGRAPHY

Ahmed, W., Xu, T., Mahmood, M., Núñez-Delgado, A., Ali, S., Shakoor, A., Qaswar, M., Zhao, H., Liu, W., Li, W. & Mehmood, S. (2022). Nano-hydroxyapatite modified biochar: Insights into the dynamic adsorption and performance of lead (II) removal from aqueous solution. *Environmental Research*. 214 (July).

Anon (n.d.). *PUG102 Regione PUGLIA*.

Baker, J.R. (1997). Evaluation of estimation methods for organic carbon normalized sorption coefficients. *Water Environment Research*. 69 (2). p.pp. 136–145.

Barjoveanu, G., De Gisi, S., Casale, R., Todaro, F., Notarnicola, M. & Teodosiu, C. (2018). A life cycle assessment study on the stabilization/solidification treatment processes for contaminated marine sediments. *Journal of Cleaner Production*. 201. p.pp. 391–402.

Bartolozzi, I., Daddi, T., Punta, C., Fiorati, A. & Iraldo, F. (2020). Life cycle assessment of emerging environmental technologies in the early stage of development: A case study on nanostructured materials. *Journal of Industrial Ecology*. 24 (1). p.pp. 101–115.

Bhardwaj, N. & Kundu, S.C. (2010). Electrospinning: A fascinating fiber fabrication technique. *Biotechnology Advances*. 28 (3) p.pp. 325–347.

Biswas, A., Bayer, I.S., Biris, A.S., Wang, T., Dervishi, E. & Faupel, F. (2012). Advances in top-down and bottom-up surface nanofabrication: Techniques, applications & future prospects. *Advances in Colloid and Interface Science*. 170 (1–2) p.pp. 2–27.

Calderon, B. & Fullana, A. (2015). Heavy metal release due to aging effect during zero valent iron nanoparticles remediation. *Water Research*. 83. p.pp. 1–9.

Capello, C., Fischer, U. & Hungerbühler, K. (2007). What is a green solvent? A comprehensive framework for the environmental assessment of solvents. *Green Chemistry*. 9 (9). p.pp. 927–93.

Cecchi, G., Cutroneo, L., Di Piazza, S., Besio, G., Capello, M. & Zotti, M. (2021). Port sediments: Problem or resource? a review concerning the treatment and decontamination of port sediments by fungi and bacteria. *Microorganisms*. 9 (6).

Chapman, E.E.V., Moore, C. & Campbell, L.M. (2020). Evaluation of a nanoscale zero-valent iron amendment as a potential tool to reduce mobility, toxicity, and

bioaccumulation of arsenic and mercury from wetland sediments. *Environmental Science and Pollution Research*. 27 (15). p.pp. 18757–18772.

Chen, C., Feng, X. & Yao, S. (2021). Ionic liquid-multi walled carbon nanotubes composite tablet for continuous adsorption of tetracyclines and heavy metals. *Journal of Cleaner Production*. 286. p.p. 124937.

Chen, W. fang, Zhang, J., Zhang, X., Wang, W. & Li, Y. (2016). Investigation of heavy metal (Cu, Pb, Cd, and Cr) stabilization in river sediment by nano-zero-valent iron/activated carbon composite. *Environmental Science and Pollution Research*. 23 (2). p.pp. 1460–1470.

Chen, X., Wright, J. V, Conca, J.L. & Peurrung, L.M. (2000). *EVALUATION OF HEAVY METAL REMEDIATION USING MINERAL APATITE The United States Environmental Protection Agency ( US EPA ) Land Disposal Restrictions ( LDR ) Program sets treatment standards for the wastes banned from land disposal ( US EPA , 1990 ). The tr*. p.pp. 57–78.

Cheng, H., Li, Y., Wang, B., Mao, Z., Xu, H., Zhang, L., Zhong, Y. & Sui, X. (2018). Chemical crosslinking reinforced flexible cellulose nanofiber-supported cryogel. *Cellulose*. 25 (1). p.pp. 573–582.

Crane, R.A. & Scott, T.B. (2012). Nanoscale zero-valent iron: Future prospects for an emerging water treatment technology. *Journal of Hazardous Materials*. 211–212. p.pp. 112–125.

Crocetti, P., González-Camejo, J., Li, K., Foglia, A., Eusebi, A.L. & Fatone, F. (2022). An overview of operations and processes for circular management of dredged sediments. *Waste Management*. 146 p.pp. 20–35.

Deb, H., Xiao, S., Morshed, M.N. & Al Azad, S. (2018). Immobilization of Cationic Titanium Dioxide (TiO2+) on Electrospun Nanofibrous Mat: Synthesis, Characterization, and Potential Environmental Application. *Fibers and Polymers*. 19 (8). p.pp. 1715–1725.

Deng, R. & Zhan, X. (2023). High performance self-assembled nano-chlorapatite in the presence of lactonic sophorolipid for the immobilization of cadmium in polluted sediment. *Journal of Hazardous Materials*. 445 (November 2022).

Deng, S., Zhang, G., Chen, S., Xue, Y., Du, Z. & Wang, P. (2016). Rapid and effective preparation of a HPEI modified biosorbent based on cellulose fiber with a

microwave irradiation method for enhanced arsenic removal in water. *Journal of Materials Chemistry A*. 4 (41). p.pp. 15851–15860.

Dong, H., Deng, J., Xie, Y., Zhang, C., Jiang, Z., Cheng, Y., Hou, K. & Zeng, G. (2017). Stabilization of nanoscale zero-valent iron (nZVI) with modified biochar for Cr(VI) removal from aqueous solution. *Journal of Hazardous Materials*. 332. p.pp. 79–86.

Egbosiuba, T.C., Abdulkareem, A.S., Tijani, J.O., Ani, J.I., Krikstolaityte, V., Srinivasan, M., Veksha, A. & Lisak, G. (2021). Taguchi optimization design of diameter-controlled synthesis of multi walled carbon nanotubes for the adsorption of Pb(II) and Ni(II) from chemical industry wastewater. *Chemosphere*. 266. p.p. 128937.

Erten, M.B., Reible, D.D., Gilbert, R.B. & El Mohtar, C.S. (2012). The performance of organophilic clay on nonaqueous phase liquid contaminated sediments under anisotropic consolidation. *ASTM Special Technical Publication*. 1554 STP. p.pp. 32–44.

Fajardo, C., Ortíz, L.T., Rodríguez-Membibre, M.L., Nande, M., Lobo, M.C. & Martin, M. (2012). Assessing the impact of zero-valent iron (ZVI) nanotechnology on soil microbial structure and functionality: A molecular approach. *Chemosphere*. 86 (8). p.pp. 802–808.

Feng, Y., Gong, J.L., Zeng, G.M., Niu, Q.Y., Zhang, H.Y., Niu, C.G., Deng, J.H. & Yan, M. (2010). Adsorption of Cd (II) and Zn (II) from aqueous solutions using magnetic hydroxyapatite nanoparticles as adsorbents. *Chemical Engineering Journal*. 162 (2). p.pp. 487–494.

Fiorati, A., Turco, G., Travan, A., Caneva, E., Pastori, N., Cametti, M., Punta, C. & Melone, L. (2017). Mechanical and drug release properties of sponges from cross-linked cellulose nanofibers. *ChemPlusChem*. 82 (6). p.pp. 848–858.

Gavankar, S., Suh, S. & Keller, A.A. (2015). The Role of Scale and Technology Maturity in Life Cycle Assessment of Emerging Technologies: A Case Study on Carbon Nanotubes. *Journal of Industrial Ecology*. 19 (1). p.pp. 51–60.

Ge, H., Huang, H., Xu, M. & Chen, Q. (2016). Cellulose/poly(ethylene imine) composites as efficient and reusable adsorbents for heavy metal ions. *Cellulose*. 23 (4). p.pp. 2527–2537.

Ghasemi, E., Ziyadi, H., Afshar, A.M. & Sillanpää, M. (2015). Iron oxide nanofibers: A new magnetic catalyst for azo dyes degradation in aqueous solution. *Chemical Engineering Journal*. 264. p.pp. 146–151.

Gheitasi Zarooni, M., Hoseini, S.J., Bahrami, M., Roushani, M. & Nabavizadeh, S.M. (2020). Pd/[C2NH2mim][Br] Thin Film Versus Pd/[C8mim][Cl] or Pd/[C8mim][BF4]: Catalytic Applications in Electrooxidation of Methanol, p-Nitrophenol Reduction and C–C Coupling Reaction. *Journal of Inorganic and Organometallic Polymers and Materials*. 30 (9). p.pp. 3448–3475.

Ghosh, U., Luthy, R.G., Cornelissen, G., Werner, D. & Menzie, C.A. (2011). In-situ sorbent amendments: A new direction in contaminated sediment management. *Environmental Science and Technology*. 45 (4). p.pp. 1163–1168.

Gil-Díaz, M., Alonso, J., Rodríguez-Valdés, E., Gallego, J.R. & Lobo, M.C. (2017). Comparing different commercial zero valent iron nanoparticles to immobilize As and Hg in brownfield soil. *Science of the Total Environment*. 584–585. p.pp. 1324–1332.

Gong, J.L., Wang, B., Zeng, G.M., Yang, C.P., Niu, C.G., Niu, Q.Y., Zhou, W.J. & Liang, Y. (2009). Removal of cationic dyes from aqueous solution using magnetic multi-wall carbon nanotube nanocomposite as adsorbent. *Journal of Hazardous Materials*. 164 (2–3). p.pp. 1517–1522.

Guégan, R. (2019). Organoclay applications and limits in the environment. *Comptes Rendus Chimie*. 22 (2–3) p.pp. 132–141.

Guerra, F.D., Attia, M.F., Whitehead, D.C. & Alexis, F. (2018). Nanotechnology for environmental remediation: Materials and applications. *Molecules*. 23 (7).

He, M., Shi, H., Zhao, X., Yu, Y. & Qu, B. (2013). Immobilization of Pb and Cd in Contaminated Soil Using Nano-Crystallite Hydroxyapatite. *Procedia Environmental Sciences*. 18. p.pp. 657–665.

Hong, Y.S., Kinney, K.A. & Reible, D.D. (2011a). Acid volatile sulfides oxidation and metals (Mn, Zn) release upon sediment resuspension: Laboratory experiment and model development. *Environmental Toxicology and Chemistry*. 30 (3). p.pp. 564–575.

Hong, Y.S., Kinney, K.A. & Reible, D.D. (2011b). Effects of cyclic changes in pH and salinity on metals release from sediments. *Environmental Toxicology and Chemistry*. 30 (8). p.pp. 1775–1784.

Hristozov, D. & Malsch, I. (2009). Hazards and Risks of engineered nanoparticles for the environment and human health. *Sustainability*. 1 (4). p.pp. 1161–1194.

Huang, D., Deng, R., Wan, J., Zeng, G., Xue, W., Wen, X., Zhou, C., Hu, L., Liu, X., Xu, P., Guo, X. & Ren, X. (2018a). Remediation of lead-contaminated sediment by biochar-supported nano-chlorapatite: Accompanied with the change of available phosphorus and organic matters. *Journal of Hazardous Materials*. 348 (August 2017). p.pp. 109–116.

Huang, D., Hu, Z., Peng, Z., Zeng, G., Chen, G., Zhang, C., Cheng, M., Wan, J., Wang, X. & Qin, X. (2018b). Cadmium immobilization in river sediment using stabilized nanoscale zero-valent iron with enhanced transport by polysaccharide coating. *Journal of Environmental Management*. 210. p.pp. 191–200.

Huang, D., Hu, Z., Peng, Z., Zeng, G., Chen, G., Zhang, C., Cheng, M., Wan, J., Wang, X. & Qin, X. (2018c). Cadmium immobilization in river sediment using stabilized nanoscale zero-valent iron with enhanced transport by polysaccharide coating. *Journal of Environmental Management*. 210. p.pp. 191–200.

Huang, D., Xue, W., Zeng, G., Wan, J., Chen, G., Huang, C., Zhang, C., Cheng, M. & Xu, P. (2016). Immobilization of Cd in river sediments by sodium alginate modified nanoscale zero-valent iron: Impact on enzyme activities and microbial community diversity. *Water Research*. 106. p.pp. 15–25.

Ihsanullah, Abbas, A., Al-Amer, A.M., Laoui, T., Al-Marri, M.J., Nasser, M.S., Khraisheh, M. & Atieh, M.A. (2016). Heavy metal removal from aqueous solution by advanced carbon nanotubes: Critical review of adsorption applications. *Separation and Purification Technology*. 157. p.pp. 141–161.

Ingrao, C., Vesce, E., Evola, R.S., Rebba, E., Arcidiacono, C., Martra, G. & Beltramo, R. (2021). Chemistry behind leather: Life Cycle Assessment of nano-hydroxyapatite preparation on the lab-scale for fireproofing applications. *Journal of Cleaner Production*. 279. p.p. 123837.

Jin, X., Xiang, Z., Liu, Q., Chen, Y. & Lu, F. (2017). Polyethyleneimine-bacterial cellulose bioadsorbent for effective removal of copper and lead ions from aqueous solution. *Bioresource Technology*. 244. p.pp. 844–849.

Joshi, P. & Manocha, S. (2017a). Sorption of cadmium ions onto synthetic hydroxyapatite nanoparticles. *Materials Today: Proceedings*. 4 (9). p.pp. 10460–10464.

Joshi, P. & Manocha, S. (2017b). Sorption of cadmium ions onto synthetic hydroxyapatite nanoparticles. *Materials Today: Proceedings*. 4 (9). p.pp. 10460–10464.

Keochaiyom, B., Wan, J., Zeng, G., Huang, D., Xue, W., Hu, L., Huang, C., Zhang, C. & Cheng, M. (2017). Synthesis and application of magnetic chlorapatite nanoparticles for zinc (II), cadmium (II) and lead (II) removal from water solutions. *Journal of Colloid and Interface Science*. 505. p.pp. 824–835.

Kharisov, B.I., Rasika Dias, H. V., Kharissova, O. V., Manuel Jiménez-Pérez, V., Olvera Pérez, B. & Muñoz Flores, B. (2012). Iron-containing nanomaterials: Synthesis, properties, and environmental applications. *RSC Advances*. 2 (25). p.pp. 9325–9358.

Knox, A.S., Paller, M.H. & Roberts, J. (2012a). Active capping technology-New approaches for in situ remediation of contaminated sediments. *Remediation*. 22 (2). p.pp. 93–117.

Knox, A.S., Paller, M.H. & Roberts, J. (2012b). Active capping technology-New approaches for in situ remediation of contaminated sediments. *Remediation*. 22 (2). p.pp. 93–117.

Labianca, C., De Gisi, S., Todaro, F., Notarnicola, M. & Bortone, I. (2022). A review of the in-situ capping amendments and modeling approaches for the remediation of contaminated marine sediments. *Science of The Total Environment*. 806. p.p. 151257.

Lee, C.H., Chiang, C.L. & Liu, S.J. (2013). Electrospun nanofibrous rhodanine/polymethylmethacrylate membranes for the removal of heavy metal ions. *Separation and Purification Technology*. 118. p.pp. 737–743.

Li, Y., Qiu, T. & Xu, X. (2013). Preparation of lead-ion imprinted crosslinked electro-spun chitosan nanofiber mats and application in lead ions removal from aqueous solutions. *European Polymer Journal*. 49 (6). p.pp. 1487–1494.

Li, Y.H., Ding, J., Luan, Z., Di, Z., Zhu, Y., Xu, C., Wu, D. & Wei, B. (2003). Competitive adsorption of Pb2+, Cu2+ and Cd 2+ ions from aqueous solutions by multiwalled carbon nanotubes. *Carbon*. 41 (14). p.pp. 2787–2792.

Liang, J., Liu, J., Yuan, X., Dong, H., Zeng, G., Wu, H., Wang, H., Liu, J., Hua, S., Zhang, S., Yu, Z., He, X. & He, Y. (2015). Facile synthesis of alumina-decorated multi-walled

carbon nanotubes for simultaneous adsorption of cadmium ion and trichloroethylene. *Chemical Engineering Journal*. 273. p.pp. 101–110.

Liberatori, G., Grassi, G., Guidi, P., Bernardeschi, M., Fiorati, A., Scarcelli, V., Genovese, M., Faleri, C., Protano, G., Frenzilli, G., Punta, C. & Corsi, I. (2020). Effect-based approach to assess nanostructured cellulose sponge removal efficacy of zinc ions from seawater to prevent ecological risks. *Nanomaterials*. 10 (7). p.pp. 1–20.

Liu, C., Jin, R.N., Ouyang, X. kun & Wang, Y.G. (2017). Adsorption behavior of carboxylated cellulose nanocrystal—polyethyleneimine composite for removal of Cr(VI) ions. *Applied Surface Science*. 408. p.pp. 77–87.

Liu, R. & Zhao, D. (2013). Synthesis and characterization of a new class of stabilized apatite nanoparticles and applying the particles to in situ Pb immobilization in a fire-range soil. *Chemosphere*. 91 (5). p.pp. 594–601.

Ma, Z., Ji, H., Teng, Y., Dong, G., Zhou, J., Tan, D. & Qiu, J. (2011). Engineering and optimization of nano- and mesoporous silica fibers using sol-gel and electrospinning techniques for sorption of heavy metal ions. *Journal of Colloid and Interface Science*. 358 (2). p.pp. 547–553.

Melone, L., Rossi, B., Pastori, N., Panzeri, W., Mele, A. & Punta, C. (2015a). TEMPO-Oxidized Cellulose Cross-Linked with Branched Polyethyleneimine: Nanostructured Adsorbent Sponges for Water Remediation. *ChemPlusChem*. 80 (9). p.pp. 1408–1415.

Melone, L., Rossi, B., Pastori, N., Panzeri, W., Mele, A. & Punta, C. (2015b). TEMPO-Oxidized Cellulose Cross-Linked with Branched Polyethyleneimine: Nanostructured Adsorbent Sponges for Water Remediation. *ChemPlusChem*. 80 (9). p.pp. 1408–1415.

Meric, D., Hellweger, F., Barbuto, S., Rahbar, N., Alshawabkeh, A.N. & Sheahan, T.C. (2013). Model Prediction of Long-Term Reactive Core Mat Efficacy for Capping Contaminated Aquatic Sediments. *Journal of Environmental Engineering*. 139 (4). p.pp. 564–575.

Meric, D., Rad, M.N., Barbuto, S., Sheahan, T.C., Alshawabkeh, A.N. & Shine, J. (2011). *Testing the Efficiency of a Reactive Core Mat to Remediate Subaqueous, Contaminated Sediments*.

Mobasherpour, I., Salahi, E. & Pazouki, M. (2012). Comparative of the removal of Pb 2+, Cd 2+ and Ni 2+ by nano crystallite hydroxyapatite from aqueous solutions: Adsorption isotherm study. *Arabian Journal of Chemistry*. 5 (4). p.pp. 439–446.

Mobasherpour, I., Salahi, E. & Pazouki, M. (2011). Removal of nickel (II) from aqueous solutions by using nano-crystalline calcium hydroxyapatite. *Journal of Saudi Chemical Society*. 15 (2). p.pp. 105–112.

Mohammad, A.M., Salah Eldin, T.A., Hassan, M.A. & El-Anadouli, B.E. (2017). Efficient treatment of lead-containing wastewater by hydroxyapatite/chitosan nanostructures. *Arabian Journal of Chemistry*. 10 (5). p.pp. 683–690.

Mubarak, N.M., Sahu, J.N., Abdullah, E.C., Jayakumar, N.S. & Ganesan, P. (2016). Microwave-assisted synthesis of multi-walled carbon nanotubes for enhanced removal of Zn(II) from wastewater. *Research on Chemical Intermediates*. 42 (4). p.pp. 3257–3281.

Olsta, J. (2010). In-situ capping of contaminated sediments with organophilic clay. *Ports 2010: Building on the Past, Respecting the Future - Proceedings of the 12th Triannual International Conference*. (Patmont 2006). p.pp. 603–610.

Olsta, J.T. & Asce, M. (2007). *In-Situ Capping of Contaminated Sediments with Reactive Materials*.

Olsta, J.T. & Darlington, J.W. (2006). Innovative systems for dredging, dewatering or for in-situ capping of contaminated sediments. *Association for Environmental Health and Sciences - 21st Annual International Conference on Contaminated Soils, Sediments and Water 2005*. 11 (January). p.pp. 286–294.

Peld, M., Tõnsuaadu, K. & Bender, V. (2002). Natural and synthetic apatites as sorbents for Cd2+ ions from aqueous solutions. *Phosphorus, Sulfur and Silicon and Related Elements*. 177 (8–9). p.p. 2239.

Peng, J. feng, Song, Y. hui, Yuan, P., Cui, X. yu & Qiu, G. lei (2009). The remediation of heavy metals contaminated sediment. *Journal of Hazardous Materials*. 161 (2–3) p.pp. 633–640.

Peng, W., Li, X., Xiao, S. & Fan, W. (2018a). Review of remediation technologies for sediments contaminated by heavy metals. *Journal of Soils and Sediments*. 18 (4). p.pp. 1701–1719.

Peng, W., Li, X., Xiao, S. & Fan, W. (2018b). Review of remediation technologies for sediments contaminated by heavy metals. *Journal of Soils and Sediments*. 18 (4). p.pp. 1701–1719.

Perelo, L.W. (2010). Review: In situ and bioremediation of organic pollutants in aquatic sediments. *Journal of Hazardous Materials*. 177 (1–3). p.pp. 81–89.

Qian, G., Chen, W., Lim, T.T. & Chui, P. (2009). In-situ stabilization of Pb, Zn, Cu, Cd and Ni in the multi-contaminated sediments with ferrihydrite and apatite composite additives. *Journal of Hazardous Materials*. 170 (2–3). p.pp. 1093–1100.

Qian, W., Liang, J.Y., Zhang, W.X., Huang, S.T. & Diao, Z.H. (2022). A porous biochar supported nanoscale zero-valent iron material highly efficient for the simultaneous remediation of cadmium and lead contaminated soil. *Journal of Environmental Sciences (China)*. 113. p.pp. 231–241.

Qiao, L., Li, S., Li, Y., Liu, Y. & Du, K. (2020). Fabrication of superporous cellulose beads via enhanced inner cross-linked linkages for high efficient adsorption of heavy metal ions. *Journal of Cleaner Production*. 253.

Que, W., Zhou, Y. hui, Liu, Y. guo, Wen, J., Tan, X. fei, Liu, S. jia & Jiang, L. hua (2019). Appraising the effect of in-situ remediation of heavy metal contaminated sediment by biochar and activated carbon on Cu immobilization and microbial community. *Ecological Engineering*. 127. p.pp. 519–526.

Rad, L.R., Momeni, A., Ghazani, B.F., Irani, M., Mahmoudi, M. & Noghreh, B. (2014). Removal of Ni2+ and Cd2+ ions from aqueous solutions using electrospun PVA/zeolite nanofibrous adsorbent. *Chemical Engineering Journal*. 256. p.pp. 119–127.

Riva, L., Fiorati, A. & Punta, C. (2021). Synthesis and application of cellulose-polyethyleneimine composites and nanocomposites: A concise review. *Materials*. 14 (3). p.pp. 1–22.

Riva, L., Pastori, N., Panozzo, A., Antonelli, M. & Punta, C. (2020). Nanostructured cellulose-based sorbent materials for water decontamination from organic dyes. *Nanomaterials*. 10 (8). p.pp. 1–18.

Shin, W. & Kim, Y.K. (2016). Stabilization of heavy metal contaminated marine sediments with red mud and apatite composite. *Journal of Soils and Sediments*. 16 (2). p.pp. 726–735.

Silva, M.M., Pérez, D.V., Wasserman, J.C., Santos-Oliveira, R. & Wasserman, M.A.V. (2017). The effect of nanohydroxyapatite on the behavior of metals in a microcosm simulating a lentic environment. *Environmental Nanotechnology, Monitoring and Management*. 8. p.pp. 219–227.

Silvani, L., Di Palma, P.R., Riccardi, C., Eek, E., Hale, S.E., Viotti, P. & Petrangeli Papini, M. (2017). Use of biochar as alternative sorbent for the active capping of oil contaminated sediments. *Journal of Environmental Chemical Engineering*. 5 (5). p.pp. 5241–5249.

Song, B., Zeng, G., Gong, J., Zhang, P., Deng, J., Deng, C., Yan, J., Xu, P., Lai, C., Zhang, C. & Cheng, M. (2017). Effect of multi-walled carbon nanotubes on phytotoxicity of sediments contaminated by phenanthrene and cadmium. *Chemosphere*. 172. p.pp. 449–458.

Sparrevik, M., Saloranta, T., Cornelissen, G., Eek, E., Fet, A.M., Breedveld, G.D. & Linkov, I. (2011). Use of life cycle assessments to evaluate the environmental footprint of contaminated sediment remediation. *Environmental Science and Technology*. 45 (10). p.pp. 4235–4241.

Stone, V., Nowack, B., Baun, A., van den Brink, N., von der Kammer, F., Dusinska, M., Handy, R., Hankin, S., Hassellöv, M., Joner, E. & Fernandes, T.F. (2010). Nanomaterials for environmental studies: Classification, reference material issues, and strategies for physico-chemical characterisation. *Science of The Total Environment*. 408 (7). p.pp. 1745–1754.

Su, H., Fang, Z., Tsang, P.E., Fang, J. & Zhao, D. (2016). Stabilisation of nanoscale zero-valent iron with biochar for enhanced transport and in-situ remediation of hexavalent chromium in soil. *Environmental Pollution*. 214. p.pp. 94–100.

Su, Y., Adeleye, A.S., Keller, A.A., Huang, Y., Dai, C., Zhou, X. & Zhang, Y. (2015). Magnetic sulfide-modified nanoscale zerovalent iron (S-nZVI) for dissolved metal ion removal. *Water Research*. 74. p.pp. 47–57.

Sun, W., Jiang, B., Wang, F. & Xu, N. (2015). Effect of carbon nanotubes on Cd(II) adsorption by sediments. *Chemical Engineering Journal*. 264. p.pp. 645–653.

Taghavy, A., Costanza, J., Pennell, K.D. & Abriola, L.M. (2010). Effectiveness of nanoscale zero-valent iron for treatment of a PCE-DNAPL source zone. *Journal of Contaminant Hydrology*. 118 (3–4). p.pp. 128–142.

Tang, J., Song, Y., Zhao, F., Spinney, S., da Silva Bernardes, J. & Tam, K.C. (2019). Compressible cellulose nanofibril (CNF) based aerogels produced via a bio-inspired strategy for heavy metal ion and dye removal. *Carbohydrate Polymers*. 208. p.pp. 404–412.

Tang, W.W., Zeng, G.M., Gong, J.L., Liang, J., Xu, P., Zhang, C. & Huang, B. Bin (2014a). Impact of humic/fulvic acid on the removal of heavy metals from aqueous solutions using nanomaterials: A review. *Science of The Total Environment*. 468–469. p.pp. 1014–1027.

Tang, W.W., Zeng, G.M., Gong, J.L., Liang, J., Xu, P., Zhang, C. & Huang, B. Bin (2014b). Impact of humic/fulvic acid on the removal of heavy metals from aqueous solutions using nanomaterials: A review. *Science of The Total Environment*. 468–469. p.pp. 1014–1027.

Teng, M., Li, F., Zhang, B. & Taha, A.A. (2011). Electrospun cyclodextrin-functionalized mesoporous polyvinyl alcohol/SiO2 nanofiber membranes as a highly efficient adsorbent for indigo carmine dye. *Colloids and Surfaces A: Physicochemical and Engineering Aspects*. 385 (1–3). p.pp. 229–234.

Todaro, F., Barjoveanu, G., De Gisi, S., Teodosiu, C. & Notarnicola, M. (2021). Sustainability assessment of reactive capping alternatives for the remediation of contaminated marine sediments. *Journal of Cleaner Production*. 286 (xxxx). p.p. 124946.

Tong, L., Chen, J., Yuan, Y., Cui, Z., Ran, M., Zhang, Q., Bu, J., Yang, F., Su, X. & Xu, H. (2015). A novel lead ion-imprinted chelating nanofiber: Preparation, characterization, and performance evaluation. *Journal of Applied Polymer Science*. 132 (8).

Vandermeersch, G., Lourenço, H.M., Alvarez-Muñoz, D., Cunha, S., Diogène, J., Cano-Sancho, G., Sloth, J.J., Kwadijk, C., Barcelo, D., Allegaert, W., Bekaert, K., Fernandes, J.O., Marques, A. & Robbens, J. (2015). Environmental contaminants of emerging concern in seafood - European database on contaminant levels. *Environmental Research*. 143. p.pp. 29–45.

Velarde, L., Nabavi, M.S., Escalera, E., Antti, M.L. & Akhtar, F. (2023). Adsorption of heavy metals on natural zeolites: A review. *Chemosphere*. 328 (March). p.p. 138508.

Visentin, C., Trentin, A.W. da S., Braun, A.B. & Thomé, A. (2021). Life cycle sustainability assessment of the nanoscale zero-valent iron synthesis process for application in contaminated site remediation. *Environmental Pollution*. 268.

Wan, J., Zeng, G., Huang, D., Hu, L., Xu, P., Huang, C., Deng, R., Xue, W., Lai, C., Zhou, C., Zheng, K., Ren, X. & Gong, X. (2018). Rhamnolipid stabilized nano-chlorapatite: Synthesis and enhancement effect on Pb-and Cd-immobilization in polluted sediment. *Journal of Hazardous Materials*. 343. p.pp. 332–339.

Wan, J., Zhang, C., Zeng, G., Huang, D., Hu, L., Huang, C., Wu, H. & Wang, L. (2016). Synthesis and evaluation of a new class of stabilized nano-chlorapatite for Pb immobilization in sediment. *Journal of Hazardous Materials*. 320. p.pp. 278–288.

Wang, X.Q., Thibodeaux, L.J., Valsaraj, K.T. & Reible, D.D. (1991). *Efficiency of Capping Contaminated Bed Sediments in Situ. 1. Laboratory-Scale Experiments on Diffusion-Adsorption in the Capping Layer*. [Online]. Available from: https://pubs.acs.org/sharingguidelines.

Xiao, S., Shen, M., Guo, R., Wang, S. & Shi, X. (2009). Immobilization of Zerovalent Iron Nanoparticles into Electrospun Polymer Nanofibers: Synthesis, Characterization, and Potential Environmental Applications. *Journal of Physical Chemistry C*. 113 (42). p.pp. 18062–18068.

Xu, R., Jia, M., Zhang, Y. & Li, F. (2012). Sorption of malachite green on vinyl-modified mesoporous poly(acrylic acid)/SiO2 composite nanofiber membranes. *Microporous and Mesoporous Materials*. 149 (1). p.pp. 111–118.

Yang, Z., Fang, Z., Zheng, L., Cheng, W., Tsang, P.E., Fang, J. & Zhao, D. (2016a). Remediation of lead contaminated soil by biochar-supported nano-hydroxyapatite. *Ecotoxicology and Environmental Safety*. 132. p.pp. 224–230.

Yang, Z., Fang, Z., Zheng, L., Cheng, W., Tsang, P.E., Fang, J. & Zhao, D. (2016b). Remediation of lead contaminated soil by biochar-supported nano-hydroxyapatite. *Ecotoxicology and Environmental Safety*. 132. p.pp. 224–230.

Yin, J., Zhan, F., Jiao, T., Deng, H., Zou, G., Bai, Z., Zhang, Q. & Peng, Q. (2020). Highly efficient catalytic performances of nitro compounds via hierarchical PdNPs-loaded MXene/polymer nanocomposites synthesized through electrospinning strategy for wastewater treatment. *Chinese Chemical Letters*. 31 (4). p.pp. 992–995.

Yirsaw, B.D., Megharaj, M., Chen, Z. & Naidu, R. (2016). Environmental application and ecological significance of nano-zero valent iron. *Journal of Environmental Sciences (China)*. 44. p.pp. 88–98.

Ylng Ma, Q., Traina, S.J., Logan, T.J. & Ryan, J.A. (1993). *In Situ Lead Immobilization by Apatite*.

Zhang, C., Zhu, M. ying, Zeng, G. ming, Yu, Z. gang, Cui, F., Yang, Z. zhu & Shen, L. qing (2016a). Active capping technology: a new environmental remediation of contaminated sediment. *Environmental Science and Pollution Research*. 23 (5). p.pp. 4370–4386.

Zhang, C., Zhu, M. ying, Zeng, G. ming, Yu, Z. gang, Cui, F., Yang, Z. zhu & Shen, L. qing (2016b). Active capping technology: a new environmental remediation of contaminated sediment. *Environmental Science and Pollution Research*. 23 (5). p.pp. 4370–4386.

Zhang, J., Gong, J.L., Zeng, G.M., Yang, H.C. & Zhang, P. (2017). Carbon nanotube amendment for treating dichlorodiphenyltrichloroethane and hexachlorocyclohexane remaining in Dong-ting Lake sediment — An implication for in-situ remediation. *Science of the Total Environment*. 579. p.pp. 283–291.

Zhang, S., Shi, Q., Christodoulatos, C. & Meng, X. (2019). Lead and cadmium adsorption by electrospun PVA/PAA nanofibers: Batch, spectroscopic, and modeling study. *Chemosphere*. 233. p.pp. 405–413.

Zhang, W.-X. (2003). *Nanoscale iron particles for environmental remediation: An overview*.

Zhang, Z., Li, M., Chen, W., Zhu, S., Liu, N. & Zhu, L. (2010). Immobilization of lead and cadmium from aqueous solution and contaminated sediment using nano-hydroxyapatite. *Environmental Pollution*. 158 (2). p.pp. 514–519.

Zhu, F., Li, L., Ma, S. & Shang, Z. (2016). Effect factors, kinetics and thermodynamics of remediation in the chromium contaminated soils by nanoscale zero valent Fe/Cu bimetallic particles. *Chemical Engineering Journal*. 302. p.pp. 663–669.

US EPA, US Environmental Protection Agency, (2013). Use of amendments for in situ remediation at superfund sediment sites. Office of Superfund Remediation and Technology Innovation.

# LIST OF FIGURES

# LIST OF TABLES

# LIST OF ABREVIATIONS

| | |
|---|---|
| 4NBAld | 4-nitrobenzaldehyde |
| 4Nph | 4-nitrophenol |
| Ac | Acetone |
| Chn | Chitin |
| Cd | Cadmium |
| Cls | Cellulose |
| Cr | Chromium |
| Et | Ethanol |
| Fr | Freeze-drying |
| $H_2OD$ | Deionized Water |
| HM | Heavy Metal |
| KBr | Potassium Bromide |
| LCA | Life Cycle Assessment |
| MB | Methylene Blue |
| Me | Methanol |
| mg/kg s.s. | Concentration of the contaminant in solid sediments |
| NaClO | Sodium Hypochlorite |
| Sxl | Soxhlet extractor |
| TEMPO | 2,2,6,6 tetramethylpiperidinyloxyl |

# *CURRICULUM VITAE*


| | |
|---|---|
| Name and Surname | Milvia Elena Di Clemente |
| Mobile | +39 3278504211 |
| E-mail | milviaelena.diclemente@poliba.it |
| Nationality | Italian |
| Date of Birth | 12/04/1990 |


Born in Terlizzi, Bari (Italy) in 1990, graduated in Material Science and Technology at the University of Bari, in 2019, discussing the thesis in Organic Chemistry: “Synthesis, Characterization and Surface Chemistry of Cesium Lead Halide ($CsPbX_3$) Nanocrystals” advisors Proff. Babudri Francesco and Suranna Gian Paolo, vote 98/110. From February 2021 to May 2024, PhD student in Environmental and Building Risk and Development at the Polytechnic University of Bari. Her research program aims to develop new adsorbent materials for reactive capping of contaminated marine sediments. In particular, the object of the project was the validation of a protocol to produce cellulose- and chitin-based materials from laboratory scale to industrial scale, testing these materials with organic dyes and heavy metals. She spent a period at the Technical University of Iasi, Romania, where she improved a Life Cycle Assessment analysis to evaluate the environmental impacts of the production process and the application of these materials.

# *PUBLICATIONS*

1. A. Petrella; S. De Gisi; **M.E. Di Clemente**; F. Todaro; U. Ayr; S. Liuzzi; M. Dobiszewska; M. Notarnicola. Experimental Investigation on Environmentally Sustainable Cement Composites Based on Wheat Straw and Perlite, 2022, Materials, 15, 453.
2. **Di Clemente, M. E**.; Grisorio, R.; Petrella, A.; Suranna, G.; Todaro, F.; Notarnicola, M.. Sviluppo di materiali a base di cellulosa nanostrutturata per il trattamento in situ di sedimenti marini contaminati - STAMPA. - 2023, pp. 410-415.

La borsa di dottorato è stata cofinanziata con risorse del
Programma Operativo Nazionale Ricerca e Innovazione 2014-2020 (CCI 2014IT16M2OP005),
Fondo Sociale Europeo, Azione I.1 “Dottorati Innovativi con caratterizzazione Industriale”

UNIONE EUROPEA
Fondo Sociale Europeo